Photodynamic effects of FosPeg®/H-ALA on Epstein-Barr virus (EBV) positive and negative nasopharyngeal carcinoma cells

WU Wing Kei

Ph.D

The Hong Kong Polytechnic University

2014

The Hong Kong Polytechnic University
Department of Health Technology and Informatics

Photodynamic effects of FosPeg®/H-ALA on Epstein-Barr virus (EBV) positive and negative nasopharyngeal carcinoma cells

by

WU Wing Kei

A thesis submitted in partial fulfilment of the requirements for the degree of Doctor of Philosophy

April 2014

Certificate of Originality

I hereby declare that this thesis is my own work and that, to the best of my knowledge and belief, it reproduces no material previously published or written, nor material that has been accepted for the award of any other degree or diploma, except where due acknowledgement has been made in the text.

(Signed)

WU Wing Kei, Ricky (Name of student)

Abstract

Nasopharyngeal carcinoma (NPC) is one of the top ten cancers highly prevalent in Hong Kong with more than 800 new cases reported annually. The epidemiologic evidence implies that Epstein-Barr virus (EBV) infection is strongly associated with the NPC tumourigenesis. Among the EBV proteins expressed in NPC patients, latent membrane protein 1 (LMP1) is documented as the principal onco-protein contributes to EBV-associated oncogenesis via modulation of the intracellular signaling pathways, such as mitogen-activated protein kinases (MAPK) signaling pathways. Conventional treatment of NPC is mainly based on chemo-radiotherapy, however, the treatment outcomes of high grade (poorly differentiated and undifferentiated) NPC tumours remain poor. The extensive use of chemodrugs further complicated the situation by inducing drug resistant NPC tumours. Therefore, a novel treatment is crucial for patients suffering from high grade NPC.

Photodynamic Therapy (PDT) is FDA approved cancer treatment regimen in the USA, European Union, Japan and China. It employs a combination of light-activated photosensitizer (PSs) and oxygen to selectively destroy the tumours. The PDT efficacy could be further enhanced by improved photosensitizers and novel light source.

In the present work, two improved photosensitizers, namely H-ALA (5-aminolevulinic acid hexylester) and FosPeg® (liposomal formula of mTHPC) with LED light activation were comparatively studied on three NPC cells, namely EBV positive C666-1 cells (undifferentiated), EBV negative CNE2 cells (poorly differentiated) and EBV negative HK1 cells (well differentiated). Their antitumour mechanisms were investigated, including: uptake and localization of PSs, phototoxicity, regulation of EBV LMP1 related miRNAs, mRNA and protein, mode of cell death, and modulation of intracellular signaling proteins (MAPK and EGFR)

and their downstream proteins on NPC. Apart from these, the action of FosPeg® PDT on the drug resistant properties in NPC cells was also addressed.

Our findings indicated that both H-ALA and FosPeg® were localized in the mitochondria of all three NPC cells. FosPeg®-PDT demonstrated a better phototoxicity in NPC cells than that of H-ALA-PDT. FosPeg®-PDT showed phototoxic effect on all three tested cell lines; whereas H-ALA-PDT was ineffective in HK1 cells. In order to achieve LD_{50} FosPeg®-PDT, a 48-fold lower PDT dose was needed than that of H-ALA. Similarly, a 24-fold lower PDT dose was needed for FosPeg® than that of H-ALA in CNE2 cells. No dark toxicity was identified in both PSs.

EBV LMP1 miRNAs, mRNA and proteins were expressed only in EBV positive C666-1 cells among the three cell lines. FosPeg®-PDT induced a down-regulation of EBV encoded miRNAs (ebv-miR-BART1-5p, 16 and 17-5p). A significant up-regulation of LMP1 mRNA and protein were also obtained ($P<0.05$). H-ALA also caused a significant up-regulation of LMP1 protein in C666-1 cells.

Both H-ALA and FosPeg® mediated PDT significantly provoked a down-regulation of MAPK and EGFR signal proteins in all NPC cells at LD_{70}, thereby triggered apoptosis cell death pathway and caused cell cycle and DNA content changes in NPC cells.

The PDT efficacy towards drug resistance counterpart was investigated. FosPeg®-PDT increased the P-glycoprotein (P-gp) mRNA and protein expression levels in all NPC cells. Interestingly, FosPeg® was not the substrate of P-gp transporter proteins and the PDT efficacy was not affected by the up-regulation of P-gp/MDR transporter proteins expression.

In conclusion, this study offered new evidence and insights for potential PDT to EBV positive and EBV negative NPC cells. Further investigations are warranted for the benefit of PDT clinical applications in NPC patients.

List of Publications and presented work

Journal Articles:

1. **WU RWK**, CHU ESM, HUANG Z, XU CS, IP CW, YOW CMN. FosPeg® PDT alters the EBV miRNAs and LMP1 protein expression in EBV positive nasopharyngeal carcinoma cells. Photochem Photobiol B. 127(5): 114-122, 2013.
2. **"WU RWK**, CHU ESM, HUANG Z, XU CS, IP CW, YOW CMN. Impact of FosPeg® mediated photoactivation on P-gp/ABCB1 protein expression in human nasopharyngeal carcinoma cells." Manuscript was submitted to Cancer Letters, April.

Conference Papers from International and Local Conferences:

1. **WU RWK,** CHU ESM, Huang Z, YOW CMN. FosPeg® mediated photodynamic therapy with LED activation induced LMP1 protein expression in EBV positive C666-1 cell line. The 14th World Congress of the International Photodynamic Association. (IPA), Seoul, Republic of Korea, 28 May -31May, 2013. Abstract no.: P-47, pp. 134.
2. **WU RWK**, CHU ESM, IP CW, HUANG Z, YOW CMN. FosPeg®-mediated photocytotoxicity down-regulates the expression of epidermal growth factor receptor (EGFR) and vascular endothelial growth factor (VEGF) in EBV positive nasopharyngeal carcinoma cell line (C666-1). 1st Singapore Pathology Conference, Singapore. 19-20 October, 2012. Pp. 70.
3. **WU RWK**, CHU ESM, LO KW, YOW CMN. 5-aminolevulinic acid hexyl ester PDT induces cell cycle arrest in nasopharyngeal carcinoma cells (C666-1). 18th Hong Kong International Cancer Congress. LKS Faculty of Medicine,

The University of Hong Kong, HK. 3-5 November, 2011. Abstract no.: A33.

4. **WU RWK**, HUANG Z, YOW CMN. FosPeg® mediated photocytotoxicity suppresses cancer cell growth through down-regulation of MEK pathways. The 13th International Photodynamic Association in Association with EPPM & HNODS. Innsbruck, Austria. 10-14 May, 2011. Abstract no.: 210.

Acknowledgements

First of all, I would express my heartfelt respect and appreciation to my supervisor, Dr. Yow Christine. She has led me to the field of photodynamic therapy and guided me patiently throughout the course of this study. Her enthusiasm and insights in research inspired and delighted me to go through this project. It is my pleasure to be her student.

I would like to thank my co-supervisor, Professor Yung Benjamin, for his advice of this study.

I value Dr. Huang Zheng from the University of Colorado Denver, USA, Dr. CHU Ellie, Mr. KEUNG WT and Mr. IP CW for their invaluable advice and help in various ways throughout my study.

Thanks also go to the academic, technical staff, and my friends in the Medical Laboratory Science section, Department of Health Technology and Informatics for their encouragement and support.

Last but not least, I would like to express gratitude to my family for their patience, encouragement, and confidence. I dedicate this thesis to my wife Karen and my daughter Jade.

Preface

This thesis is presented in the form of journal articles.

Thesis overview

The thesis was present in four parts:

Part I

- **Chapter 1** literature review provided an introduction to nasopharyngeal carcinoma, photodynamic therapy and drug resistance in tumour. The aims and key objectives of this study were also listed.

Part II

This part presents a series of investigations to illustrate the H-ALA-PDT efficacy and antitumour effects on three NPC cell lines.

- **Chapter 2** addressed the H-ALA-PDT efficacy, mode of cell death, and regulation of cell cycle on three NPC cell lines by flow cytometry. The alteration of EBV LMP1 protein expression mediated by H-ALA was also addressed via Western blot analysis.
- **Chapter 3** explained the modulation of MAPK and EGFR signaling proteins and their downstream proteins mediated by H-ALA-PDT on NPC cells via Western blotting analysis.

Part III

This part presents a series of investigations to illustrate the FosPeg®-PDT efficacy and antitumour effects on three NPC cell lines.

- **Chapter 4** addressed the FosPeg® PDT efficacy and alteration of EBV LMP1 protein expression on three NPC cell lines via MTT cytotoxicity assay, Real Time PCR analysis and Western blot analysis.

- **Chapter 5** explained the modulation of MAPK and EGFR signaling proteins and their downstream proteins mediated by FosPeg®-PDT on NPC cells via Western blotting analysis. The mode of cell death and modulation of cell cycle and DNA content by FosPeg®-PDT were also addressed via flow cytometric analysis.
- **Chapter 6** illustrated the alteration of P-gp/MDR1 transporter proteins triggered by FosPeg®-PDT via Real Time PCR analysis and flow cytometric analysis.

Part IV

- **Chapter 7** included conclusion and future investigations for this study.

Table of Contents

List of Figures

Chapter 1

Chapter 2

Chapter 3

Chapter 4

Chapter 6

List of Tables

List of Abbreviations

5-ALA	5-aminolevulinic acid
5-FU	5-Fluorouracil
ABC	Adenosine triphosphate binding cassette
AJCC	American Joint Committee on Cancer
ANOVA	analysis of variance
BART	BamHI A rightward transcript
BCRP/ABCG2	breast cancer resistant protein
CPPD	Cisplatin
CST	Complementary strand transcript
Ct	cycle threshold
CTAR	C-terminal activating regions
H-ALA	hexvix / 5-ALA hexylester
DMSO	dimethylsulfoxide
DNA	deoxy-ribonucleic acid
EBV	Epstein-Barr virus
EBER	EBV-encoded nuclear RNA
EBNA	EBV-encoded nuclear antigen
ECM	extracellular matrix
EGFR	epidermal growth factor receptors
ERK	extracellular signal-regulated kinase
pERK	phosphorylated extracellular signal-regulated kinase
FBS	fetal bovine serum
FDA	Food and Drug Administration
HpD	hematoporphyrin derivative
hTERT	human telomerase reverse transcriptase
Interleukin	IL
JAK/STAT	janus kinase/signal transducer and activator of transcription

JNK	c-Jun N-terminal kinase
pJNK	phosphorylated c-Jun N-terminal kinase
LD	lethal dose
LED	Light-emitting diode
LMP1	latent membrane protein 1
LMP2A	latent membrane protein 2A
LMP2B	latent membrane protein 2B
MAbs	monoclonal antibodies
MAPK	mitogen-activated protein kinase
MDR	multidrug resistance
MDR1/ABCB1	multidrug resistance protein 1
miRNA	micro RNA
MMC	mitomycin C
MMP	matrix metalloproteinase
MMP-2	matrix metalloproteinase-2
MMP-9	matrix metalloproteinase-9
MSD	membrane spanning domain
MTT	3-(4,5-dimethylthiazol-2-yl)-2,5-diphenyltetrazolium
mRNA	messenger ribonucleic acid
MRP1	multidrug resistance associated protein 1
m-THPC	meso-tetrahydroxyphenyl chlorine
NBD	nucleotide binding domain
NF-kB	nuclear factor kappa B
NPC	nasopharyngeal carcinoma
p38	p38 mitogen-activated protein kinase
p-p38	phosphorylated p38 mitogen-activated protein kinase
PBS	phosphate buffered saline
PCR	polymerase chain reaction
PDT	photodynamic therapy
PEG	poly ethylene glycol

PEP	prophylaxis
P-gp	P-glycoprotein
PI	propidium iodide
PIT	Photoimmunotherapy
PpIX	protoporphyrin IX
PSs	photosensitizers
qPCR	quantitative polymerase chain reaction
QOL	quality of life
Rho123	rhodamin 123
RNA	ribonucleic acid
ROS	reactive oxygen species
PS	photosensitizer
RT-PCR	reverse transcription polymerase chain reaction
TMD	transmembrane domain
UICC	International Union Against Cancer
VEGF	vascular endothelial growth factor

Chapter 1

Background and Literature Review

Chapter 1

1.1 Overview of nasopharyngeal carcinoma (NPC)

Nasopharyngeal carcinoma (NPC) is endemic in Asia. It is one of the top ten cancers highly prevalent in Hong Kong with more than 800 new cases reported annually (Hong Kong Cancer Registry, 2011; Sizhong et al., 1983; Vokes et al., 1997). The overall incidence is 6.5/100,000 persons-year in southeastern Asia. However, in some cities such as Guangdong and Hong Kong, the incidence rate sharply increases to 30.94/100,000 persons-year and 12.2/100,000 persons-year, respectively (Hong Kong Cancer Registry, 2011; Jia et al., 2006).

Nasopharyngeal carcinoma (NPC) cells encompass any squamous cell carcinoma arising in the epithelial lining of the nasopharynx, a tubular space situated at the base of the skull. It is characterized by poorly differentiated or undifferentiated carcinoma with increased radio- and chemosensitivity, and a greater tendency for distance metastasis (Yoshizaki et al., 2012).

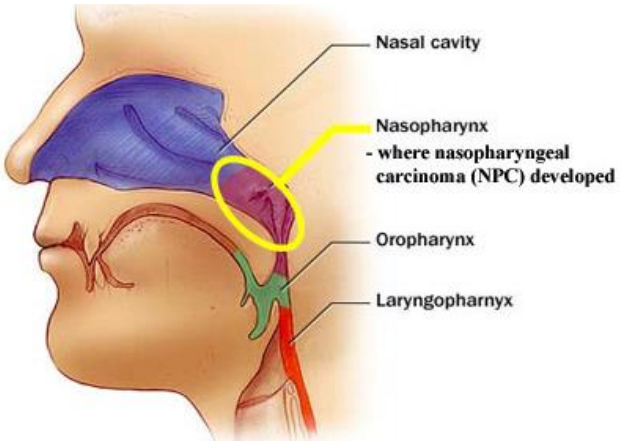

Figure 1.1 Diagram shows the region of nasopharynx, which comprises the upper portion of the pharynx that runs from nasal cavity to the top of esophagus in the neck.

(Modified from http://www.mayoclinic.com/health/nasopharyngeal-carcinoma/DS00756/DSECTION=2)

1.1.1 Classification of NPC

The histopathological classification of NPC was distinguished into three types according to the degree of differentiation by The World Health Organization. Type I is keratinizing squamous-cell carcinoma (well differentiated) similar to carcinomas that arise from other sites of the head and neck. Type II is non-keratinizing epidermoid carcinoma (poorly differentiated). Type III represents the undifferentiated carcinoma (Brennan, 2006; Vokes et al., 1997). Among these, NPC Type I is uncommon in endemic areas while type II and type III NPC are more prevalent. Reports indicated that type II and type III NPC were closely related to EBV infection (Tulalamba & Janvilisri, 2012).

NPC can also be staged clinically according to the 7th edition of the International Union Against Cancer (UICC) and the American Joint Committee on Cancer (AJCC) staging-system manual. AJCC classifies NPC into 4 stages according to the TNM system. TNM system consists of 3 key pieces of information, includes T) describes whether the primary tumour has invaded into nearby tissues or organs, N) describes whether the primary tumour has spread to nearby lymph nodes, and M) describes whether the cancer has metasisized. Different scores are given by the TNM system in order to provide more details about each of these descriptions for NPC staging. The number 0 to 4 indicate the degree of spread, while X will be given to those cases which cannot be assessed. Stage I NPC is T1-N0-M0, indicates the tumour is in the nasopharynx and may spread to nearby soft tissues. Stage II NPC is T2-N0-M0 or T1/T2-N1-M0, indicated the tumour has spread into nearby tissues. Stage III NPC is T3-N0 to N2-M0 or T1/T2-N2-M0, indicates the tumour has spread to lymph nodes. Stage IV NPC is T4-N0 to N2-M0 or any T-N3-M0 or any T-any N-M1, indicates the tumour may spread to distant sites (Zhang et al., 2013).

1.1.2 Aetiology

The aetiology of NPC is complex. The epidemiologic evidence implies that Epstein - Barr virus (EBV) infection, environmental factors and genetic factors play roles in

the tumourigenesis of NPC. EBV is listed as one of the major carcinogens and is strongly associated with NPC tumourigenesis. People with family history of NPC will have a 4 to 10 fold excess risk of NPC development (Chen & Huang, 1997; Friborg et al., 2005). Medical conditions in the ears, nose or throat have also been proposed as risk factors for NPC (Ekburanawat et al., 2010; Henderson et al., 1976). Others non-viral environmental risk factors include salted and pickled food consumption, alcohol consumption, hearable product consumption and tobacco smoking.

The first report revealed the association between salted fish intakes and NPC development was published by Ho in 1972 (Ho, 1972). A follow-up study with 2041 cases from Hong Kong was carried out by Ho to further illustrate the association between salted fish and NPC (Ho et al., 1978). The N-nitrosamine contained in salt-preserved fish and vegetables might be the source of carcinogens that act on nasopharynx. Salted fish is a traditional favourite item in the Cantonese diet and that could explain why the incidence rate of NPC is particularly high among Cantonese.

Alcohol consumption is correlated with NPC risk and is in a complex manner. Recent meta-analysis indicated large volume of alcohol intake will increase NPC risk significantly (3-4 drinks per day) while low volume of alcohol intake will result as beneficial effect (Chen et al., 2009; Marron et al., 2010).

Tobacco smoking is well documented as a risk factor for NPC. The pattern of association between tobacco smoking and NPC risk depends on the tobacco dose. The longer and greater cigarette smoking habit people have, the higher the risk of developing NPC. Current smokers with a history of more than 60 packs per year have the highest risk. People with a lifetime exposure of more than 30 packs per year have a 2 fold higher chance in NPC risk (Vaughan et al., 1996; Yu, Garabrant et al., 1990).

Studies have proposed that the use of herbal medicine was associated with NPC development through re-activation of Epstein-Barr virus (Jia & Qin, 2012; Zeng et al., 1983). However, limited evidence was found about the association between herbal tea/soups containing herbal ingredients and NPC development. Report even suggested that slow cooked soups with herbal ingredients and herbal tea decreased risk in associated with NPC development, although result was not statistically significant (Jia et al., 2010).

1.1.3 Role of Epstein-Barr Virus (EBV) in NPC tumourigenesis

It is widely accepted that Epstein–Barr virus (EBV) infection plays a major role in the tumourigenesis of NPC. EBV is a herpes virus that infects over 90% of adult population. It is a successful virus which establishes a life-long persistent relationship with human B-cell and remains asymptomatic (Farrell et al., 1997). However, EBV is also known as the most potent transforming agent for human cells. A number of malignancies are associated with EBV infection, including Burkitt's lymphoma, nasopharyngeal carcinoma, T cell lymphomas, lung carcinoma and gastric carcinoma (He et al., 2011; Herrmann & Niedobitek, 2003; Tsao et al., 2012). EBV has an envelope with viral glycoproteins carrying a double stranded DNA genome with approximately 172 kbp. The viral genome enters the infected cell nucleus and forms a circular episome. It is rare to observe viral replication in EBV-infected cells. On the other hand, EBV establishes a latent infection with a restricted set of latent genes being expressed, including two EBV-encoded nuclear RNAs (EBER1, EBER2), six EBV-encoded nuclear antigens (EBNA1, EBNA2, EBNA3A, EBNA3B, EBNA3C, EBNA-LP), and three latent membrane proteins (LMP1, LMP2A, LMP2B). It is now identified at least three different latent viral gene expression patterns in EBV associated tumours, which is known as latency I, II and III. In latency I, only the EBERs and ENBA1 are expressed. In latency II, the EBERs, EBNA1, LMP1 and LMP2 are expressed. And in latency III, all latent genes are expressed (Herrmann & Niedobitek, 2003; Raab-Traub, 2002; Zheng et al., 2007).

Chapter 1

The association between EBV and NPC was first discovered from serological studies. EBV DNA is consistently detected in NPC patients (Okano et al., 1988). There are lines of evidences showing that EBV implicated in the molecular abnormalities leading to pathogenesis of NPC. In NPC, EBV replicates and hides in cells followed by type II latency infection cycle, with expression of a limited number of viral proteins. The tumourigenic potential of EBV has been proven both *in vitro* and *in vivo*. EBV immortalizes primary primate B lymphocytes and epithelial cells *in vitro*, while EBV induces B-cell lymphomas and enhances epithelial tumour cell growth in nude mice models (Dawson et al., 2012; Eliopoulos & Young, 2001; Teramoto et al., 2000; Yoshizaki et al., 1999). The tumourigenic potential of EBV is mainly related to a unique set of latent gene products, including the latent membrane proteins (LMP1, LMP2A and LMP2B) and EBV-encoded nuclear antigens (EBNA1 and EBNA2). Among these, LMP1 is the principal oncogene involved in the process of EBV-associated oncogenesis of NPC (Figure 1.2) (Dawson et al., 2012; Goormachtigh et al., 2006; Kung & Raab-Traub, 2008; Raab-Traub, 2002).

LMP1 is a 66kDa integral membrane protein consists of 6 transmembrane domains and a carboxyl-terminus containing 3 signaling domains called C-terminal activating regions 1, 2 and 3 (CTAR 1, CTAR 2 and CTAR 3). The short cytoplasmic N-terminal segment is responsible for membrane attachment and orientates LMP1 protein to the plasma membrane while the six transmembrane loops are involved in self aggregation and oligomerization. The three CTAR domains provide docking sites for signaling adaptor proteins. Among these, CTAR 1 and CTAR 2 are two of the distinct functional domains responsible for the process of LMP1 signaling activity via directly activation of mitogen-activated protein kinases (MAPKs), nuclear factor kappa B (NF-kB), and Janus Kinase/Signal Transducer and Activator of Transcription (JAK/STAT) pathway (Dawson et al., 2012). LMP1 induced signal pathways attributed to the inhibition of apoptosis; induction of cell immortality; promotion of cell proliferation and influence the cell

invasion and metastasis (Figure 1.3) (Lo et al., 2007; Raab-Traub, 2002; Tsai et al., 2006).

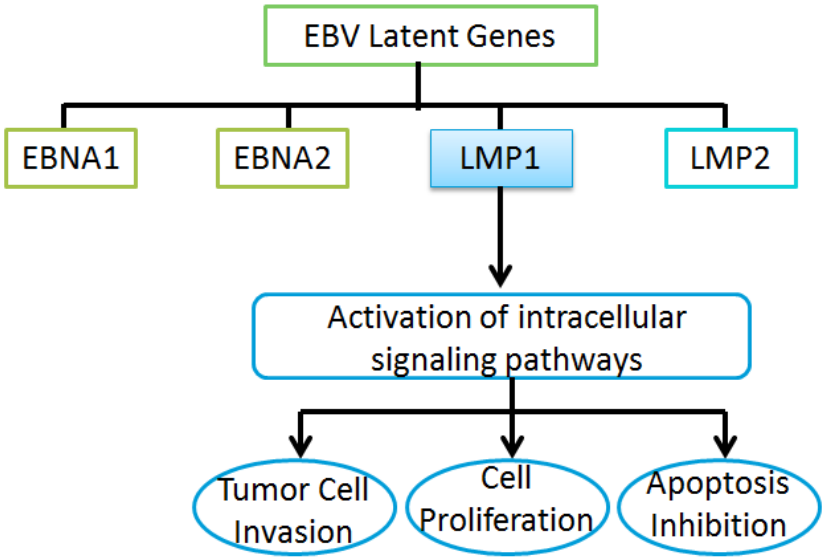

Figure. 1.2 Mechanisms of Epstein-Barr virus (EBV) latent proteins in nasopharyngeal carcinoma (NPC) development.

→ Stimulatory effect. (adopted from Josephine et al., 2008)

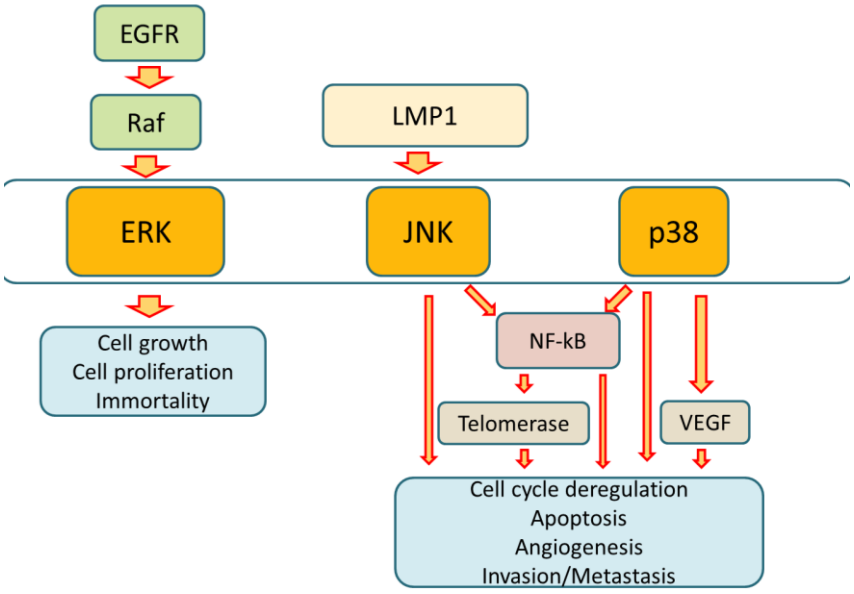

Figure 1.3 Signal transduction pathways regulated by the viral protein LMP1.
(Modified from Tsao et al., 2002)

1.1.3.1 EBV associated intracellular signaling pathways

Modulation of intracellular signaling pathways by EBV LMP1 is one of the elemental factors controlling the biological behaviors in NPC. These signaling pathways are critical for various cell functions, including cell survival, cell growth, cell differentiation and metastasis (Brennan, 2006). Researches on molecular signaling pathways reveal the role of different signaling proteins to tumourigenesis of NPC. Knowledge generated provides opportunity in the development of novel diagnostic, prognostic and therapeutic markers for NPC patients. Alteration of signaling proteins induced by EBV in NPC includes the mitogen-activated protein kinases (MAPKs) pathways and the epidermal growth factor receptors (EGFRs) pathway (Chan, 2010; He et al., 2012; Tulalamba & Janvilisri, 2012).

MAPK signaling pathways induced in the cell death mechanism

The MAPK pathway is a chain of proteins in cells which communicates a signal from cell surface receptor to the nucleus by phosphorylation, which has been proved to be very important in cancer development. The signals are transmitted by a cascade of kinases, including the extracellular signal-regulated kinase (ERK), p38 (p38 MAPK) and c-Jun N-terminal kinase (JNK) and they plays an important role in regulating cellular responses to a multitude of environmental stimuli.

JNKs are known as the stress-activated protein kinases and their normal functions are in response to growth stimuli, cellular transformation and tumour metastasis. Prolonged activation of JNK results in pro-apoptotic effect in normal cells via tumour necrosis factor. Down regulation of JNK results as increased cancer cells tolerance to cell death (Chen et al., 1996; Tang et al., 2002). Interestingly, JNK activity is consistently up-regulated in NPC via LMP1-dependent route (Eliopoulos & Young, 1998; Tsai et al., 2006). LMP1 induced JNK activity may be regarded as a growth advantage to NPC due to the versatile nature of this important signaling pathway. Constitutive activation of JNK in NPC increased p53 phosphorylation via phosphorylation of methyltransferase, resulted as reduction in E-cadherin gene

expression and leading to cell cycle deregulation (Eliopoulos & Young, 1998; Tsai et al., 2006; Tsao et al., 2002). Another possibility of JNK activation is that the pro-apoptotic effect of prolonged JNK activation is overwhelmed by other proliferative signals present in NPC.

Together with the JNK family, p38 are known as stress activated protein kinases. Evidences indicate that p38 activity is essential for normal immune and inflammatory responses. However, they could also be strongly activated *in vivo* by environmental stresses. In response to stimuli, p38 protein has been shown to regulate a wide range of cellular functions, including the self-sufficiency of growth signals, unlimited replication of proteins, angiogenesis, tissue invasion and metastasis, regulation of the cell cycle, and protection against apoptosis (Roux & Blenis, 2004). For example, p38 could induce progression or inhibition at G1/S transition depends on the cell type via regulation of cyclin proteins expression level. Any defects in p38 MAPKs function may contribute to cell cycle defects and tumourigenesis. Recent study reported that hypericin mediated PDT induced p38 expression, which counteracting the hypericin mediated PDT in HK-1/NPC cells (Chan et al., 2009).

It is not surprised that EBV induced ERK in various carcinomas, such as hepatocellular carcinoma, renal cell carcinoma and NPC. ERKs activation could be triggered via LMP1-dependent route (Oka et al., 1995; Schmidt et al., 1997). ERKs are constitutively expressed MAP kinases which regulate a diverse range of cellular functions, including cell growth and development. Phosphorylation of ERK is via the Ras/Mek/ERK cascade, resulted in activating the production of transcription factors NF-kB. The normal function of ERK activation is to control the cell growth and cell differentiation via regulation of cellular levels cyclin D1 and c-myc (Treinies et al., 1999). C-myc is critical to the regulation of G1/S phase via inhibition of p27 protein (Henderson et al., 1991; Kawanishi, 1997; Luo et al., 1997; Sheng et al., 2001). LMP1 activated ERK could also promote cell motility and

invasion by coordinating actin filament dynamics and focal adhesion turnover. Activated ERK proteins regulate the production and secretion of matrix metalloproteinases, resulting in extracellular matrix remodulation (Dawson et al., 2008; Shair et al., 2008). Studies also reported that the over-expression of the epidermal growth factor receptors (EGFRs) is associated with ERKs signal pathway activation, resulted in abnormal cell proliferation in NPC cells (Downward, 2003; Roberts & Der, 2007). Figure 1.4 illustrates the MARK signaling pathway.

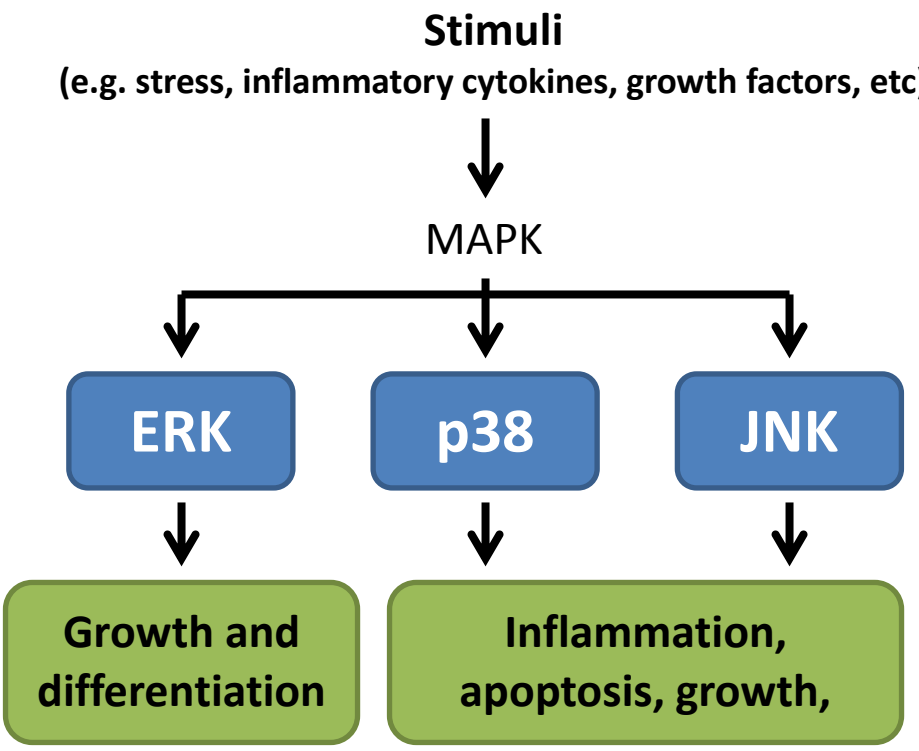

Figure 1.4 A simplified diagram of MAPK signal pathways trigger cellular responses.

The MAPK signal pathways are triggered by several extracellular stimuli, including stress, inflammatory cytokines, growth factors, mitogens, neurotransmitters etc. MAPK pathways activate through sequential phosphorylation events. Activation of ERK1/2 pathways resulted in cell growth, differentiation and development. Activation of p38 and JNK resulted in inflammation, apoptosis, growth and differentiation. (Adopted from http://www.cellsignal.com/reference/pathway/pdfs/MAPK_Cascades.pdf)

Chapter 1

The epidermal growth factor receptors (EGFRs) pathway

The epidermal growth factor receptor is a seven transmembrane receptor. It belongs to the member of tyrosine kinase receptors. Over-expression of EGFRs in NPC is quite frequent and reports indicated that as high as 80% of NPC primary biopsies with EGFRs over-expression (Kung et al., 2011; Miller et al., 1995; Ruan et al., 2011). Interestingly, LMP1 promotes growth and proliferation via the up-regulation of epidermal growth factor receptor (EGFR) expression and increase the phosphorylation of EGFR (Zheng et al., 2007). Studies indicated that LMP1 stimulated the endocytosis of EGFR and translocation into the nucleus. Intra-nuclear EGFR serves as a transcription factor to promote the expression of cellular proliferation components while cytoplasmic EGFR binds to cyclin D1 and cyclin E proteins to accelerate G1/S transition (Cho, 2007; Chou et al., 2008; Tao & Chan, 2007). Therefore, the signal pathway mediated by EGFR plays a vital role in the carcinogenesis of NPC and causes uncontrolled cell proliferation (Arteaga, 2002; Miller et al., 1995). Thus EGFR could be a rational target for antitumour strategies mediated by PDT.

NF-kB and telomerase mediated cell immortalization

In NPC, LMP1 activates NF-kB through the binding of tumour necrosis factor receptor-associated factors. NF-kB normally plays 2 main roles in normal cells, which are regulation of cell growth and modulation of inflammation. Dysregulation of NF-kB is one of the important components of NPC tumourigenesis. Studies found that NF-kB is over-expressed in almost all NPC tumours (Lee et al., 1997; Lo et al., 2006). NF-kB is a protein complex present in the cytoplasm which serves as a transcription factor (Gilmore, 2006). Translocation of activated NF-kB into the nucleus allow binding to their conjugate DNA binding sites. The binding of NF-kB to its DNA binding sites regulates a large number of genes transcription, such as cytokines (IL-6 and IL-8); anti-apoptotic proteins (Bcl-2); angiogenesis factors (VEGF); Matrix Metalloproteases-9 (MMP-9); and Epidermal Growth Factor Receptor (EGFR) signaling (Deng et al., 2003; Murono et al., 2001; Zheng et al.,

2007). Activation of NF-kB by LMP1 also contributes to NPC cell immortalization through up-regulation of telomerase activation. NF-kB binds to hTERT protein and subsequent activate the telomerase.

LMP-1 induced NF-kB activity and increased c-myc expression, lead to telomerase activation and cell immortalization. Telomerase is highly expressed in germ cells, stem cells and cancer cells. Telomerase is responsible for the maintenance of the length of the chromosome telomeres (Poole et al., 2001). Telomere is a specialized nucleoprotein complex located at the end of eukaryotic chromosomes. It is a tandem repeated DNA sequences of "TTAGGG" in Human DNA (Kim et al., 1994). The function of telomere is to stabilize and protect chromosomal ends in cells from exonucleolytic degradation and fusion. The human telomerase is a complex enzyme, which composed of a ribonucleic acid component known as hTR, a protein component, known as hTEP1 and a catalytic subunit called hTERT (Kirkpatrick & Mokbel, 2001; Poole et al., 2001). hTERT is the catalytic subunit with reverse transcriptase activity and is critical to telomerase activity (Chu et al., 2008; Guo et al., 2008; Moon et al., 2008). NPC displayed increased telomerase activity, which is EBV dependent. About 91% NPC cells demonstrate hTERT expression and 85% have telomerase activation. LMP1 increases telomerase activity through NF-kB pathway with increased c-myc expression. NF-kB mediates the activation of hTERT gene while c-myc increases hTERT promoter activity (Li et al., 2006). These findings suggest that telomerase is a necessary component for NPC development.

Matrix Metalloproteinases (MMPs) and Vascular Endothelial Growth Factor (VEGF) in tumour metastasis

LMP1 induces cell invasion and metastasis via modulation of matrix metalloproteinases and vascular endothelial growth factor at protein level (Chew et al., 2010; Horikawa et al., 2000; Lee et al., 2007; Lu et al., 2003). Matrix metalloproteinases (MMPs) are a group of zinc-dependent enzymes responsible for the proteolysis of matrix proteins. Functions of MMPs in metastasis include degradation of basement membranes and extracellular matrices; activation of

growth factors to promote cell growth and angiogenesis; and protection of tumour cells from apoptotic signals (Cawston, 1996; Chang & Werb, 2001; Lynch & Matrisian, 2002; Rosenthal et al., 1998; Stamenkovic, 2000). Studies reported that EBV virus induced MMP-1, MMP-2, MMP-3 and MMP-9 on NPC. Among these MMPs, MMP-2 and MMP-9 are two type IV collagenases thought to be correlated with tumour invasion and metastasis (Kondo et al., 2005; Takeshita et al., 1999; Yoshizaki et al., 1999). MMP-9 transcription is more EBV dependent than MMP-2 as their expression is up-regulated by LMP1 through NF-kB activation (Buettner et al., 2006; Tsao et al., 2002; Zheng et al., 2007).

Vascular endothelial growth factor (VEGF), the downstream target of NF-kB and STAT3 signal pathways, is a sub-class of growth factors. VEGF is a key regulator of angiogenesis and is associated with tumours. VEGF binds to receptor proteins (VEGFR) and activates a signal pathway, causing the endothelial cells to divide and to secrete matrix metalloproteinases. The proliferating endothelial cells migrate into the surrounding tissues and organize into hollow tubes that evolve into new networks of blood vessels.

1.1.3.2 EBV encoded MicroRNAs

In additional to the well-established viral protein expression, EBV also expressed various micro RNAs (miRNAs). These miRNAs have been referred to as complementary strand transcripts (CSTs), BamHI A rightward transcripts (BARTs) or the BARF0 RNAs (Smith, 2001; Smith et al., 2000). The possible role of these RNAs is affecting the viral transformation, as high levels of CST and BARTs expression have been detected in NPC tumours (Raab-Traub, 2002; Smith, 2001; Takada, 2012).

The recent discovery of BART microRNAs (miRNA) has shed new light on the functions of these transcripts. miRNAs are a class of 19-24 nucleotides noncoding RNAs which modulate gene expression. miRNAs are produced by endogenous

enzymatic (Dicer) digestion of RNA transcripts containing hairpins. Protein translation is inhibited by forming complementary duplexes of miRNA with their target mRNAs, causing degradation of these target mRNAs (Lo et al., 2007; Marquitz & Raab-Traub, 2012). The number of EBV miRNAs made up 23.2% of the total miRNAs in the biopsy samples in NPC patients, whereas only 0.1% EBV miRNAs was found in adjacent normal nasopharynx tissues (Chen et al., 2010). These potent gene regulators are thought to control a wide range of biological functions, including differentiation, cell growth and cancer development (Cosmopoulos et al., 2009; Marquitz & Raab-Traub, 2012; Zhao et al., 2012). Several studies revealed the function of EBV encoded miRNAs to modulate both viral and cellular gene expression in NPC cells, altering the anti-apoptotic function, immune evasion, and viral protein expression patterns.

Study indicated that miR-BART5-5p down regulated the expression of a pro-apoptotic protein, PUMA in C666-1 cells. It kept cell survival and thus the period of latency increases (Choy et al., 2008). miR-BART16 down regulated TOM22, a mitochondrial receptor for the pro-apoptotic protein Bax. miR-BART2-5p helped the host cell to escape from NK cell recognition by repressing the expression of cellular stress-induced immune molecule. miR-BART 3 targeted IPO7, a nuclear importer receptor which is responsible for the nuclear translocation of transcription factor, and is involved in cytokine and early gene expression in activated T cells. miR-BART 6-5p suppressed the viral oncoprotein EBNA2 production, preventing the transition from latency I and II to III (Iizasa et al., 2010). miR-BART 2-5p inhibited EBV lytic replication by targeting the viral DNA polymerase BALF5. miR-BART 22 down regulated the expression of LMP2A which inhibited telomerase reverse transcription and induced anti-proliferation by NF-kB suppression.

EBV constitutively expresses up to 44 mature miRNAs and their main target is its oncogene LMP1 (Lo et al., 2007). EBV BARTs produce two clusters of miRNA.

The BART Cluster 1 miRNAs target the LMP1 protein expression and BART Cluster 2 miRNAs target EBV DNA polymerase BALF5 (Barth et al., 2008; Choy et al., 2008; Cosmopoulos et al., 2009; Lo et al., 2007). Up-to-date report indicated three BARTs cluster 1 miRNAs (ebv-miR-BART1-5p, 16 and 17-5p) targeted the LMP1 gene and down regulated the LMP1 protein expression (He et al., 2012; Lo, et al., 2012; Marquitz & Raab-Traub, 2012). One possible reason for the high level expression of miRNAs in EBV is to avoid overexpression of LMP1 protein. The overexpression of LMP1 protein could result in the inhibition of cell proliferation and trigger in apoptosis. Therefore, introducing miRNAs could inhibit excessive LMP1 expression in NPC cells and results in resistant to the apoptosis (Lo et al., 2012; Marquitz & Raab-Traub, 2012).

1.1.4 Conventional treatment of NPC

Treatment selected for NPC patients is based on the AJCC classification system. The conventional treatment for NPC is chemo-radiotherapy. It is because low grade NPC cells have high radio- and chemo-sensitivity. Promising treatment outcomes were obtained, with a 5-year overall survival of 70-80% for stage I and II NPC. However, the treatment outcomes in patients with stage II NPC become less favourable than that with stage I NPC, mainly because of the distance recurrence. The treatment outcomes for loco-regionally advanced NPC are worse, as a significant drop of 5-year overall survival to 55% and 30% for stage III and IV NPC, respectively. Local recurrence, distant recurrence and development of multi-drug resistance phenotype are the most common causes of treatment failure (Larbcharoensub et al., 2008; Tulalamba & Janvilisri, 2012; Zhang et al., 2013). The distance control was unsatisfactory with a 2-year distant metastasis rate ranged from 10 to 15% and a 4-year distant metastasis rate up to 32%. Complications always resulted after chemo-radiotherapy, such as hearing impairment, endocrinological dysfunctions, temporal lobe necrosis, cranial neuropathy, haemorrhage, and bone necrosis. Complications developed depend on the tumour volume, local treatment and radiotherapy fractionation schedule. Besides, survivors of NPC always have

impaired quality of life (QOL), which is increasingly emphasized in selecting appropriate therapeutic approaches for NPC patients (Chen et al., 2011; Suarez et al., 2010). Unfortunately majority of NPC patients were diagnosed with locally advanced stages as it is difficult to be detected earlier because of its complex anatomical location (Brennan, 2006; Tao & Chan, 2007). Thus development of new treatment strategies is crucial for patients with NPC.

1.1.5 Drug resistance mechanisms in NPC

Multidrug resistance is the major obstacle to chemotherapy in tumour patients. The term multidrug resistance (MDR) refers to the ability of cancer cells being developed to cross resist with a range of antitumour drugs, which are structurally and functionally unrelated. Development of MDR was intrinsically prior to treatment or acquired during treatment (Capella & Capella, 2003). The phenomenon of MDR could be achieved by the following mechanisms, including increased drug efflux from the cells via the adenosine triphosphate binding cassette transporters (ABC), inactivation of drugs via detoxifying enzymes, and defective apoptotic pathways (Stavrovskaya, 2000; Szakacs et al., 2006). Recent studies illustrated the importance of ABC membrane transporters as one of the leading mechanisms of MDR in tumour cells (Teodori et al., 2006; Wang & Fu, 2010). The advanced studies in molecular basis elucidating the phenomenon of MDR with cell lines indicated the over-expression of plasma membrane glycoproteins, including P-glycoprotein (P-gp/ABCB1), multidrug resistance associated protein 1 (MRP-1/ABCC1) and breast cancer resistance protein (BCRP/ABCG2). Among these, P-gp is the best studied mechanisms of MDR phenotype (Aszalos, 2007a; Solazzo et al., 2006).

Multidrug resistance mechanisms developed in nasopharyngeal carcinoma

There are only few articles reported the correlation of multidrug resistance protein expression on EBV infected NPC cells. A few studies demonstrated that P-gp and MRP1 were expressed in NPC cells in different levels.

Study has shown that a small portion of NPC expressed MDR1. Study demonstrated 12.6% NPC patients and 32.6% recurrent NPC patients expressed MDR1 (Chen et al., 2001). Another group of researchers reported that 3.3% of tested NPC patients expressed MDR1 (Ji et al., 2013; Larbcharoensub et al., 2008). Study also reported a significantly higher expression level of MDR1 in keratinizing squamous cell carcinoma type NPC than those with non-keratinizing and undifferentiated types NPC. MDR1 is expressed at the apical surface of normal nasopharyngeal epithelial cells, which protects normal tissues against exogenous toxins and hydrophobic xenobiotics (Larbcharoensub et al., 2008).

Different from MDR1 expression, the expression of MRP1 varied among the NPC patients. Study reported that 40% of the tested NPC patient samples expressed MRP. The high expression rate of MPR was proved to be correlated with the clinical stage. The MRP1 expression was one of the prognostic markers at the time of diagnosis before treatment. However, study failed to illustrate the correlation between MRP and chemo-sensitivity testing with selected anticancer drugs, such as CDDP, 5-FU, PEP and MMC. Furthermore, concerning the overall 5-year survival rate, there was no difference between NPC exhibiting MRP and NPC without MRP (Larbcharoensub et al., 2008; Tsuzuki et al., 1998).

ABCB1/P-glycoprotein (P-gp)

Phenomenon of multidrug resistance was initially noticed in 1948 in leukemia patients by Farber (Farber & Diamond, 1948). In 1976, Ling's group reported that the MDR phenotype was related to decrease intracellular drug accumulation mediated by a 170kDa plasma membrane glycoprotein, P-glycoprotein (Juliano & Ling, 1976). The association of increased MDR1 mRNA expression and increased MDR1 transporter proteins expression in resistant cancers confirmed the important role of MDR1 in human cancers. Recent studies indicated that P-gp was the most typical ATP-dependent drug efflux pump contributed to multidrug resistance in

cancer cells and was the best-characterized mechanism of MDR. P-gp is a 170kDa transmembrane protein consists of two hydrophobic transmembrane domains (TMDs), three membrane spanning domains (MSD) and two nucleotide binding domains (NBDs). It is encoded by MDR1 gene and is located on chromosome 7 (Leslie et al., 2005; Sauna et al., 2007). The TMDs region formed a pore-like structure contains the drug binding sites for different drugs, while the NBDs region controlled the transportation of drug across the cell membrane via binding and hydrolysis of ATP (Ambudkar et al., 1992; Rosenberg et al., 1997). The structure of ABCB1/P-gp was shown in Figure 1.5.

Mechanism of action of P-gp

Drug binging to the pore-like structure (high-affinity drug binding site) initiates the transport cycle via binding and hydrolysis of ATP coupled with P-gp. ATP is bound to nucleotide binding domains leads to conformational change of P-gp. Changes in P-gp conformation results in reduced affinity for drug binding and re-orientation of the site so that it is exposed to the extracellular medium (Ramachandra et al., 1998; Rosenberg et al., 1997; Wang et al., 2000). Studies have also shown that the binding of ATP, rather than hydrolysis of ATP, provided the energy for drug translocation (Sauna & Ambudkar, 2000; Sauna et al., 2007; Senior & Bhagat, 1998). The hydrolysis of ATP and release of ADP from P-gp affected its conformation, through returning the drug binding site to high drug affinity status. The working principle of ABCB1/P-gp was shown in Figure 1.6

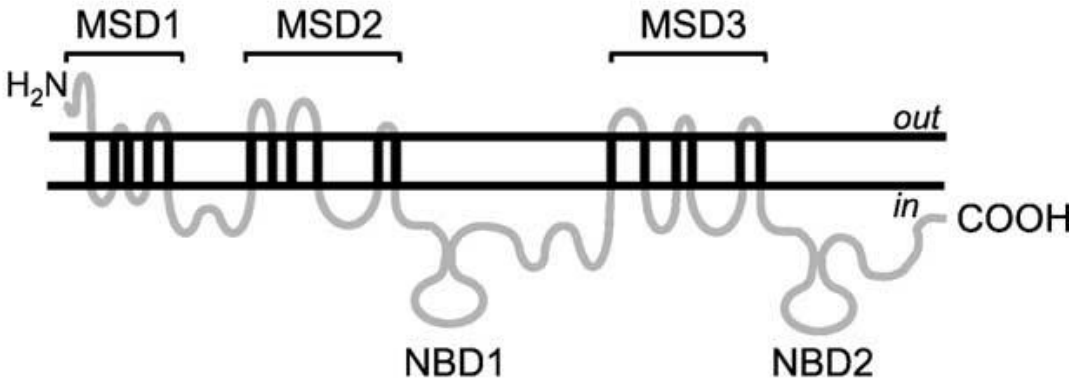

Figure 1.5 Diagram illustrate the topologic folding of human P-glycoprotein (ABCB1).

MSD: membrane-spanning domain; NBD: nucleotide binding domain. (Adopted from Leslie et al., 2005)

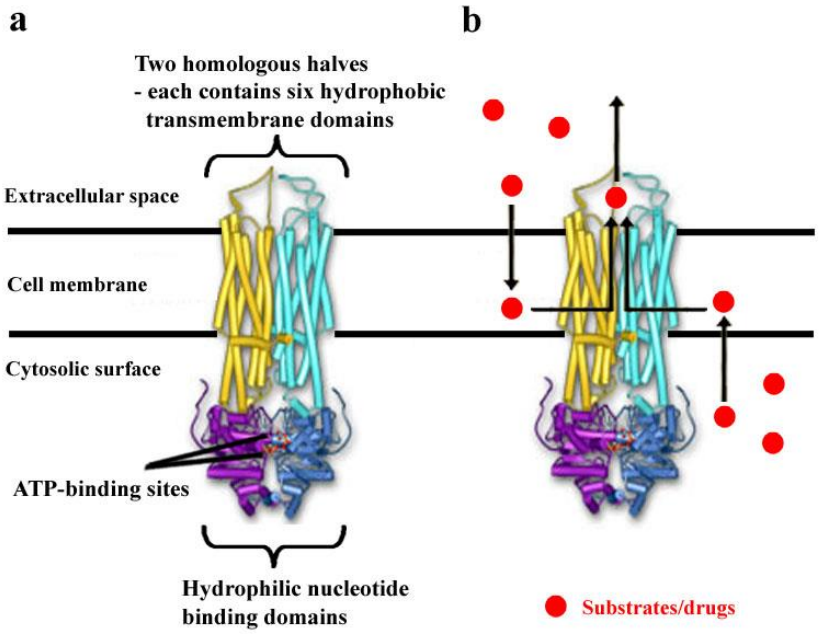

Figure 1.6 Diagram illustrate the efflux process of human P-glycoprotein (ABCB1).

(Modified from Aszalos, 2007a, 2007b)

1.2 Overview of Photodynamic Therapy (PDT)

Development of novel treatment strategies is crucial for patients with Nasopharyngeal Carcinoma in view of drug resistance phenotypes and complications developed after conventional treatment.

Photodynamic therapy (PDT) is an evolving cancer treatment regimen which was approved for use in USA, EU, Canada, Russia and Japan (Agostinis et al., 2011; Bredell et al., 2010; Brown et al., 2004). PDT uses a combination of photosensitizing agents (PSs), visible light and oxygen to selectively destroy the biological targets. None of these is individually toxic, but together they initiate phototoxicity to biological targets.

PDT function depends on the tumour localizing photosensitizer, which absorbs photon to produce photo-toxin such as singlet oxygen ($^1O_2$) and reactive oxygen species (ROS). PSs could be localized in various cellular organelles including cell membrane, mitochondria, endoplasmic reticulum and Golgi apparatus, nucleus and lysosome (Plaetzer et al., 2009; Robertson et al., 2009). ROS oxidize many biological molecules, such as proteins, lipids and nucleic acids, leading to *in vivo* and *in vitro* tumour cell disruption via apoptosis, necrosis and/or autophagy (Sasnauskiene et al., 2009; Zawacka-Pankau et al., 2008). The antitumour effects of PDT are derived from 3 mechanisms: including direct cytotoxicity effects on tumour cells, destruction of tumour-associated vasculature, and induction of inflammatory reaction against tumour cells (Agostinis et al., 2011; Calzavara-Pinton et al., 2007; Dolmans et al., 2003; Huang et al., 2008; Asta-Juzeniene & Moan, 2007; Plaetzer et al., 2009; Rumie-Vittar et al., 2013).

PDT is a FDA approved therapeutic modality for several malignant diseases, including skin cancer, bladder cancer and head and neck cancer (Plaetzer et al., 2009). It is clinically used when the patients are unable or failed to respond to chemotherapy and radiotherapy. A number of components contribute to the

efficiency of PDT, including type and dose of PSs used, drug incubation time, light dose and tumour oxygen concentration. Since PDT has limited damage to normal human cells, optimization of these components becomes one of the major goals of clinical settings to establish maximum efficacy of PDT application for cancer patients (Agostinis et al., 2011; Juarranz et al., 2008; Kolarova et al., 2008).

1.2.1 Antitumour mechanisms of PDT

The treatment of PDT consists of i) photosensitizers, ii) light in the visible wavelength, iii) molecular oxygen. PSs that is administered topically, locally or systemically will be localized and accumulated into tumour cells. The localization of PSs in various organelles depends on types of PSs. PSs have high selectivity for tumour cells. The selectivity could also be achieved through directed light delivery with specific system such as laser with optical fibres (Zamadar et al., 2011). After an incubation period, equilibrium will be reached in order to obtain the maximum drug uptake difference between normal cells and tumour cells. The region is then exposed to light of appropriate wavelength (usually red visible light with 620 – 690nm), causing photoactivating of PS, resulting in formation of ROS in the presence of oxygen (Figure 1.7) (Juarranz et al., 2008). Among these, the processes of light absorption by the PS and energy transfer are the two most important factors to determine the PDT efficacy on tumour eradication. The mechanism of photosensitizer activation to induce cell death is illustrated in Figure 1.8 (Qiang et al., 2009).

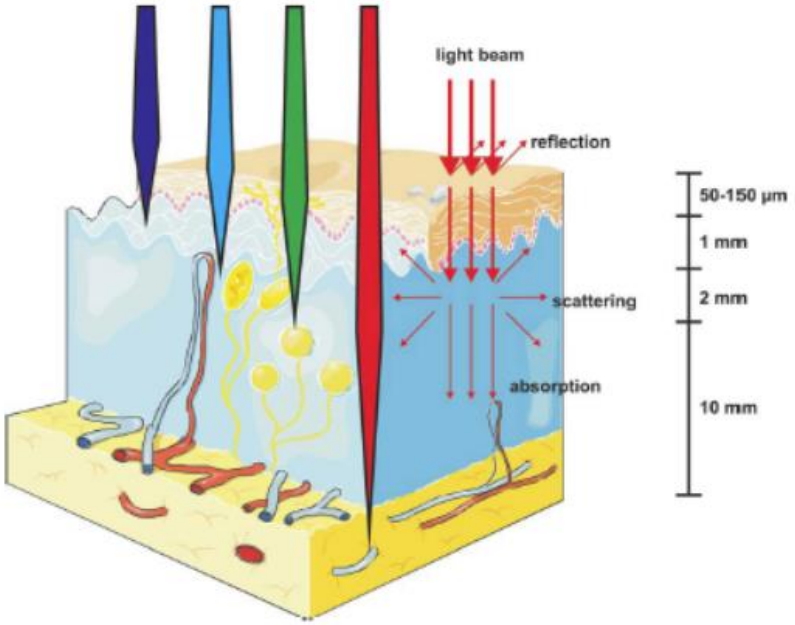

Figure 1.7 Tissue penetration depths relate to different wavelengths of light.
Near-ultra violet light provides the highest light energy but poorest tissue penetration while near-infra red light penetrates deepest into the target sites (Adopted from Agostinis et al., 2011)

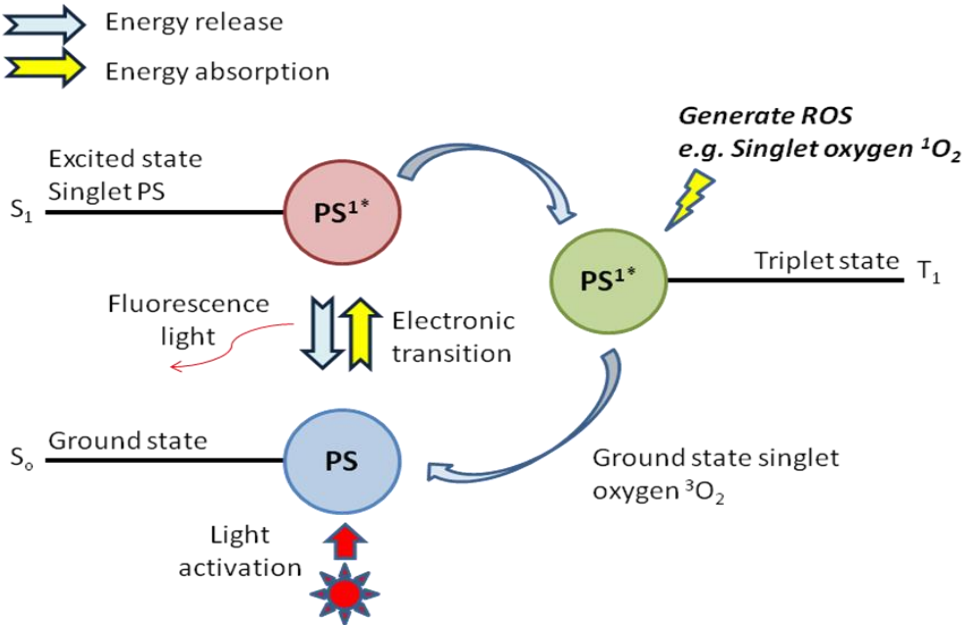

Figure 1.8 Energy level diagram for photosensitizer activation.

Figure showing the singled ground state (S_o), excited singlet state (S_1), and excited triplet state (T_1). Fluorescent photon will emit when photosensitizer decays from excited singlet state to ground state. Excited singlet-state oxygen ($^1O_2$) will be produced when the energy exchange from the photosensitizer triplet state to ground state oxygen ($^3O_2$). (Modified from Robertson et al., 2009)

In general, the photosensitizer molecules will be excited from singlet ground state (S_0) to a higher energy state (S_1) by photons from the light source (such as laser, quartz-halogen lamp or LED light) with specific wavelength. The molecules at the excited state are in nanosecond range and are usually unstable, which may easily decay to a lower energy state (T_1) by internal conversion and vibrational relaxation. Some molecules may further return to the ground state S_0 through fluorescence emission, but some will pass to the triplet excited state. Molecules in the triplet excited state can decay back to S_0 state through the emission of fluorescence light. Two processes were involved, which known as the electron transfer process (type I reaction) and the energy transfer process with molecular oxygen (type II reaction). In type I mechanism, T_1 stage molecules may generate free radical species and will further react with environmental oxygen to form oxidized products. In type II mechanism, T_1 stage molecules may generate singlet oxygen. It is believed that the singlet oxygen is the key agent for cellular damage, resulting biological damage of the proteins, lipids and various cellular constituents and thus the type II mechanism is predominate over the type I mechanism (Dolmans et al., 2003; Hilf, 2007; Robertson et al., 2009). However, the lifetime of singlet oxygen is very short (in the micro- to millisecond range) that limits its diffusion in cells. Thus the photodynamic damage is closely related with the properties and intracellular location of the photosensitizers (Figure 1.9) (Agostinis et al., 2011; Moan et al., 1989; Yano et al., 2011).

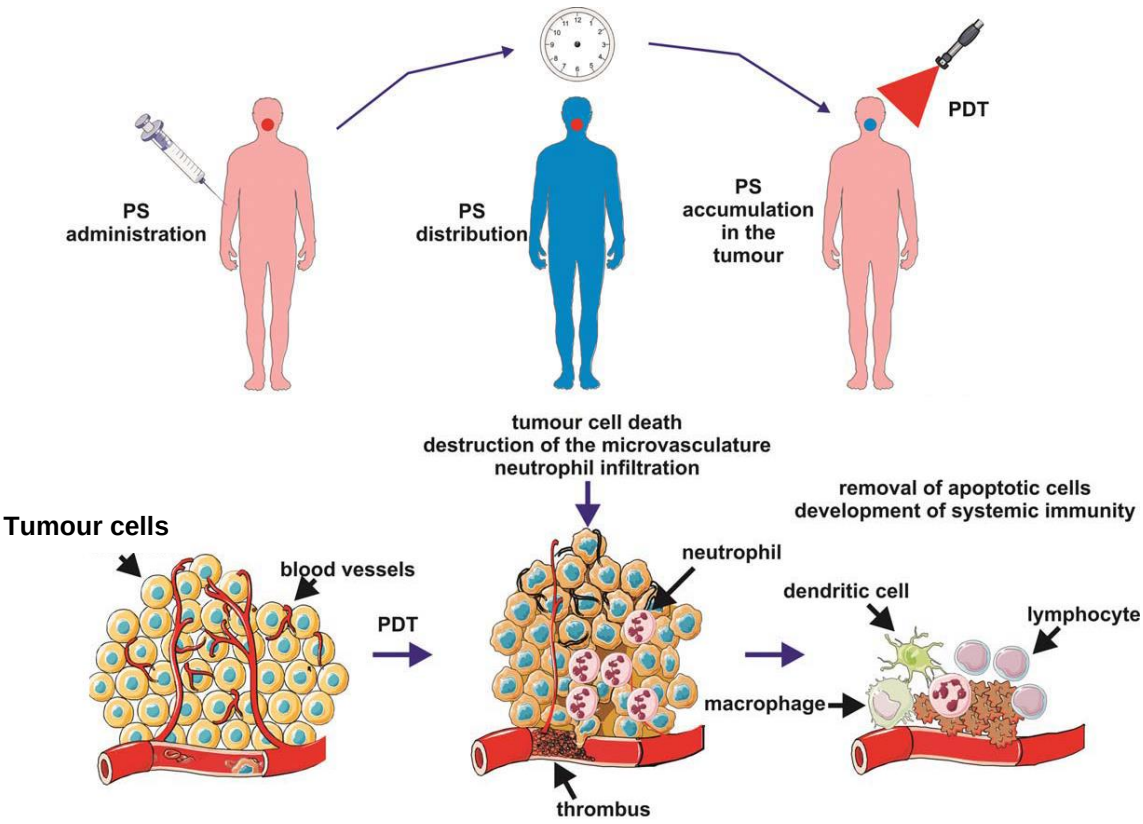

Figure 1.9 Schematic diagrams showing the sequence of photodynamic therapy and its underlying cell death mechanisms.

ROS, which would apply to execute the photodamaging process, will be generated followed by photosensitizer administration, incubation and light activation. ROS could trigger apoptosis, necrosis or autophagy and dead cells are removed by phagocytes. Dendritic cells and lymphocytes would also be recruited for development of systemic immunity. Damage to tumour vasculature may also be executed to cut the nutrient supply to tumour cell via generation of thrombus. PS: photosensitizer. (adopted from Agostinis et al., 2011)

The antitumour effects of PDT are derived from the following: i) direct cytotoxicity effects on tumour cells, and ii) modulation of intracellular signaling proteins. (Agostinis et al., 2011; Calzavara-Pinton et al., 2007; Dolmans et al., 2003; Huang et al., 2008; Asta-Juzeniene & Moan, 2007; Plaetzer et al., 2009; Rumie-Vittar et al., 2013)

i) Direct cytotoxicity effects on tumour cells

The search to define the molecular targets of PDT is one of the key questions in PDT mechanistic research. This question is closely related to the intracellular localization of PSs as ROS generated have a short half-life. ROS will only interact with intracellular structures close to their site of generation. The type of photodamage triggered by PDT thus depends on the subcellular localization of PS within the cells. Recent research has elucidated many pathways leading to cell destruction, including apoptosis, necrosis and autophargy (Castano et al., 2004).

Necrosis

The first type of cell death mechanism is known as necrosis, a quick form of degeneration affecting extensive cell population. Typical characteristics of necrosis include cell swelling, destruction of organelles and plasma membrane, leading to the release of intracellular contents and inflammation. Necrosis has been identified as accidental cell death which caused by physical or chemical damages. Decomposition of cells in necrosis is principally mediated by proteolytic activity (Calzavara-Pinton et al., 2007).

Apoptosis

Different from necrosis, apoptosis is identified in a single cell surrounded by healthy neighours. Apoptosis is referred as programmed cell death, with morphologically characterized by nucleus condensation, fragmentation of DNA, cell shrinkage, blebbing of the plasma membrane and formation of multiple membrane-enclosed spherical vesicles known as apoptotic bodies. Apoptotic bodies are then

scavenged by phagocytes *in vivo* and inflammation is prevented. Apoptosis is controlled by transcriptional activation of specific genes, including the activation of endonucleases and caspases, and DNA degradation into fragments (Hilf, 2007; Lim et al., 2011; Wu et al., 2006). Caspases consist of a group of enzymes known as the cysteine dependent aspartate-specific proteases. The apoptotic caspases could be activated by two pathways, namely extrinsic pathway and intrinsic pathway. Extrinsic pathway is triggered by binding of death ligands to their corresponding receptors; while intrinsic pathway is triggered by the mitochondria. The role of the intrinsic pathway in PDT has been documented as mitochondrium is one of the molecular targets for most of the PSs. Release of cytochrome c followed by destruction of mitochondria after PDT were observed and apoptotic caspases are being activated, resulted in PDT mediated apoptosis (Kessel, 2006; Kristjan et al., 2003).

Autophagy

The third type of cell death mechanisms is known as autophagic cell death. Autophagy is referred to the catabolic process initiated in eukaryotic cells. The purpose of autophagy is to remove damaged organelles by forming autophagosomes and recycling of cytoplasmic components. This is a survival mechanism allowing the cells to maintain normal cell functions. However, constitutive activation of autophagy can promote cell death as a result of excessive self destruction of cellular organelles. Autophagy is characteristized by a series of cellular changes, started as formation of autophagosomes, a double membrane structure which surrounded the cytoplasmic components or organelles. The autophagosomes will eventually fuse with the lysosomes. Enzymes stored in lysosomes will digest the cytoplasmic components and recycle useful materials, such as amino acids (Edinger & Thompson, 2004). Recent studies reveal that PDT may induce the formation of autophagy through photogenerated ROS. Formation of autophagy aimed to oxidatively remove damaged organelles or destruction of the mitochondria by AMP accumulation after PDT (Buytaert et al., 2007; Sasnauskiene et al., 2009).

ii) Antitumour mechanisms via modulation of intracellular signaling proteins

The generation of knowledge concerning cell biology and signal transduction pathways is one of the principal areas of mechanistic research in field of PDT. The alterations of signal transduction proteins induced by PDT include tyrosine kinase expression, transcription factors and cytokines.

Tyrosine kinase expression

Signal transduction cascades are important networks for cells to receive external stimuli and respond to the stimuli in an appropriate manner. The mitogen activated protein kinase (MAPK) signal pathways play an important role in eurkaryotic cells and modulate many cellular events including i) regulation of cell cycle, ii) regulation of embryoic development, iii) cell movement, iv) cell differetiation, and v) apoptosis (Johnson & Lapadat, 2002; Santonocito et al., 2005). The MAPK signal pathways consist of ”three kinase modules” including the extracellular signal regulated kinases (ERK), the c-Jun N-terminal kinase (JNK) and the p38 kinases. The role of JNK, ERK and p38 kinases in cell survival after PDT has been studied. Studies indicating the decrease in ERK’s expression after PDT treatment was related to PDT induced cell death. p38 kinases were found to act as stabilizers for cyclooxygenase 2 enzyme. Decrease in the p38 expression controled tumour growth via sensitizing cancer cells to apoptosis (Chan et al., 2009; Hendrickx et al., 2003; Tong et al., 2002). The epidermal growth factor receptor (EGFR) is another tyrosine kinase involved in the initiation and progression of various cancers and is related to cell proliferation, angiogenesis, invasion, and metastasis (Olayioye et al., 2000; Seymour, 2001). Many studies found that PDT induced complete loss of EGFR on different cell models, resulted as anti-proliferative responses (Ahmad et al., 2001; Martinez-Carpio & Trelles, 2010; Yang et al., 2012).

Transcritpion factors

Transcription factors are proteins which bind to the enhancer regions of genes to initiate gene expression. Transcription factors which coupled with receptor-generated signals act as intracellular messengers to activate various gene expression. Nuclear factor kappa B (NF-kB) is present in the cytoplasm and its activation typically initiate a specific signal transduction cascade, which regulates many cellular genes including a number of cytokines and growth factors. Activation of NF-kB upon photosensitization has been shown to either promote or inhibit apoptosis depending on the cell types (Castano et al., 2005; Korbelik, 2006; Li et al., 2002). In general, a number of PDT studies have shown that promotor regions of many genes, such as NF-kB, p53, B-cell lymphoma 2 (Bcl-2) and Interleukin 8 (IL-8) were activated after PDT treatment and related to both induction and prevention of apoptosis (Cogswell et al., 2000; Wolf et al., 2001).

1.2.2 Historical and clinical applications of photodynamic therapy

Treating disease with photosensitizing drugs is an old idea that the first attempts dated back to ancient Egypt, India and Greece (Moan & Peng, 2003). However, the term Photodynamic was coined by Jesionek and von Tappeiner in 1904 when they reported experiments on cancer treatment with photosensitizers. R. L. Lipson and S. Schwartz opened the door to the current research of PDT in 1960. They observed that injection of crude preparations of haematoporphyrin led to characteristic red fluorescence accumulated in neoplastic lesions during surgery. Afterward, a mixture that Schwartz obtained from treating haematoporphyrin with acetic acid and sulfuric acid was used by Lipson for tumour detection. The mixture is now known as the haematoporphyrin derivative (HpD). The expanding use of PDT in clinical applications is based on the pioneer work by Thomas J. Dougherty (USA) in the 1970s with the haematoporphyrin derivative (HpD). In 1980’s, a purified product of HpD named Photofrin, which has a wide range of proven curative effects, was approved by the US FDA as the first photosensitizer for PDT clinical application in treating or diagnosing cancers, such as skin, oral, bladder cancer and gynecological

cancer. Since then, PDT has gained increasing interests in both therapeutic and diagnostic aspects (Hopper, 2000; Huang et al., 2008; Asta-Juzeniene & Moan, 2007; Luksiene, 2003).

1.2.3 Photosensitizers

As one of the critical elements for PDT, there are a large number of photosensitizers being tested *in vivo* and *in vitro* in PDT experiments. The prerequisites of an ideal photosensitizer include: chemical purity, low dark toxicity, high quantum yield of singlet oxygen, selective accumulation in tumour cells, short time interval between drug administration and maximal accumulation within target cells, rapid clearance from the body, and being activated by longer wavelength with better tissue penetration (Garland et al., 2009).

Haematoporphyrin derivative (HpD) was the first FDA approval photosensitizer for clinical PDT with high response rate and promising results. It was developed in the 1970s and early 1980s and is now known as the 1st generation photosensitizers. The major drawback of HpD is the cutaneous photosensitivity and this drives the development of the next generation of photosensitizers.

A number of 2nd generation photosensitizers of different chemical families were synthesized in the late 1980s to offer potential advantages over the 1st generation photosensitizers, including higher chemical purity, better tumour selectivity and faster clearance (Dougherty et al., 1998; Pushpan et al., 2002). These 2nd generation photosensitizers include prophyrin precursors (5-aminolevulinic acid), chlorines (chlorine e6), meta-tetrahydroxy-phenyl chlorine (m-THPC), etc.

Current development of photosensitizers, also known as the 3rd generation of photosensitizers, aims at improving the drug delivery approach, such as biological modifications like antibody conjugate or liposome conjugate (Kuntsche et al., 2010; Paszko et al., 2011; Zamadar et al., 2011). Some selected sensitizers that are

available for intravenous administration with their main photochemical and photobiological properties are listed in Table 1.1 (Calzavara-Pinton et al., 2007; Triesscheijn et al., 2006).

Table 1.1

Main photochemical and photobiological properties of selected sensitizers available for intravenous administration or as topical solution. *(Adapted and modified from Calzavara-Pinton, et al., 2007;Triesscheijn, et al., 2006)*

	Absorption peak (nm)	Drug dose (mg/kg)	Light dose (J/cm^2)	Delay before irradiation (h)	Duration of photosensitization
Haematoporphyrin derivative	630	2.0-5.0	75-200	24-48	2-3 months
Porfimer sodium (Photofrin)	630	2.5-3.0	75-200	24-48	1-2 months
5-aminolevulinic acid (5-ALA)	635	20% *	100	3-6	
Benzoporphyrin derivative (BPD-MA)	690	0.15-0.5	100-200	0.5-2.5	4-7 days
Mesotetrahydroxyphenyl chlorine (mTHPC)	652	0.1-0.3	8-12	24-48	up to 6 weeks
Lutetium texaphyrin (Lu-tex)	732	0.6-7.2	150	3-5	up to 7 days

* Given as topical solution

1.2.3.1 Haematoporphyrin derivative (HpD) – Photofrin

Haematoporphyrin derivative is a FDA approved photosensitizer and is well known as first generation photosensitizer for the treatment of tumour, such as early and late endobronchial lesions, Barrett's esophagus and esophageal obstructing lesions (Dougherty, 1986; Dougherty, 1987; Dougherty et al., 1998; Yang et al., 2012). It is a mixture of monomers, dimers and oligomers of haematoporphyrin synthesized by chemical manipulation. It is the first photosensitizer that brought PDT to a worldwide audience. The first report of the preparation of HpD was published by Dougherty in 1983 (Dougherty, 1983). Afterward, a number of HpD formulas were available commercially, in which Photofrin from Axcan Pharma was the one commonly used for tumour treatment.

Photofrin mediated PDT is performed by intravenous injection with 24-48h incubation followed by light irradiation at wavelength 630nm. It showed promising results in controlling recurrence in breast cancer, brain tumours, and head and neck neoplasms (Cengel et al., 2007; Hsieh et al., 2003; Leunig et al., 1994).

However, drawbacks of Photofrin such as low singlet oxygen quantum yield at 630nm and long clearance time have limited the application of Photofrin in cancer treatment. It generated insufficient singlet oxygen at 630nm activation and required long incubation time for treatment. A 24-48 hour drug incubation time favours accumulation of Photofrin in rapid proliferating tissues such as tumour and to maximize the difference of Photofrin concentration in normal tissue and rapid proliferating tissues. Slow clearance rate is another drawback of Photofrin mediated PDT. Photofrin remains in tissue for 4-6 weeks after injection and thus patients are advised to protect themselves from exposure to sunlight or bright light for 4-8 weeks in order to avoid skin photosensitization (Allison & Sibata, 2010; Yano et al., 2011).

1.2.3.2 5-aminolevulinic acid hexyl ester derivatives and Protoporphyrin (PpIX)

5-aminolevulinic acid (5-ALA), the precurous substance of protoporphyrin, is one of the FDA approved 2nd generation photosensitizers and is popularly used for *in vivo* and *in vitro* studies over the past decades. It has been applied on cancers such as skin cancer, gastrointestinal adenocarcinoma, Bowen disease and basal cell carcinoma with promising results (Morton et al., 2001; Peng et al., 1997).

5-ALA is the precursor (also known as pro-drug) of an endogenous photosensitizer, protoporphyrin IX (PpIX), involved in the heme biosynthesis pathway (Figure 1.10). 5-ALA accumulates in mitochondrial region and is converted into PpIX through oxidation (Figure 1.11). It is further converted into iron (II) protoporphyrin (protoheme) by ferrochelatase in the presence of iron. By adding excess exogenous 5-ALA, more PpIX will be generated and accumulated in the cells as the rate of 5-ALA transformed into PpIX is greater than the rate of PpIX convert into protoheme. PpIX is temporary accumulated in cells with excessive exogenous 5-ALA, thus within tumour cells (Peng et al., 1997).

Photo-activation of PpIX via a specific wavelength could eradicate tumour cells. The wavelength applied depends on the absorption wavelength of photosensitizer. Short wavelength will have a poor penetration rather than long wavelength. However, long wavelength light activation may cause photo-damage to the surface cells. Thus the optimum wavelength applied is always between 620-650nm (Kennedy et al., 1996; Peng et al., 1997). There are several factors affecting the PpIX accumulation in tumour cells, such as the uptake of 5-ALA, concentration of iron and activity of the enzyme ferrochelatase (Brunner et al., 2003).

The major side effect of 5-ALA refers to its poor penetration ability via the biological membrane. The poor biological membrane penetration of 5-ALA is due to its hydrophilic properties (Peng et al., 1997). Therefore, a more effective and

powerful derivative of 5-ALA was developed and is known as the 5-ALA hexyl ester (H-ALA).

H-ALA (Figure 1.12) is one of the 5-ALA derivatives with increased in lipophilic properties by adding a long lipophilic chain (hexyl group) to 5-ALA. The hexyl group added to 5-ALA resulted in better penetration of H-ALA into cytoplasm. Study showed that 60 fold increase of ALA is needed to produce same amount of PpIX accumulation inside cells compared to H-ALA (Bruce-Micah et al., 2009; Casas et al., 2002; Dognitz et al., 2008; Eleouet et al., 2000; Juzeniene et al., 2002; Morrow et al., 2010)

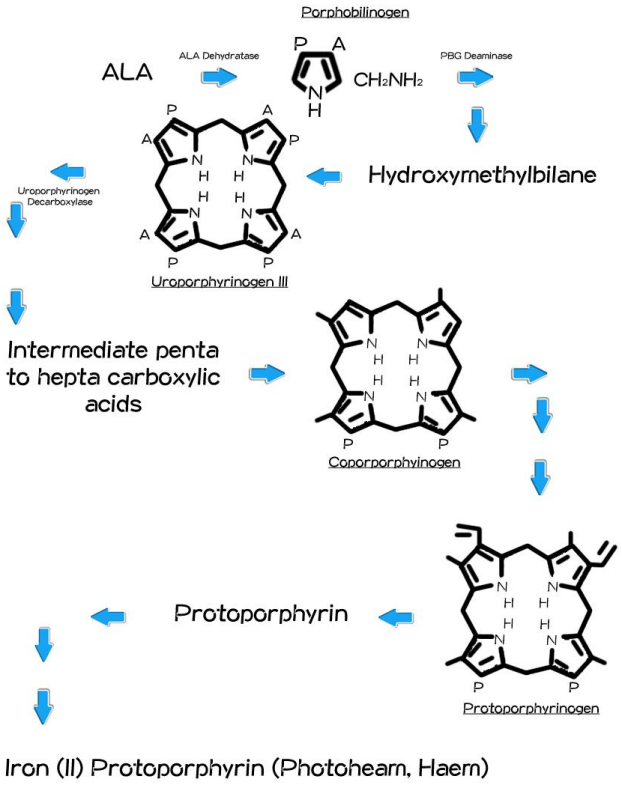

Figure 1.10 Porphyrin and haem biosynthesis in relation to porphyries.

(Modified from Schauder, Feuerstein, & Malik, 2011)

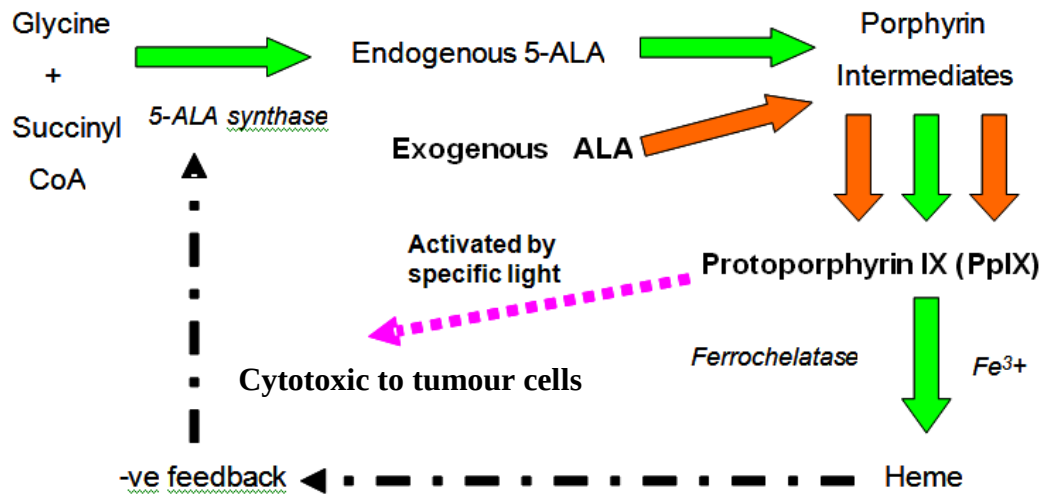

Figure 1.11 Effect of exogenous 5-ALA in the pathway of heme formation by endogenous ALA.

Increase of exogenous ALA results in higher PpIX formation and accumulation, as insufficient ferrochelatase for the conversion of PpIX to heme. Appropriate light irradiation activates the accumulated PpIX resulting in tumour cell killing.

Direction of chemical covertion; Inhibition; Activation

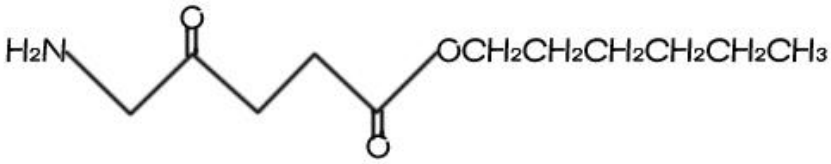

Figure 1.12 The chemical structure of H-ALA. (Adopted from Dognitz et al., 2008)

1.2.3.2.1 Foscan® and FosPeg® (Biolitec AG)-Meso tetrahydroxyphenyl chlorine (mTHPC) and its pegylated liposomes form

Meta-tetra (hydroxyphenyl) chlorine (mTHPC) is a 2nd generation photosensitizer with hyrophobic nature that has excellent photocytotoxicity. It is a clinically approved photosensitizer in USA, Europe and UK. mTHPC was highly effective in treating diseases like basal cell carcinoma, prostate and pancreatic cancer (Baas et al., 2001; Bown et al., 2002; Melnikova et al., 1999; Moore et al., 2006). The typical mTHPC mediated PDT is performed by intravenous injection and 24-96h drug incubation followed by light activation at 652nm wavelength.

The mTHPC, a chlorine-like photosensitizer that contains active ingredient temoporfin (Figure 1.13) and is derived from the reduction of porphyrins. Bonnet was the one who first synthesized temoporfin as a pure compound by reduction reaction and reported its photophysical properties and photocytotoxicity in 1989 (Bonnett et al., 1989). It has a hydrophobic nature which ensures rapid penetration across biological membrane and localization at critical intracellular membranous organelles (Pegaz et al., 2006). The absorption peak of mTHPC shifts to the longer wavelength of 652nm in the red spectrum, which is favourable for a deeper tissue penetration. It showed a 10 times higher extinction coefficient than that of Photofrin and resulted as a shorter incubation time (Bonnett, 1999). Therefore, it is a more potent photosensitizer (approxinmated 100 times greater) than Photofrin or 5-ALA (Bourre et al., 2002; Mitra et al., 2005; Yano et al., 2011; Yow et al., 2000a).

However, the major drawbacks of mTHPC are the biodistribution, clearance and selectivity of tumour uptake. These problems are related to the photochemical properties of mTHPC. The hydrophobicity leads to poor solubility of mTHPC in physiologically acceptable media, which complicated its formulation and administration. It is soluble in inorganic solvent but is insoluble in all aqueous media. Another side effect of mTHPC is the biodistribution. Hydrophobic mTHPC

forms aggregates, which decreases in photoactivity and binds strongly to serum proteins. mTHPC will also accumulate in subcutaneous fat tissues near intravenous administration and prolongs the clearance rate for 4-6 weeks after injection. All these problems of mTHPC urge the development of new drug delivery system – liposomal formulation of mTHPC (Bovis et al., 2012; Senge, 2012).

The aim of using liposomes as carriers and delivery systems is to improve its therapeutic effects by solubilizing the photosensitizer in suitable concentration, increasing drug uptake as well as eradicating tumour (Buchholz et al., 2005; Hallewin et al., 2008; Lassalle et al., 2009; Maeda et al., 2000). The formation of mTHPC contained in pegylated liposomes is known as FosPeg® (Biolitec AG). The lipocompatible polymer Polyethylene glycol (PEG) was chemically linked to the outer surface of the liposome. They function as i) stabilizer to stabilise the liposome, ii) increased their hydrophilicity to minimise the binding of liposomes to opsonins (minimize the loss of liposome from circulation), iii) inhibit the release of hydrophobic PSs to the liposomal membrane system via binding with the serum proteins, and iv) avoid recognition by the host's immune system (Bovis et al., 2012; Santos et al., 2007; Klibanov et al., 1990; Satomi et al., 2007). Modification of liposomes with long-circulating polyethylene glycol (PEG) could improve the bio-availability of m-THPC and the therapeutic index of encapsulated drugs (Bovis et al., 2012; Buchholz et al., 2005; Hallewin et al., 2008; Lassalle et al., 2009; Pegaz et al., 2006) . Figure 1.14 illustrates the different components of liposomes (Navarro et al., 2013).

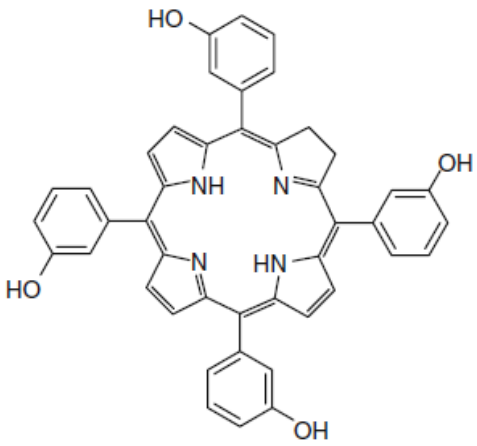

Figure 1.13 Structural formula of mTHPC (meta-tetra(hydroxyphenyl)chlorine, temoporfin).

(Adopt from Hofman et al., 2008)

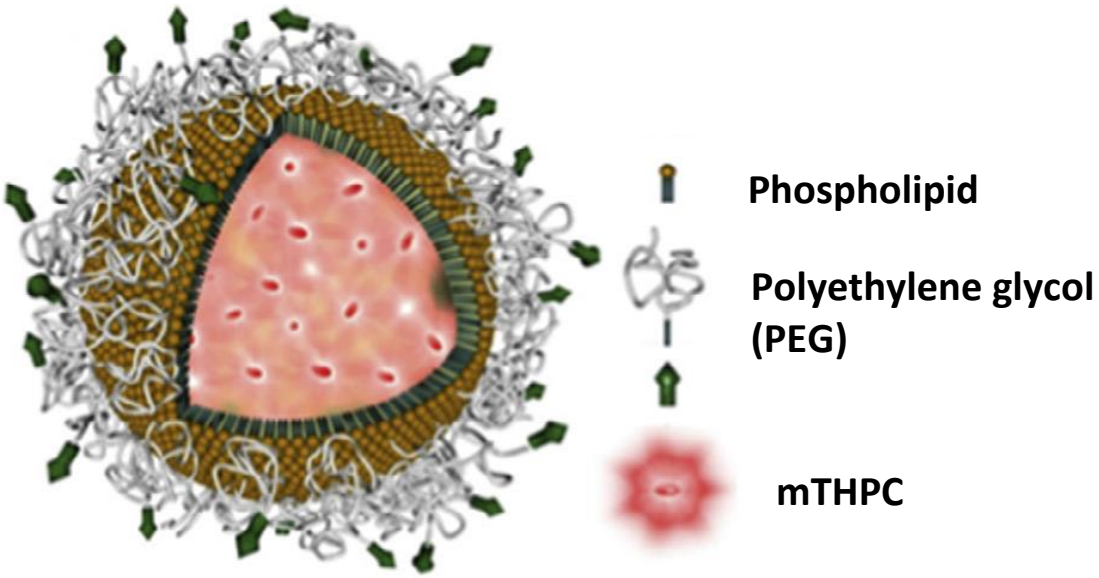

Figure 1.14 The different components of liposomes.

(Adopted from Navarro et al., 2013).

1.2.4 Light sources and light dose for PDT

Development of new light source is one of the important factors to improve the efficiency of PDT. Light sources commonly used for PDT include laser, laser diodes, light-emitting diodes and filtered broad-band light. Three main criteria must be fulfilled for an ideal light source, including i) light spectrum emitted must correspond to the absorption spectrum of the photosensitizer selected, ii) the wavelength must be long enough in order to achieve deep tissue penetration, iii) sufficient photon energy should be provided to maximize the quantum yield of singlet oxygen (Ceburkov & Gollnick, 2000; Nestor et al., 2006; Salva, 2002).

The choice of light source depends on the photosensitizer and the depth of tissue need to be penetrated. In early days, conventional light sources such as halogen lamps and xenon lamps were employed for the *in vitro* and *in vivo* PDT studies. As broad-band light sources, the specific wavelength output is achieved by adapting different filters. Usage of these non-coherence conventional light sources to activate photosensitizers mainly due to the following, i) the ease of use, ii) low cost iii) and large treatment area (Triesscheijn et al., 2006). Incoherent and coherent light are commonly employed for PDT and usually show similar efficiencies (Juzeniene et al., 2004).

Advanced light sources such as laser, laser diodes and light-emitting diodes (LED) become the choice of light source. They produce coherent light with monochromatic wavelength that allows easy calculation of light dosimetry. Light generated from these light sources could be delivered through an optical fibre to the desired site of treatment in order to achieve a greater selectivity (Castano et al., 2004; MacCormack, 2006). Among these, LED based light sources become more important and raises peoples' concern recently because of the advantages such as relatively cheap, considerably small in size and relatively mobile, without cooling units, and reliable (Mitton & Ackroyd, 2008).

Studies of light dosimetry focused on the calculation of power needed for a PDT treatment. The power applied for a PDT treatment is defined as the light dose, which is expressed as the energy delivered per unit area (J/cm^2). The term light dose is used to describe the relationship between light power density and irradiation time in order to reflect the amount of light that reaches the surface of the tumour in a period of time. There are some criteria for selecting an appropriate light dose, including the penetration depth to the tissue, low light intensity and short treatment time to avoid heating (BHenderson et al., 2006; Hopkinson et al., 1999; Kimel et al., 1992).

In parallel to the light dose, drug dose is also important to formulate the overall photodynamic dose (light dose x drug dose). Factors affecting the outcome of PDT include photosensitizers (PSs) applied, intracellular concentration of PSs, localization of PSs, quantum energy obtained by the PSs and concentration of molecular oxygen that present.

1.2.5 Advantages and limitations of PDT

The broad acceptance of PDT to tumour cells with repeatable administration without cumulative toxic effect makes PDT suitable as alternative cancer treatment. PDT has several advantages over conventional cancer treatments, including no life time limited to PSs, can be repeated as often as needed, fast clearance (depends on the types of PSs), minimial side effects, minimize damage to normal tissues, and no known interaction exists between current chemo- and radiotherapy (Agostinis et al., 2011; Bredell et al., 2010).

However, some drawbacks have limited the application of PDT in clinical practices. The well known disadvantages are the prolonged photosensitivity, which could be fatal. In order to minimize this adverse effect, patients are advised to keep in dark for weeks until the PS is eliminated from the body. Other limitations include limited choices of light sources (clinical window is between 600 to 800nm), variation of therapeutic effects according to PSs selected and tumour cell types, and the

limitation in systemic treatment for widespread metastasis (Juarranz et al., 2008; Triesscheijn et al., 2006).

1.3 PDT for nasopharyngeal carcinoma

Alternative treatment is advisable to NPC as it is often inoperable because of its complex anatomical location (Brennan, 2006; Tao & Chan, 2007). The development of improved therapeutic strategies, such as PDT and immunotherapy, shed light on the development of NPC treatment (Chan et al., 2009; Lin et al., 2010; Lutzky et al., 2010; Ma et al., 2008; Smith et al., 2012; Wu et al., 2006).

Our group demonstrated promising outcomes from a number of *in vitro* studies concerning the PDT effect on NPC cells using several PSs, including hypericin, mTHPC, merocyanine 540, 5-ALA and hexyl-ALA (Bai et al., 2011; Wu et al., 2006; Yow et al., 2009; Yow et al., 2000a; Yow et al., 2000b; Yow et al., 2000c). Lai and his colleagues showed that PDT has an immuno-enhancing effect in NPC patients by increasing natural killer cells and interleukin-2 (Lai et al., 1997). Another group from Hong Kong has illustrated similar outcomes by using other PSs, including curcumin and Zn-BC-AM on NPC/CNE2 cells and NPC/HK1 cells respectively (Koon et al., 2006; Koon et al., 2009; Koon et al., 2010). Preliminary clinical studies using hematoporphyrin and temoporfin as the treatment of the local and recurrence of NPC after curative radiotherapy found encouraging results that restricted the residual or recurrent NPC locally in the nasopharynx (Nyst et al., 2012; Tong et al., 1996).

To conclude, PDT induced apoptosis in NPC via alteration of mitogen-activated protein kinase, epidermal growth factor receptor (EGFR) pathways, or Bcl-2 protein expression level (Koon et al., 2009; Koon et al., 2010; Xie et al., 2009; Yow et al., 2009). PDT modulated the inflammatory cytokine production and angiogenic factors production (Du et al., 2006; Koon et al., 2010; Yee et al., 2005). All these findings suggested that PDT should be one of the best choices over the conventional cancer therapies for NPC.

1.4 NPC Cells employed in this study

Three NPC cell lines were used in this study, including the EBV negative well differentiated NPC cells/HK-1, EBV negative poorly differentiated NPC cells/CNE2 and EBV positive undifferentiated NPC cells/C666-1 (Figure 1.15). By comparing NPC cells with different degree of differentiation, results generated from this study would be representative to NPC population.

The C666-1/NPC cell line model is one of the authentic EBV positive cell line established from undifferentiated NPC. It is originated from an undifferentiated NPC tumour biopsy from a Southern Chinese patient. Study has shown that C666-1 cells maintained EBV positively through long term cultivation (Cheung et al., 1999). The overall BART miRNA expression in C666-1 cells was similar to the average expression in biopsy samples and thus C666-1 can be used as a representative cell line for the experiment on EBV miRNA expression in NPC (clinical relevant).

Both HK-1/NPC and CNE2/NPC are EBV negative cell lines. The HK-1/NPC cell line model was a well differentiated squamous cell carcinoma from a Chinese male patient while the NPC/CNE2 cell line was a poorly differentiated squamous cell carcinoma purchased from Shanghai Biosis Biotechnology Co., Ltd. Both cell lines are chosen for comparison in the present study (Bai et al., 2011; Gullo et al., 2008; Huang et al., 1980).

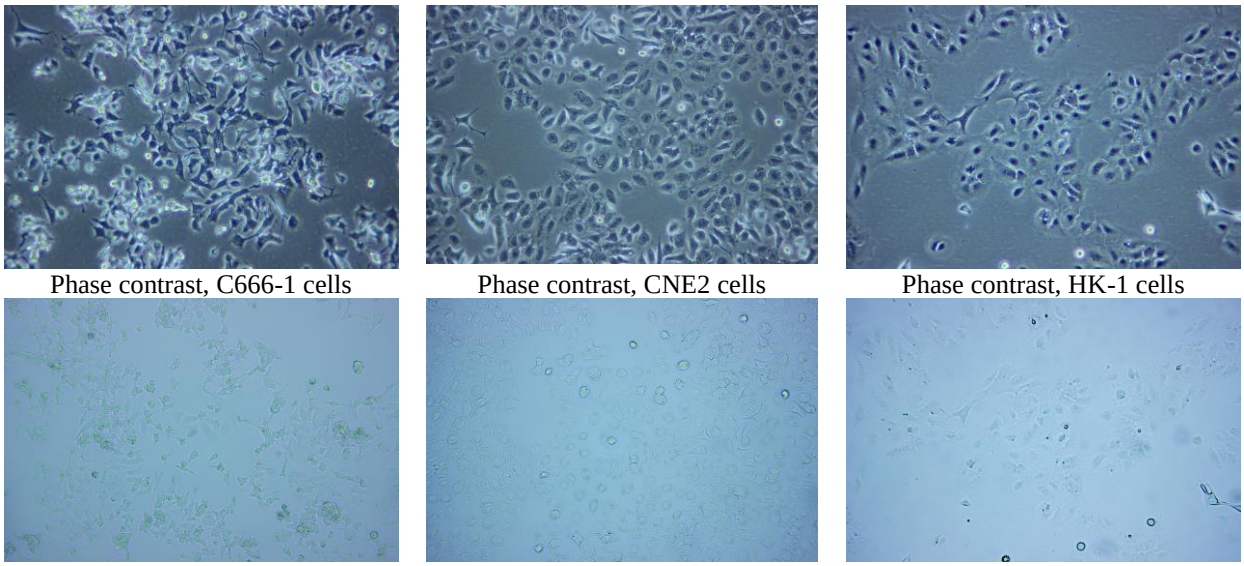

Figure 1.15 Microscopic images of C666-1 cells, CNE2 cells and HK1 cells.

1.5 Overall aims of the study

Photodynamic Therapy (PDT) involves tumour localized photosensitizer and light irradiation to destroy the tumour cells. With this inherent dual selectivity, PDT treatment outcome may have high variability due to the variation in tumour cell types, photosensitizer uptake and light dose delivered. Yet the PDT efficacy and antitumour mechanisms of two improved PSs, namely H-ALA and FosPeg® on NPC cells have not been fully investigated. To address this issue, a mechanistic study focused on H-ALA and FosPeg® mediated PDT efficacy and antitumour mechanisms was conducted.

The aim of this study was to investigate the potential of two improved 3rd generation PSs mediated PDT on three nasopharyngeal carcinoma (NPC) cells. The PDT efficacy and antitumour mechanisms for two PSs, namely H-ALA and FosPeg® on (EBV positive) undifferentiated NPC cells/C666-1, (EBV negative) poorly differentiated NPC cells/CNE2 and (EBV negative) well differentiated NPC cells/HK1 were explored.

1.5.1 Key objectives in this study were:

1. To determine the H-ALA and FosPeg® mediated PDT efficacy on three NPC cell lines by MTT assay.
2. To investigate the antitumour mechanisms of H-ALA and FosPeg® PDT on NPC cells, including uptake and localization of PSs by confocal microscopic analysis, mode of cell death and cell cycle regulation by flow cytometric analysis, and modulation of intracellular signaling proteins (MAPK and EGFR) and their downstream proteins (NF-kB, telomerase, VEGF) via western blotting analysis.
3. To examine the effects of H-ALA and FosPeg® mediated PDT on the EBV encoded LMP-1 miRNAs, mRNA and protein expression in all the three NPC cell lines by real time PCR.

4. To evaluate the modulation of P-gp/MDR1 transporter proteins triggered by FosPeg®-PDT via Western blotting and flow cytometric analysis.

1.6 References

Agostinis P, Berg K, Cengel KA, Foster TH, Girotti AW, Gollnick SO, Golab J. (2011) Photodynamic therapy of cancer: an update. *CA Cancer J Clin, 61*(4), 250-281.

Ahmad N, Kalka K, Mukhtar H. (2001) In vitro and in vivo inhibition of epidermal growth factor receptor-tyrosine kinase pathway by photodynamic therapy. *Oncogene, 20*(18), 2314-2317.

Allison RR, Sibata CH. (2010) Oncologic photodynamic therapy photosensitizers: a clinical review. *Photodiagnosis Photodyn Ther, 7*(2), 61-75.

Ambudkar SV, Lelong IH, Zhang J, Cardarelli CO, Gottesman MM, Pastan I. (1992) Partial purification and reconstitution of the human multidrug-resistance pump: characterization of the drug-stimulatable ATP hydrolysis. *Proc Natl Acad Sci U S A, 89*(18), 8472-8476.

Arteaga CL. (2002) Epidermal growth factor receptor dependence in human tumors: more than just expression? *Oncologist, 7 Suppl 4*, 31-39.

Aszalos A. (2007a) Drug-drug interactions affected by the transporter protein, P-glycoprotein (ABCB1, MDR1) I. Preclinical aspects. *Drug Discov Today, 12*(19-20), 833-837.

Aszalos A. (2007b) Drug-drug interactions affected by the transporter protein, P-glycoprotein (ABCB1, MDR1) II. Clinical aspects. *Drug Discov Today, 12*(19-20), 838-843.

Baas P, Saarnak AE, Oppelaar H, Neering H, Stewart FA. (2001) Photodynamic therapy with meta-tetrahydroxyphenylchlorin for basal cell carcinoma: a phase I/II study. *Br J Dermatol, 145*(1), 75-78.

Bai D, Xia X, Yow CMN, Chu ESM, Xu C. (2011) Hypocrellin B-encapsulated nanoparticle-mediated rev-caspase-3 gene transfection and photodynamic therapy on tumor cells. *Eur J Pharmacol, 650*(2-3), 496-500.

Barth S, Pfuhl T, Mamiani A, Ehses C, Roemer K, Kremmer E, Grasser FA. (2008) Epstein-Barr virus-encoded microRNA miR-BART2 down-regulates the viral DNA polymerase BALF5. *Nucleic Acids Res, 36*(2), 666-675.

Bonnett R, White RD, Winfield UJ, Berenbaum MC. (1989) Hydroporphyrins of the meso-tetra(hydroxyphenyl)porphyrin series as tumour photosensitizers. *Biochem J, 261*(1), 277-280.

Bourre L, Rousset N, Thibaut S, Eleouet S, Lajat Y, Patrice T. (2002) PDT effects of m-THPC and ALA, phototoxicity and apoptosis. *Apoptosis, 7*(3), 221-230.

Bovis MJ, Woodhams JH, Loizidou M, Scheglmann D, Bown SG, Macrobert AJ. (2012) Improved in vivo delivery of m-THPC via pegylated liposomes for use in photodynamic therapy. *J Control Release, 157*(2), 196-205.

Bown SG, Rogowska AZ, Whitelaw DE, Lees WR, Lovat LB, Ripley P, Hatfield AW. (2002) Photodynamic therapy for cancer of the pancreas. *Gut, 50*(4), 549-557.

Bredell MG, Besic E, Maake C, Walt H. (2010) The application and challenges of clinical PD-PDT in the head and neck region: a short review. *J Photochem Photobiol B, 101*(3), 185-190.

Brennan B. (2006). Nasopharyngeal carcinoma. *Orphanet J Rare Dis, 1*, 23.

Brown SB, Brown EA, Walker I. (2004) The present and future role of photodynamic therapy in cancer treatment. *Lancet Oncol, 5*(8), 497-508.

Bruce-Micah R, Huttenberger D, Freitag L, Cullum J, Foth HJ. (2009) Pharmacokinetic of ALA and h-ALA induced porphyrins in the models Mycobacterium phlei and Mycobacterium smegmatis. *J Photochem Photobiol B, 97*(1), 1-7.

Brunner H, Hausmann F, Knuechel R. (2003) New 5-aminolevulinic acid esters--efficient protoporphyrin precursors for photodetection and photodynamic therapy. *Photochem Photobiol, 78*(5), 481-486.

Buchholz J, Kaser-Hotz B, Khan T, Rohrer Bley C, Melzer K, Schwendener RA, Walt H. (2005) Optimizing photodynamic therapy: in vivo pharmacokinetics of liposomal meta-(tetrahydroxyphenyl)chlorin in feline squamous cell carcinoma. *Clin Cancer Res, 11*(20), 7538-7544.

Buettner M, Heussinger N, Niedobitek G. (2006) Expression of Epstein-Barr virus (EBV)-encoded latent membrane proteins and STAT3 activation in nasopharyngeal carcinoma. *Virchows Arch, 449*(5), 513-519.

Buytaert E, Dewaele M, Agostinis P. (2007) Molecular effectors of multiple cell death pathways initiated by photodynamic therapy. *Biochim Biophys Acta, 1776*(1), 86-107.

Calzavara-Pinton PG, Venturini M, Sala R. (2007) Photodynamic therapy: update 2006. Part 1: Photochemistry and photobiology. *J Eur Acad Dermatol Venereol, 21*(3), 293-302.

Capella MA, Capella LS. (2003) A light in multidrug resistance: photodynamic treatment of multidrug-resistant tumors. *J Biomed Sci, 10*(4), 361-366.

Casas A, Perotti C, Saccoliti M, Sacca P, Fukuda H, Batlle AC. (2002) ALA and ALA hexyl ester in free and liposomal formulations for the photosensitisation of tumor organ cultures. *Br J Cancer, 86*, 837-842.

Castano AP, Demidova TN, Hamblin MR. (2004) Mechanisms in photodynamic therapy: part one—photosensitizers, photochemistry and cellular localization. *Photodiagnosis Photodyn Ther, 1*(4), 279-293.

Castano AP, Demidova TN, Hamblin MR. (2005) Mechanisms in photodynamic therapy: part two—cellular signaling, cell metabolism and modes of cell death. *Photodiagnosis Photodyn Ther, 2*(1), 1-23.

Cawston TE. (1996) Metalloproteinase inhibitors and the prevention of connective tissue breakdown. *Pharmacol Ther, 70*(3), 163-182.

Ceburkov O, Gollnick H. (2000) Photodynamic therapy in dermatology. *Eur J Dermatol, 10*(7), 568-575.

Cengel KA, Glatstein E, Hahn SM. (2007) Intraperitoneal photodynamic therapy. *Cancer Treat Res, 134*, 493-514.

Chan AT. (2010) Nasopharyngeal carcinoma. *Ann Oncol, 21 Suppl 7*, 308-312.

Chan PS, Koon HK, Wu ZG, Wong RN, Lung ML, Chang CK, Mak NK. (2009) Role of p38 MAPKs in hypericin photodynamic therapy-induced apoptosis of nasopharyngeal carcinoma cells. *Photochem Photobiol, 85*(5), 1207-1217.

Chang C, Werb Z. (2001) The many faces of metalloproteases: cell growth, invasion, angiogenesis and metastasis. *Trends Cell Biol, 11*(11), 37-43.

Chen CL, Sheen TS, Lou IU, Huang AC. (2001) Expression of multidrug resistance 1 and glutathione-S-transferase-Pi protein in nasopharyngeal carcinoma. *Hum Pathol, 32*(11), 1240-1244.

Chen DL, Huang TB. (1997) A case-control study of risk factors of nasopharyngeal carcinoma. *Cancer Lett, 117*(1), 17-22.

Chen J, Dassarath M, Yin Z, Liu H, Yang K, Wu G. (2011) Radiation induced temporal lobe necrosis in patients with nasopharyngeal carcinoma: a review of new avenues in its management. *Radiat Oncol, 6*, 128.

Chen J, Liu TW, Lo PC, Wilson BC, Zheng G. (2009) "Zipper" molecular beacons: a generalized strategy to optimize the performance of activatable protease probes. *Bioconjug Chem, 20*(10), 1836-1842.

Chen J, Lovell JF, Lo PC, Stefflova K, Niedre M, Wilson BC, Zheng, G. (2008) A tumor mRNA-triggered photodynamic molecular beacon based on oligonucleotide hairpin control of singlet oxygen production. *Photochem Photobiol Sci, 7*(7), 775-781.

Chen L, Gallicchio L, Boyd-Lindsley K, Tao XG, Robinson KA, Lam TK, Alberg AJ. (2009) Alcohol consumption and the risk of nasopharyngeal carcinoma: a systematic review. *Nutr Cancer, 61*(1), 1-15.

Chen R, Huang Z, Chen G, Li Y, Chen X, Chen J, Zeng H. (2008) Kinetics and subcellular localization of 5-ALA-induced PpIX in DHL cells via two-photon excitation fluorescence microscopy. *Int J Oncol, 32*(4), 861-867.

Chen SJ, Chen GH, Chen YH, Liu CY, Chang KP, Chang YS, Chen HC. (2010) Characterization of Epstein-Barr virus miRNAome in nasopharyngeal carcinoma by deep sequencing. *PLoS One, 5*(9).

Chen YR, Wang X, Templeton D, Davis RJ, Tan TH. (1996) The role of c-Jun N-terminal kinase (JNK) in apoptosis induced by ultraviolet C and gamma radiation. Duration of JNK activation may determine cell death and proliferation. *J Biol Chem, 271*(50), 31929-31936.

Cheung ST, Huang DP, Hui AB, Lo KW, Ko CW, Tsang YS, Lee JC. (1999) Nasopharyngeal carcinoma cell line (C666-1) consistently harbouring Epstein-Barr virus. *Int J Cancer, 83*(1), 121-126.

Chew MM, Gan SY, Khoo AS, Tan EL. (2010) Interleukins, laminin and Epstein - Barr virus latent membrane protein 1 (EBV LMP1) promote metastatic phenotype in nasopharyngeal carcinoma. *BMC Cancer, 10*, 574.

Cho WC. (2007) Nasopharyngeal carcinoma: molecular biomarker discovery and progress. *Mol Cancer, 6*, 1.

Chou J, Lin YC, Kim J, You L, Xu Z, He B, Jablons DM. (2008) Nasopharyngeal carcinoma--review of the molecular mechanisms of tumorigenesis. *Head Neck, 30*(7), 946-963.

Choy EY, Siu KL, Kok KH, Lung RW, Tsang CM, To KF, Jin DY. (2008) An Epstein-Barr virus-encoded microRNA targets PUMA to promote host cell survival. *J Exp Med, 205*(11), 2551-2560.

Chu ESM, Yow CMN, Shi M, Ho RJ. (2008) Effects of photoactivated 5-aminolevulinic acid hexyl ester on MDR1 over-expressing human uterine sarcoma cells. *Toxicol Lett, 181*(1), 7-12.

Cogswell P, Guttridge D, Funkhouser W, Baldwin AJ. (2000) Selective activation of NF-κB subunits in human breast cancer: potential roles for NF-κB2/p52 and for Bcl-3. *Oncogene, 19*, 9.

Cosmopoulos K, Pegtel M, Hawkins J, Moffett H, Novina C, Middeldorp J, Thorley-Lawson DA. (2009) Comprehensive profiling of Epstein-Barr virus microRNAs in nasopharyngeal carcinoma. *J Virol, 83*(5), 2357-2367.

D'Hallewin MA, Kochetkov D, Viry-Babel Y, Leroux A, Werkmeister E, Dumas D, Bezdetnaya L. (2008) Photodynamic therapy with intratumoral administration of Lipid-Based mTHPC in a model of breast cancer recurrence. *Lasers Surg Med, 40*(8), 543-549.

Dawson CW, Laverick L, Morris MA, Tramoutanis G, Young LS. (2008) Epstein-Barr virus-encoded LMP1 regulates epithelial cell motility and invasion via the ERK-MAPK pathway. *J Virol, 82*(7), 3654-3664.

Dawson CW, Port RJ, Young LS. (2012) The role of the EBV-encoded latent membrane proteins LMP1 and LMP2 in the pathogenesis of nasopharyngeal carcinoma (NPC). *Semin Cancer Biol., 22*(2), 144-153.

Deng L, Yang J, Zhao XR, Deng XY, Zeng L, Gu HH, Cao Y. (2003) Cells in G2/M phase increased in human nasopharyngeal carcinoma cell line by EBV-LMP1 through activation of NF-kappaB and AP-1. *Cell Res, 13*(3), 187-194.

Dognitz N, Salomon D, Zellweger M, Ballini JP, Gabrecht T, Lange N, Wagnieres G. (2008) Comparison of ALA- and ALA hexyl-ester-induced PpIX depth distribution in human skin carcinoma. *J Photochem Photobiol B, 93*(3), 140-148.

Dolmans DE, Fukumura D, Jain RK. (2003) Photodynamic therapy for cancer. *Nat Rev Cancer, 3*(5), 380-387.

Dos Santos N, Allen C, Doppen AM, Anantha M, Cox KA, Gallagher RC, Bally MB. (2007) Influence of poly(ethylene glycol) grafting density and polymer length on liposomes: relating plasma circulation lifetimes to protein binding. *Biochim Biophys Acta, 1768*(6), 1367-1377.

Dougherty TJ. (1983) Hematoporphyrin as a photosensitizer of tumors. *Photochem Photobiol, 38*(3), 377-379.

Dougherty TJ. (1986) Photosensitization of malignant tumors. *Semin Surg Oncol, 2*(1), 24-37.

Dougherty TJ. (1987) Studies on the structure of porphyrins contained in Photofrin II. *Photochem Photobiol, 46*(5), 569-573.

Dougherty TJ, Gomer CJ, Henderson BW, Jori G, Kessel D, Korbelik M, Peng Q. (1998) Photodynamic therapy. *J Natl Cancer Inst, 90*(12), 889-905.

Downward J. (2003) Targeting RAS signalling pathways in cancer therapy. *Nat Rev Cancer, 3*(1), 11-22.

Du H, Bay BH, Mahendran R, Olivo M. (2006) Hypericin-mediated photodynamic therapy elicits differential interleukin-6 response in nasopharyngeal cancer. *Cancer Lett, 235*(2), 202-208.

Edinger AL, Thompson CB. (2004) Death by design: apoptosis, necrosis and autophagy. *Curr Opin Cell Biol, 16*(6), 663-669.

Ekburanawat W, Ekpanyaskul C, Brennan P, Kanka C, Tepsuwan K, Temiyastith S, Sangrajrang S. (2010) Evaluation of non-viral risk factors for nasopharyngeal carcinoma in Thailand: results from a case-control study. *Asian Pac J Cancer Prev, 11*(4), 929-932.

Eleouet S, Rousset N, Carre J, Bourre L, Vonarx V, Lajat Y, Patrice T. (2000) In vitro fluorescence, toxicity and phototoxicity induced by delta-aminolevulinic acid (ALA) or ALA-esters. *Photochem Photobiol, 71*(4), 447-454.

Eliopoulos AG, Young LS. (1998) Activation of the cJun N-terminal kinase (JNK) pathway by the Epstein-Barr virus-encoded latent membrane protein 1 (LMP1). *Oncogene, 16*(13), 1731-1742.

Eliopoulos AG, Young LS. (2001) LMP1 structure and signal transduction. *Semin Cancer Biol, 11*(6), 435-444.

Farber S, Diamond LK. (1948) Temporary remissions in acute leukemia in children produced by folic acid antagonist, 4-aminopteroyl-glutamic acid. *N Engl J Med, 238*(23), 787-793.

Farrell PJ, Cludts I, Stuhler A. (1997) Epstein-Barr virus genes and cancer cells. *Biomed Pharmacother, 51*(6-7), 258-267.

Friborg J, Wohlfahrt J, Koch A, Storm H, Olsen OR, Melbye M. (2005) Cancer susceptibility in nasopharyngeal carcinoma families--a population-based cohort study. *Cancer Res, 65*(18), 8567-8572.

Garland MJ, Cassidy CM, Woolfson D, Donnelly RF. (2009) Designing photosensitizers for photodynamic therapy: strategies, challenges and promising developments. *Future Med Chem, 1*(4), 667-691.

Gilmore TD. (2006) Introduction to NF-kappaB: players, pathways, perspectives. *Oncogene, 25*(51), 6680-6684.

Goormachtigh G, Ouk TS, Mougel A, Tranchand-Bunel D, Masy E, Le Clorennec C, Coll J. (2006) Autoactivation of the Epstein-Barr virus oncogenic protein LMP1 during type II latency through opposite roles of the NF-kappaB and JNK signaling pathways. *J Virol, 80*(15), 7382-7393.

Guelluy PH, Fontaine-Aupart MP, Grammenos A, Lecart S, Piette J, Hoebeke M. (2010) Optimizing photodynamic therapy by liposomal formulation of the photosensitizer pyropheophorbide-a methyl ester: in vitro and ex vivo comparative biophysical investigations in a colon carcinoma cell line. *Photochem Photobiol Sci, 9*(9), 1252-1260.

Gullo C, Low WK, Teoh G. (2008) Association of Epstein-Barr Virus with Nasopharyngeal Carcinoma and Current Status of Development of Cancer-derived Cell Lines. *Ann Acad Med Singapore, 37*, 9.

Guo X, Wang W, Zhou F, Lu Z, Fang R, Jia F, Wei L. (2008) siRNA-mediated inhibition of hTERT enhances chemosensitivity of hepatocellular carcinoma. *Cancer Biol Ther, 7*(10), 1555-1560.

He JR, Tang LY, Yu, D. D., Su, F. X., Song, E. W., Lin, Y., Ren, Z. F. (2011). Epstein-Barr virus and breast cancer: serological study in a high-incidence area of nasopharyngeal carcinoma. *Cancer Lett, 309*(2), 128-136. doi: 10.1016/j.canlet.2011.05.012

He ML, Luo MX, Lin MC, Kung HF. (2012) MicroRNAs: potential diagnostic markers and therapeutic targets for EBV-associated nasopharyngeal carcinoma. *Biochim Biophys Acta, 1825*(1), 1-10.

Henderson BE, Louie E, SooHoo Jing J, Buell P, Gardner MB. (1976) Risk factors associated with nasopharyngeal carcinoma. *N Engl J Med, 295*(20), 1101-1106.

Henderson BW, Busch TM, Snyder JW. (2006) Fluence rate as a modulator of PDT mechanisms. *Lasers Surg Med, 38*(5), 489-493.

Henderson S, Rowe M, Gregory C, Croom-Carter D, Wang F, Longnecker R, Rickinson A. (1991) Induction of bcl-2 expression by Epstein-Barr virus latent membrane protein 1 protects infected B cells from programmed cell death. *Cell, 65*(7), 1107-1115.

Hendrickx N, Volanti C, Moens U, Seternes OM, de Witte P, Vandenheede JR, Agostinis P. (2003) Up-regulation of cyclooxygenase-2 and apoptosis resistance by p38 MAPK in hypericin-mediated photodynamic therapy of human cancer cells. *J Biol Chem, 278*(52), 52231-52239.

Herrmann K, Niedobitek G. (2003) Epstein-Barr virus-associated carcinomas: facts and fiction. *J Pathol., 199*(2), 140-145.

Hilf R. (2007) Mitochondria are targets of photodynamic therapy. *J Bioenerg Biomembr, 39*(1), 85-89.

Ho JH. (1972) Nasopharyngeal carcinoma (NPC). *Adv Cancer Res, 15*, 57-92.

Ho JH, Huang DP, Fong YY. (1978) Salted fish and nasopharyngeal carcinoma in southern Chinese. *Lancet, 2*(8090), 626.

Hofman JW, Carstens MG, van Zeeland F, Helwig C, Flesch FM, Hennink WE, van Nostrum CF. (2008) Photocytotoxicity of mTHPC (temoporfin) loaded polymeric micelles mediated by lipase catalyzed degradation. *Pharm Res, 25*(9), 2065-2073.

Hopkinson HJ, Vernon DI, Brown SB. (1999) Identification and partial characterization of an unusual distribution of the photosensitizer meta-tetrahydroxyphenyl chlorin (temoporfin) in human plasma. *Photochem Photobiol, 69*(4), 482-488.

Hopper C. (2000) Photodynamic therapy: a clinical reality in the treatment of cancer. *Lancet Oncol, 1*, 212-219.

Horikawa T, Yoshizaki T, Sheen TS, Lee SY, Furukawa M. (2000) Association of latent membrane protein 1 and matrix metalloproteinase 9 with metastasis in nasopharyngeal carcinoma. *Cancer, 89*(4), 715-723.

Hospital Authority: Hong Kong Cancer Registry. (2011) from http://www3.ha.org.hk/cancereg/Statistics.html

Hsieh YJ, Wu CC, Chang CJ, Yu JS. (2003) Subcellular localization of Photofrin determines the death phenotype of human epidermoid carcinoma A431 cells triggered by photodynamic therapy: when plasma membranes are the main targets. *J Cell Physiol, 194*(3), 363-375.

Huang DP, Ho JH, Poon YF, Chew EC, Saw D, Lui M, Lau WH. (1980) Establishment of a cell line (NPC/HK1) from a differentiated squamous carcinoma of the nasopharynx. *Int J Cancer, 26*(2), 127-132.

Huang Z, Xu H, Meyers AD, Musani AI, Wang L, Tagg R, Chen YK. (2008) Photodynamic therapy for treatment of solid tumors--potential and technical challenges. *Technol Cancer Res Treat, 7*(4), 309-320.

Iizasa H, Wulff BE, Alla NR, Maragkakis M, Megraw M, Hatzigeorgiou A, Nishikura K. (2010) Editing of Epstein-Barr virus-encoded BART6 microRNAs controls their dicer targeting and consequently affects viral latency. *J Biol Chem, 285*(43), 33358-33370.

Ji XN, Yang F, Sui XM, Wang FG, Ge RG, Quan XL, Zhao T, Gao BW, Wang RY. (2013) Effect of fractionated irradiation on the expression of multidrug resistance genes in the CNE1 human nasopharyngeal carcinoma cell line. *Mol Med Rep*, 7(1), 187-194.

Jia WH, Huang QH, Liao J, Ye W, Shugart YY, Liu Q, Zeng YX. (2006) Trends in incidence and mortality of nasopharyngeal carcinoma over a 20-25 year period (1978/1983-2002) in Sihui and Cangwu counties in southern China. *BMC Cancer, 6*, 178.

Jia WH, Luo XY, Feng BJ, Ruan HL, Bei JX, Liu WS, Zeng YX. (2010) Traditional Cantonese diet and nasopharyngeal carcinoma risk: a large-scale case-control study in Guangdong, China. *BMC Cancer, 10*, 446.

Jia WH, Qin HD. (2012) Non-viral environmental risk factors for nasopharyngeal carcinoma: a systematic review. *Semin Cancer Biol, 22*(2), 117-126.

Johnson GL, Lapadat R. (2002) Mitogen-activated protein kinase pathways mediated by ERK, JNK, and p38 protein kinases. *Science, 298*(5600), 1911-1912.

Juarranz, A., Jaen, P., Rodriguez, F. S., Cuevas, J., & Gonzailez, S. (2008). Photodynamic therapy of cancer: Basic principles and applications. *Clin Trans Oncol, 10*, 7.

Juarranz A, Jaen P, Sanz-Rodriguez F, Cuevas J, Gonzalez S. (2008) Photodynamic therapy of cancer. Basic principles and applications. *Clin Transl Oncol, 10*(3), 148-154.

Juliano RL, Ling V. (1976) A surface glycoprotein modulating drug permeability in Chinese hamster ovary cell mutants. *Biochim Biophys Acta, 455*(1), 152-162.

Juzeniene A, Juzenas P, Ma LW, Iani V, Moan J. (2004) Effectiveness of different light sources for 5-aminolevulinic acid photodynamic therapy. *Lasers Med Sci, 19*(3), 139-149.

Juzeniene A, Ma LW, Juzenas P, Iani V, Lange N, Moan J. (2002) Production of protoporphyrin IX from 5-aminolevulinic acid and two of its esters in cells in vitro and tissues in vivo. *Cell Mol Biol (Noisy-le-grand), 48*(8), 911-916.

Juzeniene A, Moan J. (2007) The history of PDT in Norway Part one: Identification of basic mechanisms of general PDT. *PPT, 4*, 9.

Kawanishi M. (1997) Expression of Epstein-Barr virus latent membrane protein 1 protects Jurkat T cells from apoptosis induced by serum deprivation. *Virology, 228*(2), 244-250.

Kennedy JC, Marcus SL, Pottier RH. (1996) Photodynamic therapy (PDT) and photodiagnosis (PD) using endogenous photosensitization induced by 5-aminolevulinic acid (ALA): mechanisms and clinical results. *J Clin Laser Med Surg, 14*(5), 289-304.

Kessel D. (2006) Death pathways associated with photodynamic therapy. *Med Laser Appl, 21*(4), 219-224.

Kim NW, Piatyszek MA, Prowse KR, Harley CB, West MD, Ho PL, Shay JW. (1994) Specific association of human telomerase activity with immortal cells and cancer. *Science, 266*(5193), 2011-2015.

Kimel S, Svaasand LO, Hammer-Wilson M, Gottfried V, Cheng S, Svaasand E, Berns MW. (1992) Demonstration of synergistic effects of hyperthermia and photodynamic therapy using the chick chorioallantoic membrane model. *Lasers Surg Med, 12*(4), 432-440.

Kirkpatrick KL, Mokbel K. (2001) The significance of human telomerase reverse transcriptase (hTERT) in cancer. *Eur J Surg Oncol, 27*(8), 754-760.

Klibanov AL, Maruyama K, Torchilin VP, Huang L. (1990) Amphipathic polyethyleneglycols effectively prolong the circulation time of liposomes. *FEBS Lett, 268*(1), 235-237.

Kolarova H, Nevrelova P, Tomankova K, Kolar P, Bajgar R, Mosinger J. (2008) Production of reactive oxygen species after photodynamic therapy by porphyrin sensitizers. *Gen Physiol Biophys, 27*(2), 101-105.

Kondo S, Wakisaka N, Schell MJ, Horikawa T, Sheen TS, Sato H, Yoshizaki T. (2005) Epstein-Barr virus latent membrane protein 1 induces the matrix metalloproteinase-1 promoter via an Ets binding site formed by a single nucleotide polymorphism: enhanced susceptibility to nasopharyngeal carcinoma. *Int J Cancer, 115*(3), 368-376.

Koon H, Leung AW, Yue KK, Mak NK. (2006) Photodynamic effect of curcumin on NPC/CNE2 cells. *J Environ Pathol Toxicol Oncol, 25*(1-2), 205-215.

Koon HK, Chan PS, Wong RN, Wu ZG, Lung ML, Chang CK, Mak NK. (2009) Targeted inhibition of the EGFR pathways enhances Zn-BC-AM PDT-induced apoptosis in well-differentiated nasopharyngeal carcinoma cells. *J Cell Biochem, 108*(6), 1356-1363.

Koon HK, Chan PS, Wu ZG, Wong RN, Lung ML, Chang CK, Mak NK. (2010a) Role of mitogen-activated protein kinase in Zn-BC-AM PDT-induced apoptosis in nasopharyngeal carcinoma cells. *Cell Biochem Funct, 28*(3), 239-248.

Koon HK, Lo KW, Leung KN, Lung ML, Chang CC, Wong RN, Mak NK. (2010b) Photodynamic therapy-mediated modulation of inflammatory cytokine production by Epstein-Barr virus-infected nasopharyngeal carcinoma cells. *Cellular & Molecular Immunology, 7*(4), 323-326.

Korbelik M. (2006) PDT-associated host response and its role in the therapy outcome. *Lasers Surg Med, 38*(5), 500-508.

Kung CP, Meckes DG Jr, Raab-Traub N. (2011) Epstein-Barr virus LMP1 activates EGFR, STAT3, and ERK through effects on PKCdelta. *J Virol, 85*(9), 4399-4408.

Kung CP, Raab-Traub N. (2008) Epstein-Barr virus latent membrane protein 1 induces expression of the epidermal growth factor receptor through effects on Bcl-3 and STAT3. *J Virol, 82*(11), 5486-5493.

Kuntsche J, Freisleben I, Steiniger F, Fahr A. (2010) Temoporfin-loaded liposomes: physicochemical characterization. *Eur J Pharm Sci, 40*(4), 305-315.

Lai JP, Tao ZD, Xiao JY, Zhao SP, Tian YQ. (1997) Effect of photodynamic therapy on selected laboratory values of patients with nasopharyngeal carcinoma. *Ann Otol Rhinol Laryngol, 106*(8), 680-682.

Larbcharoensub N, Leopairat J, Sirachainan E, Narkwong L, Bhongmakapat T, Rasmeepaisarn K, Janvilisri T. (2008) Association between multidrug resistance-associated protein 1 and poor prognosis in patients with nasopharyngeal carcinoma treated with radiotherapy and concurrent chemotherapy. *Hum Pathol, 39*(6), 837-845.

Lassalle HP, Dumas D, Grafe S, D'Hallewin MA, Guillemin F, Bezdetnayaz L. (2009) Correlation between in vivo pharmacokinetics, intratumoral distribution and photodynamic efficiency of liposomal mTHPC. *J Control Release, 134*(2), 118-124.

Lee AW, Foo W, Law SC, Poon YF, Sze WM, O SK, Lau WH. (1997) Nasopharyngeal carcinoma: presenting symptoms and duration before diagnosis. *Hong Kong Med J, 3*(4), 355-361.

Lee DC, Chua DT, Wei WI, Sham JS, Lau AS. (2007) Induction of matrix metalloproteinases by Epstein-Barr virus latent membrane protein 1 isolated from nasopharyngeal carcinoma. *Biomed Pharmacother, 61*(9), 520-526.

Leslie EM, Deeley RG, Cole SP. (2005) Multidrug resistance proteins: role of P-glycoprotein, MRP1, MRP2, and BCRP (ABCG2) in tissue defense. *Toxicol Appl Pharmacol, 204*(3), 216-237.

Leunig A, Staub F, Peters K, Heimann A, Csapo C, Kempski P, Goetz AE. (1994) Relation of early photofrin uptake to photodynamically induced phototoxicity and changes of cell volume in different cell lines. *European Journal of Cancer, 30A*(1), 6.

Li HL, Chen DD, Li XH, Zhang HW, Lu YQ, Ye CL, Ren XD. (2002) Changes of NF-kB, p53, Bcl-2 and caspase in apoptosis induced by JTE-522 in human gastric adenocarcinoma cell line AGS cells: role of reactive oxygen species. *World J Gastroenterol, 8*(3), 431-435.

Li XP, Li CY, Li X, Ding Y, Chan LL, Yang PH, Peng Y. (2006) Inhibition of human nasopharyngeal carcinoma growth and metastasis in mice by adenovirus-associated virus-mediated expression of human endostatin. *Mol Cancer Ther, 5*(5), 1290-1298.

Lim SH, Lee HB, Ho AS. (2011) A new naturally derived photosensitizer and its phototoxicity on head and neck cancer cells. *Photochem Photobiol, 87*(5), 1152-1158.

Lin ML, Lu YC, Chung JG, Wang SG, Lin HT, Kang SE, Chen SS. (2010) Down-regulation of MMP-2 through the p38 MAPK-NF-kappaB-dependent pathway by aloe-emodin leads to inhibition of nasopharyngeal carcinoma cell invasion. *Mol Carcinog, 49*(9), 783-797.

Lo AK, Dawson CW, Jin DY, Lo KW. (2012) The pathological roles of BART miRNAs in nasopharyngeal carcinoma. *J Pathol, 227*(4), 392-403.

Lo AK, Lo KW, Tsao SW, Wong HL, Hui JW, To KF, Huang DP. (2006) Epstein-Barr virus infection alters cellular signal cascades in human nasopharyngeal epithelial cells. *Neoplasia, 8*(3), 173-180.

Lo AK, To KF, Lo KW, Lung RW, Hui JW, Liao G, Hayward SD. (2007) Modulation of LMP1 protein expression by EBV-encoded microRNAs. *Proc Natl Acad Sci U S A., 104*(41), 16164-16169.

Lu J, Chua HH, Chen SY, Chen JY, Tsai CH. (2003) Regulation of matrix metalloproteinase-1 by Epstein-Barr virus proteins. *Cancer Res, 63*(1), 256-262.

Luksiene Z. (2003) Photodynamic therapy: mechanism of action and ways to improve the efficiency of treatment. *Medicina (Kaunas), 39*(12), 1137-1150.

Luo J, Xiao J, Tao Z, Li X. (1997) Detection of c-myc gene expression in nasopharyngeal carcinoma by nonradioactive in situ hybridization and immunohistochemistry. *Chin Med J (Engl), 110*(3), 229-232.

Lutzky VP, Corban M, Heslop L, Morrison LE, Crooks P, Hall DF, Moss DJ. (2010) Novel approach to the formulation of an Epstein-Barr virus antigen-based nasopharyngeal carcinoma vaccine. *J Virol, 84*(1), 407-417.

Lynch CC, Matrisian LM. (2002) Matrix metalloproteinases in tumor-host cell communication. *Differentiation, 70*(9-10), 561-573.

Ma BB, Hui EP, Chan AT. (2008) Systemic approach to improving treatment outcome in nasopharyngeal carcinoma: current and future directions. *Cancer Sci, 99*(7), 1311-1318.

MacCormack M. (2006) Photodynamic therapy. *Adv Dermatol, 22*, 40.

Maeda H, Wu J, Sawa T, Matsumura Y, Hori K. (2000) Tumor vascular permeability and the EPR effect in macromolecular therapeutics: a review. *J Control Release, 65*(1-2), 271-284.

Marquitz AR, Raab-Traub N. (2012) The role of miRNAs and EBV BARTs in NPC. *Semin Cancer Biol., 22*(2), 166-172.

Marron M, Boffetta P, Zhang ZF, Zaridze D, Wunsch-Filho V, Winn DM, Hashibe M. (2010) Cessation of alcohol drinking, tobacco smoking and the reversal of head and neck cancer risk. *Int J Epidemiol, 39*(1), 182-196.

Martinez-Carpio PA, Trelles MA. (2010) The role of epidermal growth factor receptor in photodynamic therapy: a review of the literature and proposal for future investigation. *Lasers Med Sci, 25*(6), 767-771.

Melnikova VO, Bezdetnaya LN, Bour C, Festor E, Gramain MP, Merlin JL, Guillemin F. (1999) Subcellular localization of meta-

teta(hydroxyphenyl)chlorine in human tumor cells subjected to photodynamic treatment. *J. Photochem Photobiol. B., 49*, 8.

Miller WE, Earp HS, Raab-Traub N. (1995) The Epstein-Barr virus latent membrane protein 1 induces expression of the epidermal growth factor receptor. *J Virol, 69*(7), 4390-4398.

Mitra S, Maugain E, Bolotine L, Guillemin F, Foster TH. (2005) Temporally and spatially heterogeneous distribution of mTHPC in a murine tumor observed by two-color confocal fluorescence imaging and spectroscopy in a whole-mount model. *Photochem Photobiol, 81*(5), 1123-1130.

Mitton D, Ackroyd R. (2008) A brief overview of photodynamic therapy in Europe. *Photodiagnosis Photodyn Ther, 5*(2), 103-111.

Moan J, Berg K, Kvam E, Western A, Malik Z, Ruck A, Schneckenburger H. (1989) Intracellular localization of photosensitizers. *Ciba Found Symp, 146*, 95-107; discussion 107-111.

Moan J, Peng Q. (2003) An outline of the hundred-year history of PDT. *Anticancer Res, 23*(5A), 3591-3600.

Moon DO, Kim MO, Choi YH, Lee HG, Kim ND, Kim GY. (2008) Gossypol suppresses telomerase activity in human leukemia cells via regulating hTERT. *FEBS Lett, 582*(23-24), 3367-3373.

Moore CM, Nathan TR, Lees WR, Mosse CA, Freeman A, Emberton M, Bown SG. (2006) Photodynamic therapy using meso tetra hydroxy phenyl chlorin (mTHPC) in early prostate cancer. *Lasers Surg Med, 38*(5), 356-363.

Morrow DI, McCarron PA, Woolfson AD, Juzenas P, Juzeniene A, Iani V, Donnelly RF. (2010) Hexyl aminolaevulinate is a more effective topical photosensitiser precursor than methyl aminolaevulinate and 5-aminolaevulinic acids when applied in equimolar doses. *J Pharm Sci, 99*(8), 3486-3498.

Morton CA, Whitehurst C, McColl JH, Moore JV, MacKie RM. (2001) Photodynamic therapy for large or multiple patches of Bowen disease and basal cell carcinoma. *Arch Dermatol, 137*(3), 319-324.

Murono S, Inoue H, Tanabe T, Joab I, Yoshizaki T, Furukawa M, Pagano JS. (2001) Induction of cyclooxygenase-2 by Epstein-Barr virus latent membrane protein 1 is involved in vascular endothelial growth factor production in nasopharyngeal carcinoma cells. *Proc Natl Acad Sci U S A, 98*(12), 6905-6910.

Navarro FP, Creusat G, Frochot C, Moussaron A, Verhille M, Vanderesse R, Thomann JS, Boisseau P, Texier I, Couffin AC, Barberi-Heyob M. (2013) Preparation and characterization of mTHPC-loaded solid lipid nanoparticles for photodynamic therapy. *J Photochem Photobiol B.* 130, 161-69.

Nestor M, Gold M, Kauvar A, Taub A, Geronemus R, Ritvo E, Gilbert D. (2006) The use of photodynamic therapy in dermatology: results of a consensus conference. *J Drugs Dermatol, 5*, 15.

Nguyen T D. (2012) Portraits of colloidal hybrid nanostructures: Controlled synthesis and potential applications. *Colloids Surf B Biointerfaces, 103C*, 326-344.

Nyst HJ, Wildeman MA, Indrasari SR, Karakullukcu B, van Veen RL, Adham M, Tan IB. (2012) Temoporfin mediated photodynamic therapy in patients with local persistent and recurrent nasopharyngeal carcinoma after curative radiotherapy: a feasibility study. *Photodiagnosis Photodyn Ther, 9*(3), 274-281.

Oka H, Chatani Y, Hoshino R, Ogawa O, Kakehi Y, Terachi T, Yoshida O. (1995) Constitutive activation of mitogen-activated protein (MAP) kinases in human renal cell carcinoma. *Cancer Res, 55*(18), 4182-4187.

Okano M, Thiele GM, Davis JR, Grierson HL, Purtilo DT. (1988) Epstein-Barr virus and human diseases: recent advances in diagnosis. *Clin Microbiol Rev, 1*(3), 300-312.

Olayioye MA, Neve RM, Lane HA, Hynes NE. (2000) The ErbB signaling network: receptor heterodimerization in development and cancer. *EMBO J, 19*(13), 3159-3167.

Paszko E, Ehrhardt C, Senge MO, Kelleher DP, Reynolds JV. (2011) Nanodrug applications in photodynamic therapy. *Photodiagnosis Photodyn Ther, 8*(1), 14-29.

Pegaz B, Debefve E, Ballini JP, Wagnieres G, Spaniol S, Albrecht V, Konan-Kouakou YN. (2006) Photothrombic activity of m-THPC-loaded liposomal formulations: pre-clinical assessment on chick chorioallantoic membrane model. *Eur J Pharm Sci, 28*(1-2), 134-140.

Peng Q, Warloe T, Berg K, Moan J, Kongshaug M, Giercksky KE, Nesland JM. (1997) 5-Aminolevulinic acid-based photodynamic therapy. Clinical research and future challenges. *Cancer, 79*(12), 2282-2308.

Plaetzer K, Kiesslich T, Verwanger T, Krammer B. (2003) The Modes of Cell Death Induced by PDT: An Overview. *Medical Laser Application, 18*(1), 7-19.

Plaetzer K, Krammer B, Berlanda J, Berr F, Kiesslich T. (2009) Photophysics and photochemistry of photodynamic therapy: fundamental aspects. *Lasers Med Sci, 24*(2), 259-268.

Poole JC, Andrews LG, Tollefsbol TO. (2001) Activity, function, and gene regulation of the catalytic subunit of telomerase (hTERT). *Gene, 269*(1-2), 1-12.

Pushpan SK, Venkatraman S, Anand VG, Sankar J, Parmeswaran D, Ganesan S, Chandrashekar TK. (2002) Porphyrins in photodynamic therapy - a search for ideal photosensitizers. *Curr Med Chem Anticancer Agents, 2*(2), 187-207.

Qiang YG, Yow CMN, Huang Z. (2008) Combination of photodynamic therapy and immunomodulation: current status and future trends. *Med Res Rev, 28*(4), 632-644.

Bonnett R. (1999) Photodynamic therapy in historical perspective. *Rev Contemp Pharmacother, 10*, 17.

Raab-Traub N. (2002) Epstein-Barr virus in the pathogenesis of NPC. *Semin Cancer Biol, 12*(6), 431-441.

Ramachandra M, Ambudkar SV, Chen D, Hrycyna CA, Dey S, Gottesman MM, Pastan I. (1998) Human P-glycoprotein exhibits reduced affinity for

substrates during a catalytic transition state. *Biochemistry, 37*(14), 5010-5019.

Roberts PJ, Der CJ. (2007) Targeting the Raf-MEK-ERK mitogen-activated protein kinase cascade for the treatment of cancer. *Oncogene, 26*(22), 3291-3310.

Robertson CA, Evans DH, Abrahamse H. (2009) Photodynamic therapy (PDT): a short review on cellular mechanisms and cancer research applications for PDT. *J Photochem Photobiol B, 96*(1), 1-8.

Rosenberg MF, Callaghan R, Ford RC, Higgins CF. (1997) Structure of the multidrug resistance P-glycoprotein to 2.5 nm resolution determined by electron microscopy and image analysis. *J Biol Chem, 272*(16), 10685-10694.

Rosenthal EL, Johnson TM, Allen ED, Apel IJ, Punturieri A, Weiss SJ. (1998) Role of the plasminogen activator and matrix metalloproteinase systems in epidermal growth factor- and scatter factor-stimulated invasion of carcinoma cells. *Cancer Res, 58*(22), 5221-5230.

Roux PP, Blenis J. (2004) ERK and p38 MAPK-activated protein kinases: a family of protein kinases with diverse biological functions. *Microbiol Mol Biol Rev, 68*(2), 320-344.

Ruan L, Li XH, Wan XX, Yi H, Li C, Li MY, Xiao ZQ. (2011) Analysis of EGFR signaling pathway in nasopharyngeal carcinoma cells by quantitative phosphoproteomics. *Proteome Sci, 9*, 35.

Rumie Vittar NB, Lamberti MJ, Pansa MF, Vera RE, Rodriguez ME, Cogno IS, Rivarola VA. (2013) Ecological photodynamic therapy: New trend to disrupt the intricate networks within tumor ecosystem. *Biochim Biophys Acta, 1835*(1), 86-99.

Safari J, Zarnegar Z. (2013) Advanced Drug Delivery Systems; Nanotechnology of Health Design A review. *Journal of Saudi Chemical Society*.

Salva KA. (2002) Photodynamic therapy: unapproved uses, dosages, or indications. *Clin Dermatol, 20*(5), 571-581.

Santonocito C, Concolino P, Lavieri MM, Ameglio F, Gentileschi S, Capizzi R, Capoluongo E. (2005) Comparison between three molecular methods for detection of blood melanoma tyrosinase mRNA. Correlation with melanoma stages and S100B, LDH, NSE biochemical markers. *Clin Chim Acta, 362*(1-2), 85-93.

Sasnauskiene A, Kadziauskas J, Vezelyte N, Jonusiene V, Kirveliene V. (2009) Apoptosis, autophagy and cell cycle arrest following photodamage to mitochondrial interior. *Apoptosis, 14*(3), 276-286.

Satomi T, Nagasaki Y, Kobayashi H, Tateishi T, Kataoka K, Otsuka H. (2007) Physicochemical characterization of densely packed poly(ethylene glycol) layer for minimizing nonspecific protein adsorption. *J Nanosci Nanotechnol, 7*(7), 2394-2399.

Sauna ZE, Ambudkar SV. (2000) Evidence for a requirement for ATP hydrolysis at two distinct steps during a single turnover of the catalytic cycle of human P-glycoprotein. *Proc Natl Acad Sci U S A, 97*(6), 2515-2520.

Sauna ZE, Ambudkar SV. (2001) Characterization of the catalytic cycle of ATP hydrolysis by human P-glycoprotein. The two ATP hydrolysis events in a single catalytic cycle are kinetically similar but affect different functional outcomes. *J Biol Chem, 276*(15), 11653-11661.

Sauna ZE, Kim IW, Ambudkar SV. (2007) Genomics and the mechanism of P-glycoprotein (ABCB1). *J Bioenerg Biomembr, 39*(5-6), 481-487.

Schauder A, Feuerstein T, Malik Z. (2011) The centrality of PBGD expression levels on ALA-PDT efficacy. *Photochem Photobiol Sci, 10*(8), 1310-1317.

Schmidt CM, McKillop IH, Cahill PA, Sitzmann JV. (1997) Increased MAPK expression and activity in primary human hepatocellular carcinoma. *Biochem Biophys Res Commun, 236*(1), 54-58.

Senge MO. (2012) mTHPC--a drug on its way from second to third generation photosensitizer? *Photodiagnosis Photodyn Ther, 9*(2), 170-179.

Senior AE, Bhagat S. (1998) P-glycoprotein shows strong catalytic cooperativity between the two nucleotide sites. *Biochemistry, 37*(3), 831-836.

Seymour LK. (2001) Epidermal growth factor receptor as a target: recent developments in the search for effective new anti-cancer agents. *Curr Drug Targets, 2*(2), 117-133.

Shair KH, Schnegg CI, Raab-Traub N. (2008) EBV latent membrane protein 1 effects on plakoglobin, cell growth, and migration. *Cancer Res, 68*(17), 6997-7005.

Sheng W, Decaussin G, Sumner S, Ooka T. (2001) N-terminal domain of BARF1 gene encoded by Epstein-Barr virus is essential for malignant transformation of rodent fibroblasts and activation of BCL-2. *Oncogene, 20*(10), 1176-1185.

Sizhong Z, Xiukung G, Yi Z. (1983) Cytogenetic studies on an epithelial cell line derived from poorly differentiated nasopharyngeal carcinoma. *Int J Cancer, 31*(5), 587-590.

Smith C, Tsang J, Beagley L, Chua D, Lee V, Li V, Khanna R. (2012) Effective treatment of metastatic forms of Epstein-Barr virus-associated nasopharyngeal carcinoma with a novel adenovirus-based adoptive immunotherapy. *Cancer Res, 72*(5), 1116-1125.

Smith P. (2001) Epstein-Barr virus complementary strand transcripts (CSTs/BARTs) and cancer. *Semin Cancer Biol, 11*(6), 469-476.

Smith PR, de Jesus O, Turner D, Hollyoake M, Karstegl CE, Griffin BE, Farrell PJ. (2000) Structure and coding content of CST (BART) family RNAs of Epstein-Barr virus. *J Virol, 74*(7), 3082-3092.

Solazzo M, Fantappie O, Lasagna N, Sassoli C, Nosi D, Mazzanti R. (2006) P-gp localization in mitochondria and its functional characterization in multiple drug-resistant cell lines. *Exp Cell Res, 312*(20), 4070-4078.

Stamenkovic I. (2000) Matrix metalloproteinases in tumor invasion and metastasis. *Semin Cancer Biol, 10*(6), 415-433.

Starkey JR, Rebane AK, Drobizhev MA, Meng F, Gong A, Elliott A, Spangler CW. (2008) New two-photon activated photodynamic therapy sensitizers induce xenograft tumor regressions after near-IR laser treatment through the body of the host mouse. *Clin Cancer Res, 14*(20), 6564-6573.

Stavrovskaya AA. (2000) Cellular mechanisms of multidrug resistance of tumor cells. *Biochemistry (Mosc), 65*(1), 95-106.

Suarez C, Rodrigo JP, Rinaldo A, Langendijk JA, Shaha AR, Ferlito A. (2010) Current treatment options for recurrent nasopharyngeal cancer. *Eur Arch Otorhinolaryngol, 267*(12), 1811-1824.

Szakacs G, Paterson JK, Ludwig JA, Booth-Genthe C, Gottesman MM. (2006) Targeting multidrug resistance in cancer. *Nat Rev Drug Discov, 5*(3), 219-234.

Takada K. (2012) Role of EBER and BARF1 in nasopharyngeal carcinoma (NPC) tumorigenesis. *Semin Cancer Biol, 22*(2), 162-165.

Takeshita H, Yoshizaki T, Miller WE, Sato H, Furukawa M, Pagano JS, Raab-Traub N. (1999) Matrix metalloproteinase 9 expression is induced by Epstein-Barr virus latent membrane protein 1 C-terminal activation regions 1 and 2. *J Virol, 73*(7), 5548-5555.

Tang F, Tang G, Xiang J, Dai Q, Rosner MR, Lin A. (2002) The absence of NF-kappaB-mediated inhibition of c-Jun N-terminal kinase activation contributes to tumor necrosis factor alpha-induced apoptosis. *Mol Cell Biol, 22*(24), 8571-8579.

Tao Q, Chan AT. (2007) Nasopharyngeal carcinoma: molecular pathogenesis and therapeutic developments. *Expert Rev Mol Med, 9*(12), 1-24.

Teodori, E., Dei, S., Martelli, C., Scapecchi, S., & Gualtieri, F. (2006). The functions and structure of ABC transporters: implications for the design of new inhibitors of Pgp and MRP1 to control multidrug resistance (MDR). *Curr Drug Targets, 7*(7), 893-909.

Teramoto N, Maeda A, Kobayashi K, Hayashi K, Oka T, Takahashi K, Akagi T. (2000) Epstein-Barr virus infection to Epstein-Barr virus-negative nasopharyngeal carcinoma cell line TW03 enhances its tumorigenicity. *Lab Invest, 80*(3), 303-312.

Tong MC, van Hasselt CA, Woo JK. (1996) Preliminary results of photodynamic therapy for recurrent nasopharyngeal carcinoma. *Eur Arch Otorhinolaryngol, 253*(3), 189-192.

Tong Z, Singh G, Rainbow AJ. (2002) Sustained activation of the extracellular signal-regulated kinase pathway protects cells from photofrin-mediated photodynamic therapy. *Cancer Res, 62*(19), 5528-5535.

Treinies I, Paterson HF, Hooper S, Wilson R, Marshall CJ. (1999) Activated MEK stimulates expression of AP-1 components independently of phosphatidylinositol 3-kinase (PI3-kinase) but requires a PI3-kinase signal To stimulate DNA synthesis. *Mol Cell Biol, 19*(1), 321-329.

Triesscheijn M, Ruevekamp M, Antonini N, Neering H, Stewart FA, Baas P. (2006) Optimizing meso-tetra-hydroxyphenyl-chlorin-mediated photodynamic therapy for basal cell carcinoma. *Photochem Photobiol, 82*(6), 1686-1690.

Tsai CL, Li HP, Lu YJ, Hsueh C, Liang Y, Chen CL, Chang YS. (2006) Activation of DNA methyltransferase 1 by EBV LMP1 Involves c-Jun NH(2)-terminal kinase signaling. *Cancer Res, 66*(24), 11668-11676.

Tsao SW, Tramoutanis G, Dawson CW, Lo AK, Huang DP. (2002) The significance of LMP1 expression in nasopharyngeal carcinoma. *Semin Cancer Biol, 12*(6), 473-487.

Tsao SW, Tsang CM, Pang PS, Zhang G, Chen H, Lo KW. (2012) The biology of EBV infection in human epithelial cells. *Seminars in Cancer Biology, 22*(2), 137-143.

Tsuzuki H, Fujieda S, Sunaga H, Sugimoto C, Tanaka N, Saito H. (1998) Expression of multidrug resistance-associated protein (MRP) in head and neck squamous cell carcinoma. *Cancer Lett, 126*(1), 89-95.

Tulalamba W, Janvilisri T. (2012) Nasopharyngeal carcinoma signaling pathway: an update on molecular biomarkers. *Int J Cell Biol. , 2012,* 594681.

Vaughan TL, Shapiro JA, Burt RD, Swanson GM, Berwick M, Lynch CF, Lyon JL. (1996) Nasopharyngeal cancer in a low-risk population: defining risk factors by histological type. *Cancer Epidemiol Biomarkers Prev, 5*(8), 587-593.

Vokes EE, Liebowitz DN, Weichselbaum RR. (1997) Nasopharyngeal carcinoma. *Lancet, 350*(9084), 1087-1091.

Wang EJ, Casciano CN, Clement RP, Johnson WW. (2000) Two transport binding sites of P-glycoprotein are unequal yet contingent: initial rate kinetic analysis by ATP hydrolysis demonstrates intersite dependence. *Biochim Biophys Acta, 1481*(1), 63-74.

Wang XK, Fu LW. (2010). Interaction of tyrosine kinase inhibitors with the MDR-related ABC transporter proteins. *Curr Drug Metab, 11*(7), 618-628.

Wolf JS, Chen Z, Dong G, Sunwoo JB, Bancroft CC, Capo DE, Van Waes C. (2001) IL (interleukin)-1alpha promotes nuclear factor-kappaB and AP-1-induced IL-8 expression, cell survival, and proliferation in head and neck squamous cell carcinomas. *Clin Cancer Res, 7*(6), 1812-1820.

Wu RWK, Chu ESM, Yow CMN, Chen JY. (2006) Photodynamic effects on nasopharyngeal carcinoma (NPC) cells with 5-aminolevulinic acid or its hexyl ester. *Cancer Lett., 242*(1), 112-119.

Xie Y, Wei ZB, Zhang Z, Wen W, Huang GW. (2009) Effect of 5-ALA-PDT on VEGF and PCNA expression in human NPC-bearing nude mice. *Oncol Rep, 22*(6), 1365-1371.

Yang PW, Hung MC, Hsieh CY, Tung EC, Wang YH, Tsai JC, Lee JM. (2013) The effects of Photofrin-mediated photodynamic therapy on the modulation of EGFR in esophageal squamous cell carcinoma cells. *Lasers Med Sci*. 28(2), 605-14.

Yano S, Hirohara S, Obata M, Hagiya Y, Ogura Si, Ikeda A, Joh T. (2011) Current states and future views in photodynamic therapy. *Journal of Photochemistry and Photobiology C: Photochemistry Reviews, 12*(1), 46-67.

Yee KK, Soo KC, Olivo M. (2005) Anti-angiogenic effects of Hypericin-photodynamic therapy in combination with Celebrex in the treatment of human nasopharyngeal carcinoma. *Int J Mol Med, 16*(6), 993-1002.

Yoshizaki T, Ito M, Murono S, Wakisaka N, Kondo S, Endo K. (2012) Current understanding and management of nasopharyngeal carcinoma. *Auris Nasus Larynx, 39*(2), 137-144.

Yoshizaki T, Sato H, Murono S, Pagano JS, Furukawa M. (1999) Matrix metalloproteinase 9 is induced by the Epstein-Barr virus BZLF1 transactivator. *Clin Exp Metastasis, 17*(5), 431-436.

Yow CMN, Chen JY, Mak NK, Cheung NH, Leung AW. (2000a) Cellular uptake, subcellular localization and photodamaging effect of temoporfin (mTHPC) in nasopharyngeal carcinoma cells: comparison with hematoporphyrin derivative. *Cancer Lett, 157*(2), 123-131.

Yow CMN, Mak NK, Leung AW, Huang Z. (2009) Induction of early apoptosis in human nasopharyngeal carcinoma cells by mTHPC-mediated photocytotoxicity. *Photodiagnosis Photodyn Ther, 6*(2), 122-127.

Yow CMN, Mak NK, Szeto S, Chen JY, Lee YL, Cheung NH, Leung AW. (2000b) Photocytotoxic and DNA damaging effect of temoporfin (mTHPC) and merocyanine 540 (MC540) on nasopharyngeal carcinoma cell. *Toxicology Letters, 115*(1), 53-61.

Yow CMN, Chen JY, Mak NK, Cheung NH, Leung AWN. (2000c) Cellular uptake, subcellular localization and photodamaging effect of Temopor®n (mTHPC) in nasopharyngeal carcinoma cells:comparison with hematoporphyrin derivative. *Cancer Lett, 157*, 9.

Yu MC, Garabrant DH, Huang TB, Henderson BE. (1990) Occupational and other non-dietary risk factors for nasopharyngeal carcinoma in Guangzhou, China. *Int J Cancer, 45*(6), 1033-1039.

Zamadar M, Ghosh G, Mahendran A, Minnis M, Kruft BI, Ghogare A, Greer A. (2011) Photosensitizer drug delivery via an optical fiber. *J Am Chem Soc, 133*(20), 7882-7891.

Zawacka-Pankau J, Krachulec J, Grulkowski I, Bielawski KP, Selivanova G. (2008) The p53-mediated cytotoxicity of photodynamic therapy of cancer: recent advances. *Toxicol Appl Pharmacol, 232*(3), 487-497.

Zeng Y, Zhong JM, Mo YK, Miao XC. (1983) Epstein-Barr virus early antigen induction in Raji cells by Chinese medicinal herbs. *Intervirology, 19*(4), 201-204.

Zhang L, Chen QY, Liu H, Tang LQ, Mai HQ. (2013) Emerging treatment options for nasopharyngeal carcinoma. *Drug Des Devel Ther, 7*, 37-52.

Zhao Y, Wang Y, Zeng S, Hu X. (2012). LMP1 expression is positively associated with metastasis of nasopharyngeal carcinoma: evidence from a meta-analysis. *J Clin Pathol, 65*(1), 41-45.

Zheng G, Chen J, Stefflova K, Jarvi M, Li H, Wilson BC. (2007) Photodynamic molecular beacon as an activatable photosensitizer based on protease-controlled singlet oxygen quenching and activation. *Proc Natl Acad Sci U S A, 104*(21), 8989-8994.

Zheng H, Li LL, Hu DS, Deng XY, Cao Y. (2007) Role of Epstein-Barr virus encoded latent membrane protein 1 in the carcinogenesis of nasopharyngeal carcinoma. *Cellular & Molecular Immunology, 4*(3), 185-196.

Chapter 2

H-ALA-PDT effect on EBV LMP1 protein expression in NPC cells

Chapter 2

2.1 Abstract

5-aminolevulinic acid (5-ALA), the precursor substance of protoporphyrin, is one of the FDA approved 2nd generation photosensitizers and is popularly used for *in vitro* and *in vivo* studies over past decades. 5-aminolevulinic acid hexyl derivative (H-ALA) is one of the 5-ALA derivatives with an additional long lipophilic chain (hexyl group) than 5-ALA. The hexyl group added to 5-ALA increased the lipophilic property of 5-ALA, resulted in better penetration of PSs into cell cytoplasm.

Nasopharyngeal carcinoma (NPC) is highly prevalent in Southern China and its tumuorigenesis is strongly associated with Epstein-Barr virus (EBV). The latent membrane protein 1 (LMP1) is the major oncoprotein expressed by EBV. This is evident that the level of LMP1 protein expression determines the tumour properties. Low level of LMP1 could induce cell growth and cell survival, while high level of LMP1 could suppress cell growth and trigger apoptosis.

The aim of this study was to investigate the effect of H-ALA-mediated phototoxicity on three human NPC cell lines, including (EBV positive) undifferentiated NPC cells/C666-1, (EBV negative) poorly differentiated NPC cells/CNE2 and (EBV negative) well differentiated NPC cells/HK1. Intracellular accumulation of PpIX was measured to reflect the H-ALA uptake by NPC cells. The phototoxic efficacies of LED activated H-ALA on three NPC cell lines were determined by MTT assay. Effects of H-ALA-PDT on the expression of LMP1 protein was examined by Western blotting analysis. Effect of H-ALA-PDT on the cell cycle regulation was evaluated by flow cytometry.

Our data reported that H-ALA was uptaken by all three NPC cell lines. LED-activated H-ALA-PDT eradicated C666-1 cells and CNE2 cells effectively, while it was ineffective to HK1 cells. In C666-1 cells, LD_{70} was obtained at 7.56μg/ml H-

ALA with 4J/cm^2 LED activation. In CNE2 cells, LD_{70} was obtained at 7.56μg/ml H-ALA with 2J/cm^2 LED activation.

EBV LMP1 proteins only expressed in EBV positive C666-1 cells among the three NPC cell lines tested. A 55% increase in LMP1 protein expression was obtained at LD_{70} in response to H-ALA-PDT in a dose-dependent manner ($P<0.01$).

This is the first report to reveal the action of H-ALA mediated PDT on EBV positive and EBV negative NPC cells. Our pioneer work revealed the potential of LMP1 protein as a therapeutic marker for H-ALA on C666-1 NPC cells.

Key words: H-ALA, LMP1 protein, EBV, PDT

Chapter 2

2.2 Introduction

Nasopharyngeal Carcinoma (NPC) cell is one of the top ten cancers highly prevalent in Southern China, especially in Hong Kong and Guangdong (Hong Kong Cancer registry 2011, Sizhong et al., 1983; Wei et al., 2011). The epidemiologic evidence implies that Epstein - Barr virus (EBV) infection is strongly associated with the tumourigenesis of NPC. EBV is a herpes virus that infects over 90% of adult population worldwide (Tsao et al., 2012b). A number of malignancies were associated with EBV infection, including nasopharyngeal carcinoma, Burkett's lymphoma, and lung carcinoma (Herrmann & Niedobitek, 2003; Pattle & Farrell, 2006). The tumourigenic potential of EBV mainly related to a unique set of latent gene products including the latent membrane proteins (LMP1, LMP2A, and LMP2B) and EBV-encoded nuclear antigens (EBNA1 and EBNA2) (Miller et al., 1995; Raab-Traub, 2002; Tsao et al., 2012a). Among these, LMP1 is the principal oncoprotein involved in the process of EBV-associated oncogenesis of NPC (Dawson et al., 2012; Lang, 2009; Lo et al., 2007). A number of signaling pathways were associated with EBV LMP1 expression in NPC cells including the mitogen-activated protein kinases (MAPK) signaling pathways. Alteration of MAPK pathways resulted in inhibiting apoptosis; inducing cell immortality; promoting cell proliferation and influencing the cell invasion and metastasis in NPC (Li et al., 2007; Lo et al., 2007; Raab-Traub, 2002; Tulalamba & Janvilisri, 2012).

Photodynamic Therapy (PDT) is a novel therapy shedding light on NPC (Koon et al., 2010; Wu et al., 2006; Yow et al., 2009). PDT is an evolving cancer treatment regimen with approval for use in USA, EU, Canada, Russia and Japan. PDT effect depends on the tumour localizing photosensitizer (PS), which absorbs photon to produce photo-toxin such as reactive oxygen species (ROS) (Agostinis et al., 2011; Bredell et al., 2010; Robertson et al., 2009). 5-aminolevulinic acid (5-ALA), the precurous substance of protoporphyrin IX (PpIX), is one of the FDA approved 2nd generation PSs and is prevalent applied for *in vivo* and *in vitro* studies over the past decades. Addition of exogenous 5-ALA increased the intracellular accumulation of

PpIX via the heme biosynthesis pathway. Several factors affect the PpIX accumulation in tumour cells, such as the uptake of 5-ALA, concentration of iron and activity of the enzyme ferrochelatase (Brunner et al., 2003).

The major limitation of 5-ALA refers to its poor penetration ability via the biological membrane (Peng et al., 1997). Therefore, a modified derivative of 5-ALA was developed, which is known as the H-ALA (5-ALA hexyl ester). 5-ALA is chemically modified by adding a hexyl lipophilic chain to form H-ALA. The hexyl group inserted to 5-ALA increase its lipophilic properties, resulted in better penetration to cytoplasm. A study showed that only 60-fold of decrease in H-ALA concentration was needed to produce the same amount of PpIX accumulated inside cells compared to 5-ALA (Bruce-Micah et al., 2009; Casas et al., 2002; Dognitz et al., 2008; Eleouet et al., 2000; Juzeniene et al., 2002; Morrow et al., 2010). Besides improving the PSs, development of light source could also enhance the PDT efficacy. A novel light source from light emitting diode (LED) has been setup by our group with promising results in activation of the nano-photosensitizer Hypocrellin-B in nasopharyngeal carcinoma cells (Bai et al., 2010).

In this study, the PDT efficacy of LED activated H-ALA on three NPC cell lines was evaluated. The action of H-ALA-PDT to EBV LMP1 protein expression and cell cycle progression analysis were investigated via western blotting analysis and flow cytometry.

2.3 Materials and Methods

2.3.1 Materials

The photosensitizer, H-ALA, was kindly provided by Photocure (Oslo, Norway). The stock and working solutions were prepared in phosphate-buffered saline (PBS, pH 7.4) and freshly prepared with RPMI-1640 culture medium, respectively.

3-(4,5-dimethylthiazol-2-yl)-2,5-diphenyltetrazolium bromide (MTT) and propidium iodide (PI) were purchased from Sigma Chemical Co. (St. Louis, MO). Primary mouse monoclonal anti-LMP1 antibody (CS1-4) was purchased from Dako (Singapore). Secondary anti-mouse antibody was purchased from Cell Signaling Technology, Inc. (Danvers, MA).

NPC cells (3×10^4 cells/well) were seeded in 96-well tissue culture plates, incubated with various H-ALA concentrations ranged from 1.26 μg/ml to 251.75μg/ml for 4 hours. Cells were then irradiated with 0 – 4 J/cm^2 of light emitting diode (LED) light as described by Bai et al. (2010).

2.3.2 Cell culture

EBV positive undifferentiated NPC cell/C666-1 and EBV negative well differentiated NPC cell/HK1 were kindly provided by Anatomical and Cellular Pathology Department, The Chinese University of Hong Kong. EBV negative poorly differentiated NPC cells/CNE2 was purchased from Shanghai Biosis Biotechnology Co., Ltd. (Shanghai China). The C666-1 cells were cultured in RPMI-1640 supplemented with 10% fetal bovine serum (FBS; Gibco BRL), 1% glutamax and 1% antibiotics PSN (5 mg/ml penicillin, 5 mg/ml streptomycin and 10 mg/ml neomycin) (Gibco BRL). HK1 and CNE2 cells were cultured in RPMI-1640 supplemented with 10% fetal bovine serum (FBS; Gibco BRL) and 1% antibiotics PSN. Cells were grown at 37 ^{o}C in a humidified 5% CO_2 incubator.

2.3.3 Examination of intracellular drug uptake by flow cytometry

Subconfluent NPC cells were incubated with H-ALA (7.56μg/ml) in the dark for 1, 2, 4, 8 or 24 hours, respectively. Cells were then washed and resuspended in PBS. Cellular uptake of H-ALA was determined by flow cytometry (Cytomics FC500, Beckman Coulter, CA) equipped with a 15 mW argon ion laser providing the excitation at 488 nm. Cell suspensions were excited and the fluorescence signal of drug uptake by the cells was detected by a photomultiplier tube with a 610 nm long-pass filter. A minimum of 10,000 cells per sample were analyzed in three independent experiments. The uptake of H-ALA in terms of PpIX fluorescence intensity at single-cell level was acquired (Wu et al., 2006).

2.3.4 3-(4,5-dimethylthiazol-2-yl)-2,5-diphenyltetrazolium bromide (MTT) assay

Light irradiated cells were washed and further incubated for 24 hours. MTT (5 mg/ml) was added to each well and incubated for 3 hours. Viable cells took up MTT and reduced it to form dark blue, water insoluble formazan by the mitochondrial dehydrogenase from the cells. The ability to form formazan refers to the normal function of the mitochondria and is used for the study of cell viability. To lyse cells and dissolve formazan crystals, 100 μl of dimethyl sulfoxide (DMSO) was added to each well and the optical density was measured at 570 nm using the spectrophotometer (Benchmark Plus, Bio-Rad). Cell viability was calculated as:

Cell viability (%) = (mean OD value of treated cells ÷ mean OD value of control cells) × 100%

2.3.5 Western blot analysis

The control cells and H-ALA-PDT treated cells from both adherent and non-adherent floating cells were washed with ice-cold PBS and lysed in 0.2 ml lysis buffer (50 mM Tris-HCl, 150 mM NaCl, 1% Nonidet 40, 0.5% (w/v) Na-deoxycholate, 2 mM phenylmethylsulfonyl fluoride, 1x protease inhibitors).

Supernatant was collected from lysates by centrifugation at 14,000g for 30 minutes at 4 ^{o}C. An equal amount of protein was subjected to 10% sodium dodecyl sulphate polyacrylamide gel electrophoresis before blotting onto a polyvinylidene difluoride membrane (Amersham Pharmacia Biotech, Piscataway, NJ). The membrane was blocked with 5% skimmed milk in tris-buffered saline with 0.05% Tween 20 (pH 7.6) for 1 hour at room temperature. After blocking, the membrane was probed with a LMP1-primary antibody at 4 ^{o}C overnight. After washing, the membrane was incubated with a secondary anti-mouse antibody coupled to horseradish peroxidase (Amersham and Pharmacia Biotech) for 1 hour at room temperature. The antibody-antigen binding was then detected using an ECL chemiluminescence detection system according to the manufacturer's instructions and visualized by Bio-Rad Chemi Doc™ EQ densitometer (Bio-Rad laboratories, USA). The intensities of the protein bands were compared and normalized with GAPDH protein by Bio-Rad Quantity One software (Bio-Rad laboratories, USA).

2.3.6 Cell cycle and DNA content analysis

Cell cycle and DNA content were analyzed by flow cytometry with propidium iodide (PI) staining. NPC cells (5×10^5 cells/dish) were cultured and synchronized in RPMI-1640 without FBS (iRPMI) for 24 hours. At 4, 24, 48 and 72 hours post PDT, treated cells were harvested, washed and suspended in PBS. Cells were fixed with ice cold 80% ethanol overnight at -20 °C. Fixed cells were washed twice with PBS, then re-suspended in 300 µl PBS containing PI staining solution (10 µg/ml PI, 10 mg/ml RNase A and triton X-100) followed by incubation at 37 °C for 30 minutes. For each sample, 10,000 events in triplicate were counted by Cytomics FC500 (Beckman Coulter). The data were analyzed by the FlowJo Software (Version 5.7.2) to estimate the proportion of the cell cycle phases in form of the cell number against DNA content histograms. The debris and doublet were gated out and excluded by the software.

2.3.7 Statistical analysis

All data were processed and presented by GraphPad Prism (GraphPad Software, Inc.). Mean and standard deviation (SD) were used to present data and all graphical error bars were represented in SD. Quantitative data from three independent experiments were used for analysis of the western blotting and the cell cycle progression. One-way analysis of variance (ANOVA) followed by Dunnett correction or two-way ANOVA followed by Bonferroni's correction post-hoc test were used to analyze differences between groups by the GraphPad Prism (GraphPad Software, Inc.). A P-value of less than 0.05 was considered as statistically significant different.

2.4 Results

2.4.1. Intracellular localization of PpIX generated by hexyl-ALA in NPC cells

Intracellular PpIX fluorescence was determined by flow cytometer at different time points. As expected, the intracellular PpIX formation in NPC cells was mainly influenced by the time of incubation. Figure 2.1 shows the formation of PpIX in C666-1 cells, CNE2 cells and HK1 cells at different time points. Similar fluorescence intensity was obtained in C666-1 cells and CNE2 cells at H-ALA concentration 7.56μg/ml (30μM) with 4 hours incubation. A higher PpIX concentration was obtained in C666-1 cells and CNE2 cells than in HK1 cells at all measured time points. For instance, after incubating with 7.56μg/ml (30μM) of H-ALA for 4 hours, the PpIX concentration in C666-1 cells and CNE2 cells were 1.7-fold higher than that in HK1 cells. To facilitate follow-up studies, 4 hours H-ALA incubation time was selected for all subsequent experiments (Agostinis et al., 2011; Radakovic-Fijan et al., 1999).

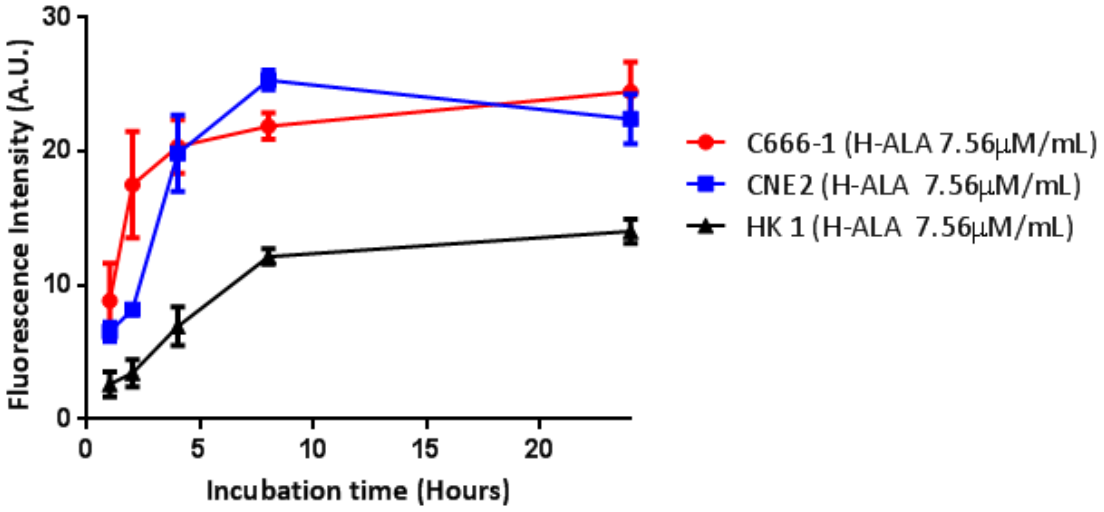

Figure 2.1. Kinetics of cellular PpIX accumulation in NPC cells.

The fluorescence intensity represented the cellular PpIX content (relative). Error bars (SD) were obtained from 3 to 6 independent experiments.

2.4.2. Phototoxicity of H-ALA mediated PDT in NPC cells

MTT assay was used to evaluate the phototoxicity of H-ALA-PDT on C666-1, CNE2 cell lines and HK1 cells. The results of H-ALA mediated phototoxicity in three NPC cells were presented in Figure 2.2. The phototoxicity induced by the LED irradiated PpIX varied due to different concentration of prodrug and LED light dose applied. The phototoxic effect of H-ALA on C666-1 cells and CNE2 cells increased progressively with H-ALA concentrations ranged from 1.26 to 7.56μg/ml, at the light dose of 2-4 J/cm^2. There was no toxic effect on H-ALA alone or light alone (data not shown). In CNE2 cells, LD_{30}, LD_{50} and LD_{70} were obtained at 1.26μg/ml, 2.52μg/ml and 7.56μg/ml at 2J/cm^2 respectively. In C666-1 cells, LD_{30}, LD_{50} and LD_{70} were obtained at 1.26μg/ml, 2.52μg/ml and 7.56μg/ml at 4J/cm^2 respectively. CNE2 cells required a 50% lower PDT dose (2.25μg/ml, 2J) to generate LD_{50} than that of C666-1 cells (2.25μg/ml, 4J), indicated that H-ALA-PDT is more effective to CNE2 cells than to C666-1 cells. It was found that H-ALA was inefficient to HK1 cells. LD_{50} of HK1 cells was obtained only at high PDT dose (251.75μg/ml, 3J/cm^2). A 150-fold higher PDT dose was needed to achieve LD50 in HK1 cells than that of CNE2 cells. Similarly, a 75-fold higher PDT dose was needed for HK1 cells than that of C666-1 cells.

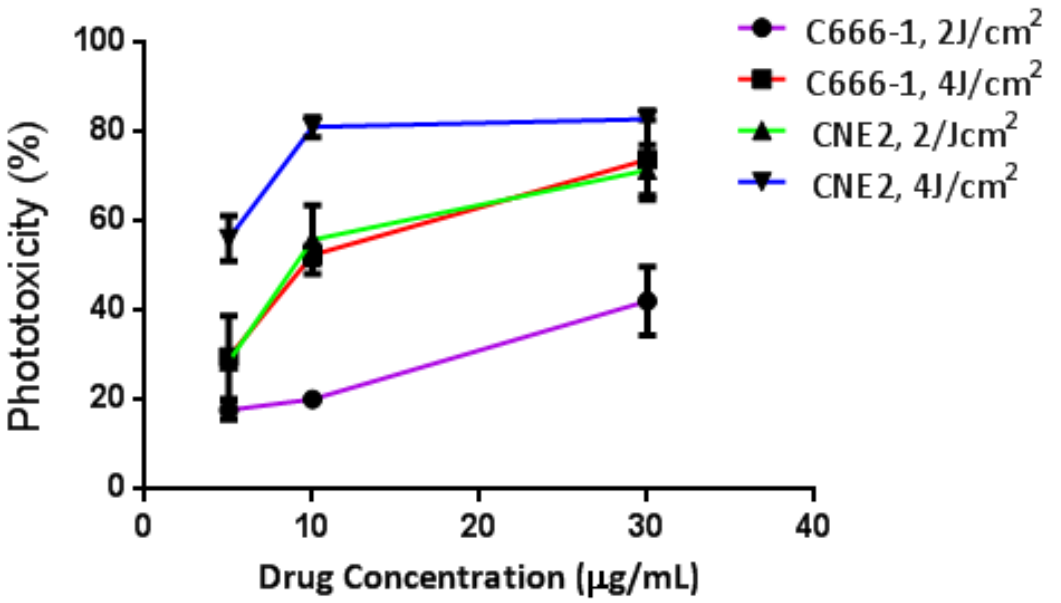

Figure 2.2. Photocytotoxicity of H-ALA on NPC cells.

Cells were incubated with H-ALA at different concentrations for 4 h, and then irradiated with light at 2 or 4 J/cm^2. The percentage of photocytotoxicity was measured by MTT assay. Error bars (SD) were from 3 to 6 independent experiments.

2.4.3. Quantitative evaluation of H-ALA-PDT effect on EBV LMP1 Protein expression

The effect of H-ALA mediated PDT to LMP1 protein expression was evaluated by Western blot analysis. Among the three NPC cell lines, LMP1 protein was only expressed in EBV positive C666-1 cells. Figure 2.3 shows the action of H-ALA-PDT to LMP1 protein expression in C666-1 cells. LMP1 protein was found in both control and dark control C666-1 cells with similar expression level, indicated that H-ALA alone could not affect the LMP1 protein expression. However, H-ALA-PDT promoted LMP1 protein expression in C666-1 cells in a dose dependent manner. Up to 55% increase of LMP1 protein expression was obtained at LD_{70} H-ALA-PDT ($P<0.01$).

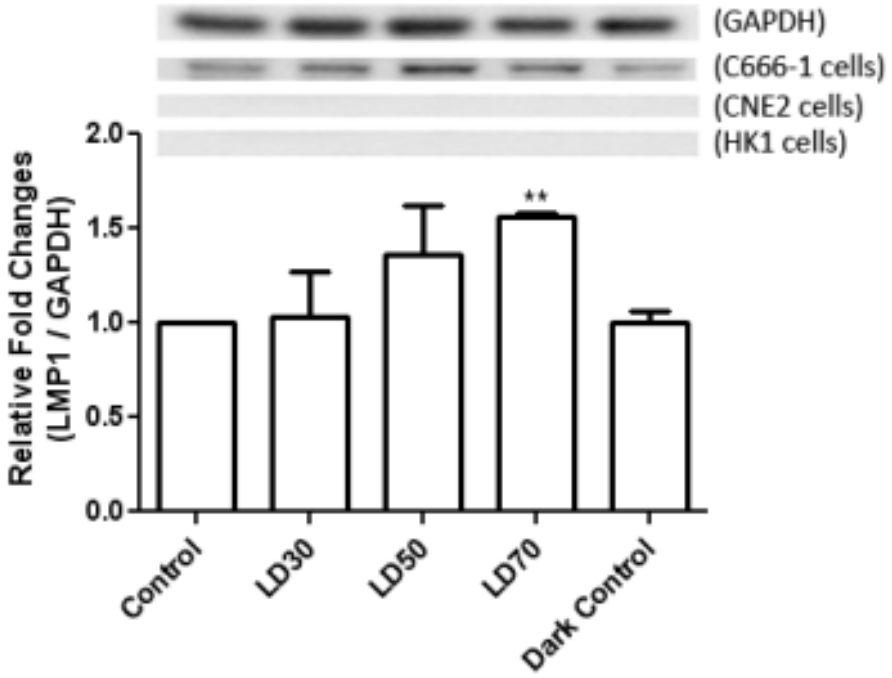

Figure 2.3. Effect of H-ALA mediated PDT on the LMP1 protein expression in C666-1 cells.

A 55% increase of LMP1 protein expression was obtained after H-ALA mediated PDT at LD_{70}. Total cellular proteins were extracted from control and PDT treated cells for the detection of LMP1 protein by western blot analysis. Protein amount was normalized by GAPDH. Significant differences between treatment and control groups were analyzed by one-way ANOVA and followed by Dunnett's post-tests (**: $p<0.01$).

2.4.4. H-ALA induced cell cycle and DNA content change in NPC cells

Flow cytometric analysis was applied to explore the effect of the H-ALA-PDT to cell cycle phase distribution. Data showed that H-ALA-PDT induced a time dependent cell cycle arrest in both C666-1 cells and CNE2 cells (Table 2.1). The representative cell cycle distributions were shown in Figure 2.4. In figure 2.4, (A) represented the Sub-G1 phase; (B) represented the G1 phase of the cell cycle; (C) represented the S-phase; and (D) represented the G2 phase. Table 2.1 summarizes the percentage of cell cycle phase induced by H-ALA in C666-1 cells and CNE2 cells. There were 16.7% of C666-1 cells and 8.8% CNE2 cells undergoing apoptosis, respectively. At 72 hours post-H-ALA-PDT with LD_{50}, a significant increase in percentage of cells in sub-G1 phase cells with a decline in that of S phase and G2/M phase were obtained in C666-1 cells ($p<0.05$).

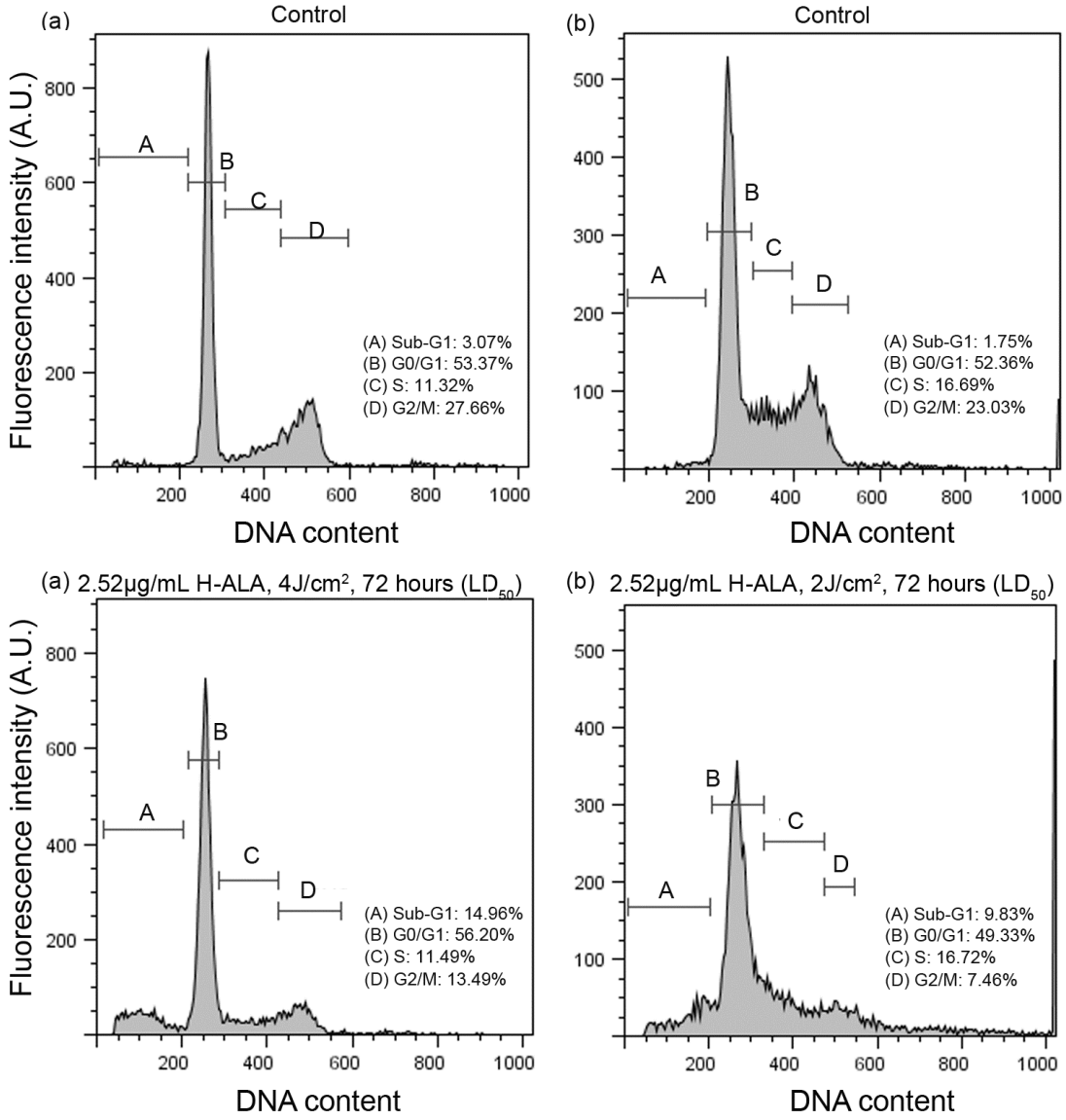

Figure 2.4 Flow cytometric analysis for effect of H-ALA-PDT on cell cycle distribution in NPC cells at 72 hours after treatment at LD_{50}.

Representative data: (a) C666-1 cells; (b) CNE2 cells. (A: percentage of cells in Sub G1 phase; B: percentage of cells in G0/G1 phase; C: percentage of cells in S phase; D: percentage of cells in G2/M phase)

Table 2.1 Flow cytometric analysis for time-effect of H-ALA-PDT on cell cycle phase distribution in NPC cells 4-72 hours after treatment at LD_{50}.

(a) C666-1	**Control**	**4 hours**	**24 hours**	**48 hours**	**72 hours**
Sub-G1	3.01 ± 1.71%	4.14 ± 1.78%	5.29 ± 5.16%	5.02 ± 1.95%	**16.69 ± 2.08%** *
G0/G1	50.41 ± 9.24%	71.79 ± 2.73% ***	56.40 ± 10.36%	57.09 ± 7.94%	49.89 ± 10.82%
S	13.96 ± 4.60%	7.70 ± 0.64% *	12.04 ± 4.26%	14.47 ± 2.64%	11.80 ± 2.57%
G2/M	28.70 ± 9.72%	6.73 ± 0.58% *	22.13 ± 10.27%	19.08 ± 8.87%	11.74 ± 5.23%

(b) CNE2	**Control**	**4 hours**	**24 hours**	**48 hours**	**72 hours**
Sub-G1	2.40 ± 2.47%	4.01 ± 1.12%	6.37 ± 2.12%	9.90 ± 3.04%	**8.78 ± 1.72%**
G0/G1	63.63 ± 11.98%	48.79 ± 5.32%	49.95 ± 13.79%	67.89 ± 6.35%	61.05 ± 16.64%
S	16.06 ± 6.43%	19.72 ± 3.94%	21.50 ± 8.72%	10.48 ± 2.65%	13.06 ± 3.62%
G2/M	16.27 ± 9.71%	23.69 ± 6.51%	17.72 ± 10.11%	7.86 ± 6.30%	4.44 ± 2.31%

(a) C666-1 cells; (b) CNE2 cells. The cell percentages at different cell cycle phases expressed as mean±SD from three independent experiments. Significant difference between treatment and control groups were analyzed by two-way ANOVA and followed by Bonferroni's post-tests (* $p<0.05$; ** $p<0.01$; *** $p<0.001$).

2.5 Discussion

According to our previous publication, 5-ALA was proved to be an effective treatment on NPC. Tumour cell eradication was obtained using 5-ALA on CNE2 cells and HK1 cells. However, the poor membrane penetration of 5-ALA limited its application as high dosage is required for tumour eradication. We reported previously that 100-fold less H-ALA was required to produce the same phototoxic effect in CNE2 cells than that of 5-ALA. We also reported that no genotoxicity were obtained in normal human lymphocytes with H-ALA-PDT (Wu et al., 2006; Yow et al., 2012). However, limited data were provided on H-ALA-PDT efficacy on EBV positive undifferentiated NPC cells. Taken together, the PDT efficacy of H-ALA mediated PDT on C666-1 cells, CNE2 cells and HK1 cells were explored in this study. The *in vitro* modulation of H-ALA to LMP1 protein expression and cell cycle progression on three NPC cell lines were also explored.

H-ALA-PDT efficacy was evaluated through PSs uptake, phototoxicity, mode of cell death and cell cycle regulation. With increased H-ALA incubation time, more PpIX were accumulated in all three NPC cells (Figure 2.1). The PpIX formation was obviously higher in C666-1 cells and CNE2 cells than in HK1 cells. At the H-ALA concentration 7.56μg/ml with 4 hours of incubation, similar PpIX were obtained in C666-1 cells and CNE2 cells. While a 1.7-fold higher PpIX were obtained in C666-1 cells and CNE2 cells than in HK1 cells. These results explained why the H-ALA-PDT phototoxicity was higher in C666-1 cells and CNE2 cells than in HK1 cells (Figure 2.2) with the same PDT dosage. Other studies also suggested that the PpIX accumulation depended on the cell type, cell size, ferrochelatase activity and cell cycle. Our finding suggested that H-ALA was favorable in generating and accumulating PpIX in undifferentiated and poorly differentiated NPC cells in *in vitro* condition.

Our study found that LMP1 protein was only expressed in EBV positive C666-1 cells but not in EBV negative HK1 cells and CNE2 cells. Data suggested that the

expression of LMP1 protein was correlated with the presence of the virus. LMP1 is one of the principal EBV encoded proteins expressed in NPC. EBV LMP1 protein activated a number of signaling pathways including the MAPK and EGFR signaling pathways, resulted in inhibition of apoptosis; induction of cell immortality; promotion of cell proliferation, and influence of cell invasion and metastasis (Dawson et al., 2012; Li et al., 2007; Lo et al., 2007; Raab-Traub, 2002; Zheng et al., 2007). Yet the LMP1 functions in NPC tumourigenesis was dose dependent. A number of studies indicated that high levels of LMP1 can suppress cell growth and sensitized cells to apoptosis (Deng et al., 2003; Yoshizaki et al., 2012).

Our finding was echoed to these studies. H-ALA-PDT triggered EBV LMP1 protein expression in a dose dependent manner, with a significantly increased in EBV LMP1 protein expression (55%) at LD_{70} ($P<0.01$). Up regulation of LMP1 protein promoted C666-1 cells undergo apoptosis. There was a 2-fold of C666-1 cells undergo apoptotic cell death than that of CNE2 cells at LD_{70}. All these findings suggested that EBV LMP1 was one of the therapeutic markers for NPC treatment.

In summary, our findings confirmed that H-ALA was effective to both EBV positive undifferentiated NPC cells/C666-1 and EBV negative poorly differentiated NPC cells/CNE2. H-ALA triggered apoptotic cell destruction in both C666-1 cells and CNE2 cells. A significant increase in EBV LMP1 protein expression was obtained in C666-1 cells. LMP1 protein could be a potential therapeutic marker for EBV positive NPC cells. Studies on the effect of H-ALA-mediated PDT on LMP1 induced signaling proteins will be reported in Chapter 3.

2.6 References

Agostinis P, Berg K, Cengel KA, Foster TH, Girotti AW, Gollnick SO, Golab J. (2011) Photodynamic therapy of cancer: an update. *CA Cancer J Clin, 61*(4), 250-281.

Bai DQ, Yow CMN, Tan Y, Chu ESM, Xu CS. (2010) Photodynamic action of LED-activated nanoscale photosensitizer in nasopharyngeal carcinoma cells. *Laser Physics, 20*(2), 7.

Bredell MG, Besic E, Maake C, Walt H. (2010) The application and challenges of clinical PD-PDT in the head and neck region: a short review. *J Photochem Photobiol B, 101*(3), 185-190.

Bruce-Micah R, Huttenberger D, Freitag L, Cullum J, Foth HJ. (2009) Pharmacokinetic of ALA and h-ALA induced porphyrins in the models Mycobacterium phlei and Mycobacterium smegmatis. *J Photochem Photobiol B, 97*(1), 1-7.

Brunner H, Hausmann F, Knuechel R. (2003) New 5-aminolevulinic acid esters--efficient protoporphyrin precursors for photodetection and photodynamic therapy. *Photochem Photobiol, 78*(5), 481-486.

Casas A, Perotti C, Saccoliti M, Sacca P, Fukuda H, Batlle AC. (2002) ALA and ALA hexyl ester in free and liposomal formulations for the photosensitisation of tumor organ cultures. *Br J Cancer, 86*, 7.

Chu ESM, Wu RWK, Yow CMN, Wong TK, Chen JY. (2006) The cytotoxic and genotoxic potential of 5-aminolevulinic acid on lymphocytes: a comet assay study. *Cancer Chemother Pharmacol, 58*(3), 408-414.

Dawson CW, Port RJ, Young LS. (2012) The role of the EBV-encoded latent membrane proteins LMP1 and LMP2 in the pathogenesis of nasopharyngeal carcinoma (NPC). *Semin Cancer Biol., 22*(2), 144-153.

Deng L, Yang J, Zhao XR, Deng XY, Zeng L, Gu HH, Cao Y. (2003) Cells in G2/M phase increased in human nasopharyngeal carcinoma cell line by EBV-LMP1 through activation of NF-κB and AP-1. *Cell Res, 13*(3), 8.

Dognitz N, Salomon D, Zellweger M, Ballini JP, Gabrecht T, Lange N, Wagnieres G. (2008) Comparison of ALA- and ALA hexyl-ester-induced PpIX depth distribution in human skin carcinoma. *J Photochem Photobiol B, 93*(3), 140-148.

Eleouet S, Rousset N, Carre J, Bourre L, Vonarx V, Lajat Y, Patrice T. (2000) In vitro fluorescence, toxicity and phototoxicity induced by delta-aminolevulinic acid (ALA) or ALA-esters. *Photochem Photobiol, 71*(4), 447-454.

Herrmann K, Niedobitek G. (2003) Epstein-Barr virus-associated carcinomas: facts and fiction. *J Pathol., 199*(2), 140-145.

Juzeniene A, Ma LW, Juzenas P, Iani V, Lange N, Moan J. (2002) Production of protoporphyrin IX from 5-aminolevulinic acid and two of its esters in cells in vitro and tissues in vivo. *Cell Mol Biol (Noisy-le-grand), 48*(8), 911-916.

Koon HK, Lo KW, Leung KN, Lung ML, Chang CC, Wong RN, Mak NK. (2010) Photodynamic therapy-mediated modulation of inflammatory cytokine

production by Epstein-Barr virus-infected nasopharyngeal carcinoma cells. *Cellular & Molecular Immunology, 7*(4), 323-326.

Lang F. (2009) *Encyclopedia of Molecular Mechanisms of Disease*: Berlin: Springer-Verlag GmbH.

Li L, Guo L, Tao Y, Zhou S, Wang Z, Luo W, Cao Y. (2007) Latent membrane protein 1 of Epstein-Barr virus regulates p53 phosphorylation through MAP kinases. *Cancer Lett., 255*(2), 219-231.

Lo AK, To KF, Lo KW, Lung RW, Hui JW, Liao G, Hayward SD. (2007) Modulation of LMP1 protein expression by EBV-encoded microRNAs. *Proc Natl Acad Sci U S A., 104*(41), 16164-16169.

Miller WE, Earp HS, Raab-Traub N. (1995) The Epstein-Barr virus latent membrane protein 1 induces expression of the epidermal growth factor receptor. *J Virol, 69*(7), 4390-4398.

Morrow DI, McCarron PA, Woolfson AD, Juzenas P, Juzeniene A, Iani V, Donnelly RF. (2010) Hexyl aminolaevulinate is a more effective topical photosensitiser precursor than methyl aminolaevulinate and 5-aminolaevulinic acids when applied in equimolar doses. *J Pharm Sci, 99*(8), 3486-3498.

Pattle SB, Farrell PJ. (2006) The role of Epstein-Barr virus in cancer. *Expert Opin Biol Ther., 6*(11), 1193-1205.

Peng Q, Warloe T, Berg K, Moan J, Kongshaug M, Giercksky KE, Nesland JM. (1997) 5-Aminolevulinic acid-based photodynamic therapy. Clinical research and future challenges. *Cancer, 79*(12), 2282-2308.

Raab-Traub N. (2002) Epstein-Barr virus in the pathogenesis of NPC. *Semin Cancer Biol, 12*(6), 431-441.

Radakovic-Fijan S, Rappersberger K, Tanew A, Honigsmann H, Ortel B. (1999) Ultrastructural Changes in PAM Cells After Photodynamic Treatment with Delta-Aminolevulinic Acid-Induced Porphyrins or Photosan. *J Invest Dermatol,* 112(3), 7.

Robertson CA, Evans DH, Abrahamse H. (2009) Photodynamic therapy (PDT): a short review on cellular mechanisms and cancer research applications for PDT. *J Photochem Photobiol B, 96*(1), 1-8.

Sizhong Z, Xiukung G, Yi Z. (1983) Cytogenetic studies on an epithelial cell line derived from poorly differentiated nasopharyngeal carcinoma. *Int J Cancer, 31*(5), 587-590.

Tsao SW, Tsang CM, Pang PS, Zhang G, Chen H, Lo KW. (2012a) The biology of EBV infection in human epithelial cells. *Semin Cancer Biol., 22*(2), 137-143.

Tulalamba W, Janvilisri T. (2012) Nasopharyngeal carcinoma signaling pathway: an update on molecular biomarkers. *Int J Cell Biol. , 2012*, 594681.

Wei KR, Xu Y, Liu J, Zhang WJ, Liang ZH. (2011) Histopathological Classification of Nasopharyngeal Carcinoma. *Asian Pac J Cancer Prev., 12*, 7.

Wu RWK, Chu ESM, Yow CMN, Chen JY. (2006) Photodynamic effects on nasopharyngeal carcinoma (NPC) cells with 5-aminolevulinic acid or its hexyl ester. *Cancer Lett., 242*(1), 112-119.

Yoshizaki T, Ito M, Murono S, Wakisaka N, Kondo S, Endo K. (2012) Current understanding and management of nasopharyngeal carcinoma. *Auris Nasus Larynx, 39*(2), 137-144.

Yow CMN, Mak NK, Leung AW, Huang Z. (2009) Induction of early apoptosis in human nasopharyngeal carcinoma cells by mTHPC-mediated photocytotoxicity. *Photodiagnosis Photodyn Ther, 6*(2), 122-127.

Yow CMN, Wu RWK, Huang Z. (2012) Comparison of Aminolevulinic Acid and Its Methyl Ester Mediated Photocytotoxicity on Human Nasopharyngeal Carcinoma Cells. *Journal of Innovative Optical Health Sciences, 05*(02), 1250007.

Zheng H, Li LL, Hu DS, Deng XY & Cao Y. (2007) Role of Epstein-Barr virus encoded latent membrane protein 1 in the carcinogenesis of nasopharyngeal carcinoma. *Cellular & Molecular Immunology, 4*(3), 185-196.

Chapter 3

H-ALA-PDT: Alteration of MAPK signaling proteins in NPC cells

Abstract was presented:

WU RWK, CHU ESM, LO KW, YOW CMN. 5-aminolevulinic acid hexyl ester (H-ALA)-PDT induces cell cycle arrest in Nasopharyngeal Carcinoma cells (C666-1). 18th Hong Kong International Cancer Congress. LKS Faculty of Medicine, The University of Hong Kong, HK. 3-5 November, 2011. Abstract no.: A33.

3.1 Abstract

Mitogen-activated protein kinases (MAPK) signaling pathway include the extracellular signal-regulated kinase (ERK), c-Jun N-terminal kinase (JNK) proteins and p38 mitogen-activated protein kinases (p38). Activation of MAPK signaling pathways was correlated with the EBV LMP1 protein expression in nasopharyngeal carcinoma (NPC) cells. Current finding also indicated that photosensitizers localized in mitochondria altered MAPK signaling pathways.

Hence in this study, the effects of H-ALA-PDT on MAPK related signaling proteins in C666-1 cells and CNE2 cells were examined.

Results indicated that H-ALA-PDT down-regulated different signaling proteins, includes EGFR signaling protein and MAPK signaling proteins (p38 and ERK).

Our study provided the first evidence of the H-ALA-PDT effect to regulate MAPK signal proteins in NPC cells. These findings echo with the previous finding of H-ALA-PDT induced apoptosis in NPC cells. *In vivo* studies of H-ALA-PDT are worth examined for the benefit of clinical PDT applications in EBV induced cancers.

3.2 Introduction

Photosensitizers are selectively localized in malignant or diseased lesions according to their physical and chemical properties. The intracellular localization of photosensitizers is vital for the determination of the primary target sites for tumour cell destruction and the alteration of signaling pathways (Joanna and Grant, 2007; Milla et al., 2013; Robertson et al., 2009).

Recent studies reported that destruction of tumour cells by photosensitizers localized in mitochondria altered MAPK signaling pathways, resulted in apoptotic cell destruction, inhibition of angiogenesis and cell migration (Bui-Xuan et al., 2010; Ji et al., 2010). Alteration of MAPK signaling pathways was also correlated with the EBV LMP1 protein expression in nasopharyngeal carcinoma (NPC) cells. Study also reported that the expression of ERK protein was regulated by the EGFR signaling proteins (Downward, 2003; Roberts & Der, 2007).

The MAPK signaling proteins consist of p38, JNK and ERK proteins. They are three important MAPK family signal proteins responsible for cell survival, cell growth and cell development via activation of downstream protein NF-kB. Up regulation of p38 protein in NPC cells regulated a wide range of cellular functions, including the self-sufficiency of growth signals, angiogenesis, tumour metastasis, regulation of the cell cycle, and protection against apoptosis (Roux & Blenis, 2004). Up regulation of JNK in NPC cells triggered cell survival via cell cycle deregulation (Eliopoulos & Young, 1998; Tsai et al., 2006). Up regulation of ERKs in NPC cells resulted in cell growth and cell development (Kung et al., 2011; Lo et al., 2013).

Our previous publication demonstrated that H-ALA was selectively localized in mitochondria, and thereby triggered apoptotic cell death (Chu et al., 2006; Wu et al., 2006). We also reported that H-ALA-PDT up-regulated LMP1 protein expression in C666-1 cells. All evidence suggested that H-ALA-PDT efficacy could be associated with MAPK signaling proteins alteration. Hence in this chapter, the effect of H-

ALA-PDT on EGFR protein; MAPK signaling proteins and their down-stream effectors and were determined using undifferentiated NPC cells/C666-1 and the poorly differentiated NPC cells/CNE2.

3.3 Methodology

3.3.1 Materials

The ALA hexylester (H-ALA) was kindly provided by Photocure (Oslo, Norway). The stock (1mM) and working solutions were prepared in PBS and freshly prepared with serum-free RPMI culture medium.

Primary antibodies of Mek, phospho-Mek, p38 and JNK were purchased from Cell Signaling Technology, Inc. (Danvers, MA). Primary antibodies of phosphorylated p38, phosphorylated JNK, ERK and phosphorylated ERK were purchased from BD transduction, Inc. Primary antibodies for EGFR and phospho-EGFR were purchased from Santa Cruz Biotech, Inc. Primary antibody for telomerase and GAPDH were purchased from Abcam, Inc. Secondary anti-mouse, anti-goat and anti-rabbit antibodies coupled with horseradish peroxidase conjugate were purchased from Cell Signaling Technology, Inc.

3.3.2 Elucidate the effect of H-ALA-PDT on MAPK and EGFR signal proteins in NPC cells

In order to elucidate the intracellular signal transduction pathways triggered by H-ALA-PDT in EBV positive and EBV negative cells, western blot analysis was applied specifically for three major members of the MAP-kinase family, namely p38MAPK, ERK, and JNK and the EGFR protein. The control cell and H-ALA-PDT treated cells from both adherent and non-adherent floating cells were washed with ice-cold PBS and lysed in 0.2 ml lysis buffer (50 mM Tris-HCl, 150 mM NaCl, 1% Nonidet 40, 0.5% (w/v) Na-deoxycholate, 2 mM phenylmethylsulfonyl fluoride, 1x protease inhibitors). Supernatant was collected from lysates by centrifugation at 14,000g for 30 minutes at 4 ^{o}C. An equal amount of protein (20µg) was subjected to 10% sodium dodecyl sulphate polyacrylamide gel electrophoresis before blotting onto a polyvinylidene difluoride membrane (Amersham Pharmacia Biotech, Piscataway, NJ). The membrane was blocked with 5% skimmed milk in tris-buffered saline with 0.05% Tween 20 (pH 7.6) for 1 hour at room temperature.

After blocking, the membrane was probed with specific-primary antibodies at 4 ^{o}C overnight. After washing, the membrane was incubated with secondary antibody coupled to horseradish peroxidase (Amersham and Pharmacia Biotech) for 1 hour at room temperature. The antibody-antigen binding was then detected using an ECL chemiluminescence detection system according to the manufacturer's instructions and visualized by Bio-Rad Chemi Doc™ EQ densitometer (Bio-Rad laboratories, USA). The intensities of the protein bands were normalized and compared by Bio-Rad Quantity One software (Bio-Rad laboratories, USA).

3.3.3 Statistical analysis

All data were processed and presented by GraphPad Prism (Version 5.01) (GraphPad Software, Inc.). Mean and standard deviation (SD) were used to present data and all graphical error bars were represented in SD. Quantitative data from three independent experiments were used for analysis from Western blotting. One-way analyze of variance (ANOVA) followed by Dunnett correction was used to analyze differences between groups by the GraphPad Prism (Version 5.01) (GraphPad Software, Inc.). A P-value of less than 0.05 was considered as significant different.

3.4 Results

3.4.1. H-ALA-PDT induced modulation of MAPK proteins and their down-stream proteins in NPC cells

Effect of H-ALA-PDT on MAPK signaling proteins modulation was evaluated by Western blot analysis. The expression of the phosphorylated and total proteins of p38, JNK, and ERK were found in both C666-1 cells and CNE2 cells. A significant decrease in phosphorylated p38 (p-p38) proteins was obtained at LD_{70} in both C666-1 cells and CNE2 cells ($P<0.05$). A significant decrease in phosphorylated ERK (p-ERK) proteins was also obtained at LD_{70} in CNE2 cells ($P<0.05$). At LD_{70}, 25% decrease of p-p38 and ERK proteins were obtained in C666-1 cells while 35% decrease of p38 and ERK proteins were obtained in CNE2 cells, respectively. These results suggested that H-ALA mediated PDT inhibited phosphorylated form of p38 and ERK protein expression in NPC cells. Down-regulation of MAPK signaling proteins by H-ALA-PDT were summarized in Figures 3.1.

The expression of MAPK downstream transcription factors, NF-kB proteins, was not altered by H-ALA-PDT. Figure 3.2 shows that no significant changes of NF-kB protein expression observed in both NPC cell lines after H-ALA-PDT.

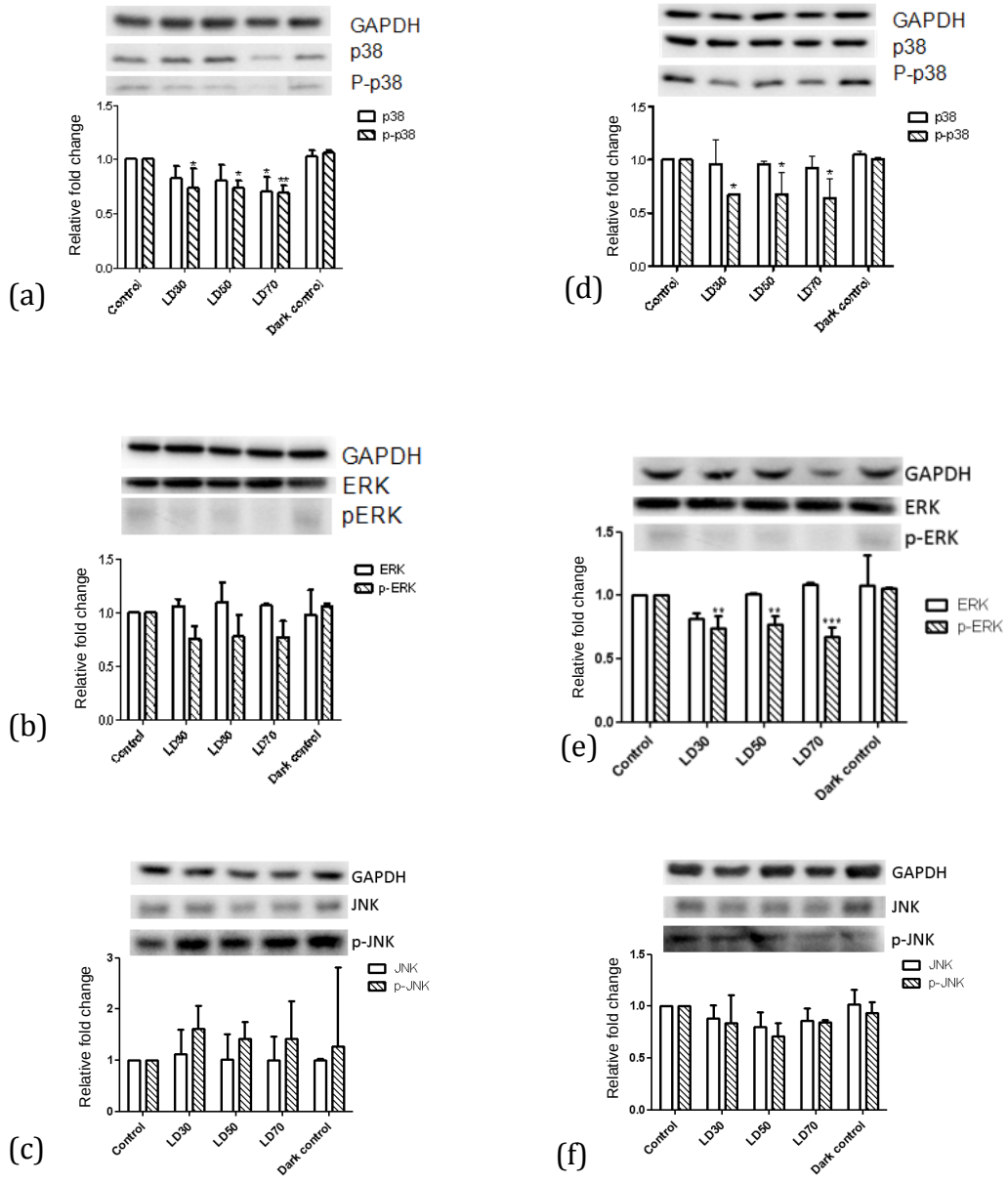

Fig 3.1 Effects of H-ALA mediated PDT on the p38, Phospho-p38, Erk, Phospho-Erk, JNK and Phospho-JNK protein expression in C666-1 cells and CNE2 cells.

Total cellular proteins were extracted from control and PDT treated cells for the detection of MAPK signal proteins by western blot analysis. Results were normalized with GAPDH protein.
a-c: C666-1 cells; d-f: CNE2 cells.
Significant difference between treatment and control groups were analyzed by one-way ANOVA and followed by Dunnett's post-tests (* $p<0.05$, ** $p<0.01$, *** $p<0.001$).

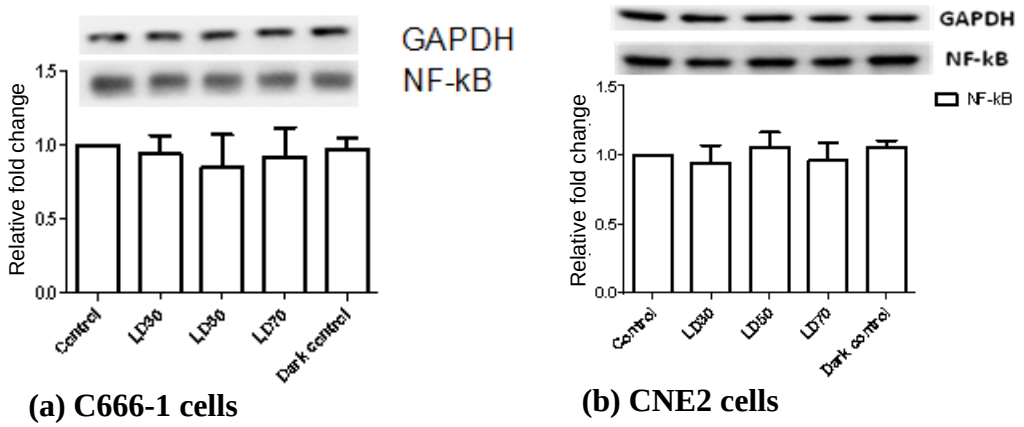

Fig 3.2 Effects of H-ALA mediated PDT on the NF-kB protein expression in C666-1 cells and CNE2 cells. Total cellular proteins were extracted from control and PDT treated cells for western blot analysis. Housekeeping protein GAPDH was used as control to normalize the protein amounts in different treatment. Figure a showed NF-kB protein expression in C666-1 cells; Figure b showed NF-kB protein expression in CNE2 cells. Significant differences between treatment and control groups were analyzed by one-way ANOVA and followed by Dunnett's post-tests (* $p<0.05$, ** $p<0.01$).

3.4.2 H-ALA altered EGFR protein expression in NPC cells

Effect of H-ALA-PDT on EGFR protein expression was determined by Western blot analysis. Results shown in Figure 3.3 indicated that H-ALA-PDT down-regulated EGFR proteins in both C666-1 cells and CNE2 cells with a 12% and 55% decrease at LD_{70}, respectively. All these results confirmed that H-ALA mediated PDT suppressed EGFR signaling pathways. It is also suggested that the down-regulation of EGFR proteins was correlated with the ERK protein expression.

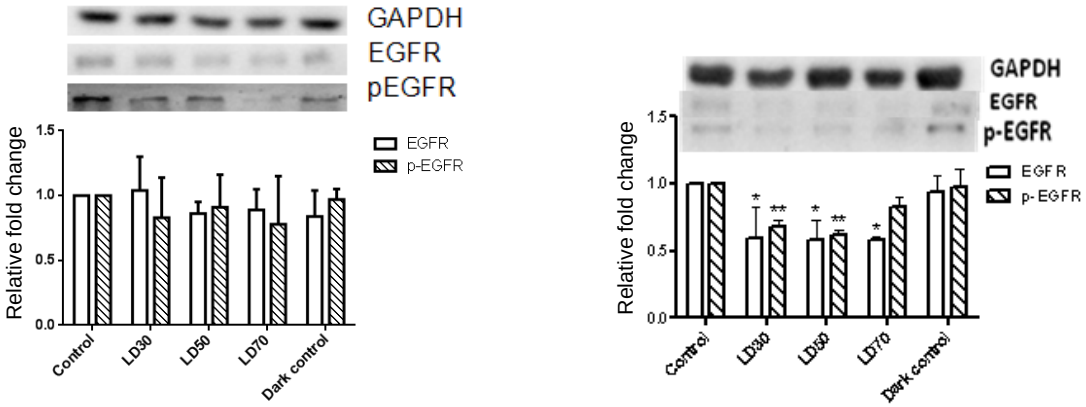

(a) C666-1 cells **(b) CNE2 cells**

Fig 3.3 Effect of H-ALA mediated PDT on the EGFR proteins expression in C666-1 cells and CNE2 cells. Total cellular proteins were extracted from control and PDT treated cells for western blot analysis. Housekeeping protein GAPDH was used as control to normalize the protein amounts in different treatment. Figure a showed EGFR proteins expression in C666-1 cells; Figure b showed EGFR proteins expression in CNE2 cells. Significant difference between treatment and control groups were analyzed by one-way ANOVA and followed by Dunnett's post-tests (* $p<0.05$, ** $p<0.01$).

3.5 Discussion

According to previous studies, it was confirmed that mitochondrion was the major target site of H-ALA induced PpIX accumulation in NPC cells regardless the differentiation status of the cells (Chu et al., 2006; Wu et al., 2006; Yow et al., 2012). Studies indicated that MAPK signaling proteins expression was altered by photosensitizers which localized in mitochondria (Chen et al., 2011; Dougherty et al., 1998). Yet the alteration of signal transduction pathways mediated by PDT varied with the cell types and photosensitizer employed.

MAPK signaling proteins work uniquely in NPC cells because of their interaction with LMP1 protein. In NPC cells, up-regulation of MAPK signaling pathways played a vital role in tumour development. Up regulation of p38 protein controlled a wide range of cellular functions, including the self-sufficiency of growth signals, tumour metastasis, regulation of the cell cycle, and prevention of apoptosis (Roux & Blenis, 2004). ERK is another MAPK signaling protein constitutively expressed in NPC with a diverse range of cellular functions, including cell growth and development. Phosphorylation of ERK was associated with EGFR signaling protein, resulted in activation of downstream effector proteins such as NF-kB (Downward, 2003; Oka et al., 1995; Roberts & Der, 2007; Schmidt et al., 1997). Constitutively active ERK protein has been reported to deregulate cell cycle in NPC cells (Kerkhoff & Rapp, 1998; Zhang et al., 2007). All these evidence suggested that down-regulation of MAPK signaling proteins could result in cell elimination.

Figure 3.3 summarized the protein targets of H-ALA-PDT. Our findings demonstrated that H-ALA-PDT down-regulated p38, EGFR and phosphorylated ERK protein expression in both C666-1 cells and CNE2 cells, resulted in cell destruction. Similar results were reported by other researchers. Deng reported that down-regulation of ERK protein expression in CNE2 cells by microRNA resulted in tumour growth suppression (Deng et al., 2011). Chan et al. (2009) reported that inhibition of p38 expression enhanced hypericin PDT efficacy in HK1 cells, resulted

as apoptotic cell death. All these evidence confirmed that modulation of p38, ERK and EGFR proteins in NPC cell are vital for cell elimination.

To sum up, H-ALA-PDT has shown to be an effective treatment option for C666-1 cells and CNE2 cells *in vitro*. Continuing work in this field will further elucidate the routes of mechanisms mediated by H-ALA-PDT, and establish H-ALA-PDT as a minimally invasive and focal treatment option for NPC treatment.

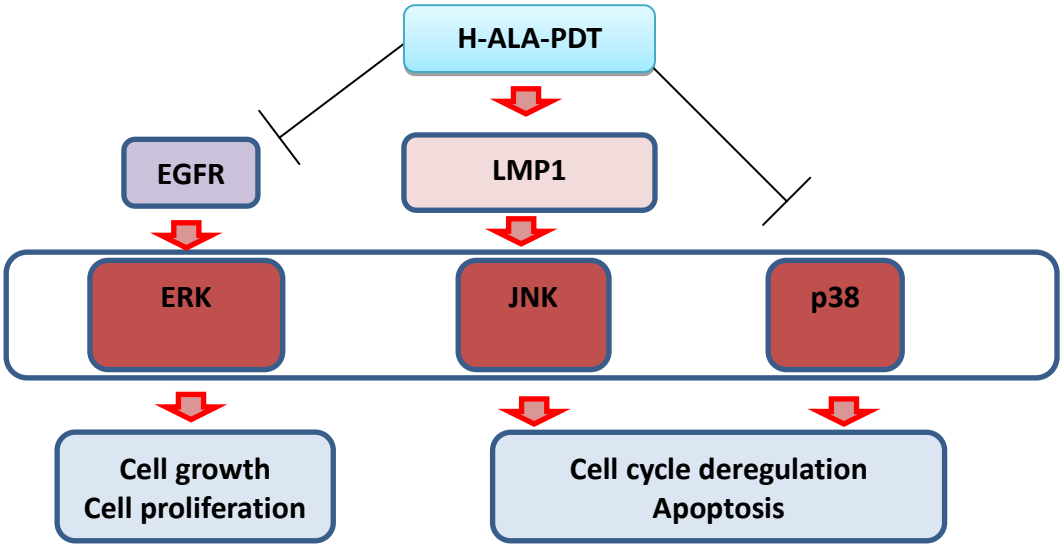

Figure 3.3 Diagram illustrates the effects of H-ALA mediated PDT on MAPK signal pathways in NPC cells.

→ Stimulatory effect. ⟞ Inhibitory effect.

3.6 References

Agostinis P, Berg K, Cengel KA, Foster TH, Girotti AW, Gollnick SO, Golab J. (2011) Photodynamic therapy of cancer: an update. *CA Cancer J Clin, 61*(4), 250-281.

Bredell MG, Besic E, Maake C, Walt H. (2010) The application and challenges of clinical PD-PDT in the head and neck region: a short review. *J Photochem Photobiol B, 101*(3), 185-190.

Brown SB, Brown EA, Walker I. (2004) The present and future role of photodynamic therapy in cancer treatment. *Lancet Oncol, 5*(8), 497-508.

Bruce-Micah R, Huttenberger D, Freitag L, Cullum J, Foth HJ. (2009) Pharmacokinetic of ALA and h-ALA induced porphyrins in the models Mycobacterium phlei and Mycobacterium smegmatis. *J Photochem Photobiol B, 97*(1), 1-7. 4

Bui-Xuan NH, Tang PM, Wong CK, Fung KP. (2010) Photo-activated pheophorbide-a, an active component of Scutellaria barbata, enhances apoptosis via the suppression of ERK-mediated autophagy in the estrogen receptor-negative human breast adenocarcinoma cells MDA-MB-231. *J Ethnopharmacol, 131*(1), 95-103.

Casas A, Perotti C, Saccoliti M, Sacca P, Fukuda H, Batlle AC. (2002) ALA and ALA hexyl ester in free and liposomal formulations for the photosensitisation of tumor organ cultures. *Br J Cancer, 86*, 7.

Chan PS, Koon HK, Wu ZG, Wong RN, Lung ML, Chang CK, Mak NK. (2009) Role of p38 MAPKs in hypericin photodynamic therapy-induced apoptosis of nasopharyngeal carcinoma cells. *Photochem Photobiol*. 85(5): 1207-17.

Chen X, Zhao P, Chen F, Li L, Luo R. (2011) Effect and mechanism of 5-aminolevulinic acid-mediated photodynamic therapy in esophageal cancer. *Lasers Med Sci, 26*(1), 69-78.

Chu ESM, Wu RWK, Yow CMN, Wong TK, Chen JY. (2006) The cytotoxic and genotoxic potential of 5-aminolevulinic acid on lymphocytes: a comet assay study. *Cancer Chemother Pharmacol, 58*(3), 408-414.

Chu ESM, Yow CMN. (2012) Modulation of telomerase and signal transduction proteins by hexyl-ALA-photodynamic therapy (PDT) in human doxorubicin resistant cancer cell models. *Photodiagnosis Photodyn Ther, 9*(3), 243-255.

Deng M, Tang H, Zhou M, Xiong W, Zheng Y, Ye Q, Zeng X, Liao Q, Guo X, Li X, Ma J, Li G. (2011) miR-216b suppresses tumor growth and invasion by targeting KRAS in nasopharyngeal carcinoma. *J Cell Sci*. 124(Pt17): 2997-3005.

Dougherty TJ, Gomer CJ, Henderson BW, Jori G, Kessel D, Korbelik M, Peng Q. (1998) Photodynamic therapy. *J Natl Cancer Inst, 90*(12), 889-905.

Downward J. (2003) Targeting RAS signalling pathways in cancer therapy. *Nat Rev Cancer, 3*(1), 11-22.

Eleouet S, Rousset N, Carre J, Bourre L, Vonarx V, Lajat Y, Patrice T. (2000) In vitro fluorescence, toxicity and phototoxicity induced by delta-aminolevulinic acid (ALA) or ALA-esters. *Photochem Photobiol, 71*(4), 447-454.

Eliopoulos AG, Young LS. (1998) Activation of the cJun N-terminal kinase (JNK) pathway by the Epstein-Barr virus-encoded latent membrane protein 1 (LMP1). *Oncogene, 16*(13), 1731-1742.

Joanna G and Grant F. (2007) The current role of photodynamic therapy in oesophageal dysplasia and cancer. *Photodiag Photodyn ther*. 4(3), 151-9.

Ji HT, Chien LT, Lin YH, Chien HF, Chen CT. (2010) 5-ALA mediated photodynamic therapy induces autophagic cell death via AMP-activated protein kinase. *Mol Cancer, 9*, 91.

Juzeniene A, Ma LW, Juzenas P, Iani V, Lange N, Moan J. (2002) Production of protoporphyrin IX from 5-aminolevulinic acid and two of its esters in cells in vitro and tissues in vivo. *Cell Mol Biol (Noisy-le-grand), 48*(8), 911-916.

Kerkhoff E, Rapp UR. (1998) Cell cycle targets of Ras/Raf signalling. *Oncogene, 17* (11), 1457-1462.

Kung CP, Meckes DG, Jr, Raab-Traub N. (2011) Epstein-Barr virus LMP1 activates EGFR, STAT3, and ERK through effects on PKCdelta. *J Virol, 85*(9), 4399-4408.

Lo AK, Lo KW, Ko CW, Young LS, Dawson CW. (2013) Inhibition of the LKB1-AMPK Pathway by the Epstein-Barr Virus-encoded LMP1 Promotes Proliferation and Transformation of Human Nasopharyngeal Epithelial Cells. *J Pathol*. 230(3), 336-346.

Milla SL, Rodriguez ME, Cogno IS, Rumie Vittar NB, Pansa MF, Lamberti MJ, Rivarola VA. (2013) Direct and indirect photodynamic therapy effects on the cellular and molecular components of the tumor microenvironment. *Biochim Biophys Acta.* 1832(1), 36-45

Oka H, Chatani Y, Hoshino R, Ogawa O, Kakehi Y, Terachi T, Yoshida O. (1995) Constitutive activation of mitogen-activated protein (MAP) kinases in human renal cell carcinoma. *Cancer Res, 55*(18), 4182-4187.

Roberts PJ, Der CJ. (2007) Targeting the Raf-MEK-ERK mitogen-activated protein kinase cascade for the treatment of cancer. *Oncogene, 26*(22), 3291-3310.

Robertson CA, Evans DH, Abrahamse H. (2009) Photodynamic therapy (PDT): a short review on cellular mechanisms and cancer research applications for PDT. *J Photochem Photobiol B.* 96(1), 1-8.

Roux, P. P., & Blenis, J. (2004). ERK and p38 MAPK-activated protein kinases: a family of protein kinases with diverse biological functions. *Microbiol Mol Biol Rev, 68*(2), 320-344.

Schmidt CM, McKillop IH, Cahill PA, Sitzmann JV. (1997) Increased MAPK expression and activity in primary human hepatocellular carcinoma. *Biochem Biophys Res Commun, 236*(1), 54-58.

Tsai CL, Li HP, Lu YJ, Hsueh C, Liang Y, Chen CL, Chang YS. (2006) Activation of DNA methyltransferase 1 by EBV LMP1 Involves c-Jun NH(2)-terminal kinase signaling. *Cancer Res, 66*(24), 11668-11676.

Wu RWK, Chu ESM, Yow CMN, Chen JY. (2006) Photodynamic effects on nasopharyngeal carcinoma (NPC) cells with 5-aminolevulinic acid or its hexyl ester. *Cancer Lett., 242*(1), 112-119.

Yow CMN, Wu RWK, Huang Z. (2012) Comparison of Aminolevulinic Acid and Its Methyl Ester Mediated Photocytotoxicity on Human Nasopharyngeal Carcinoma Cells. *Journal of Innovative Optical Health Sciences, 05*(02), 1250007. Zhang, Z., Sun, D., Van do, N., Tang, A., Hu, L., & Huang, G. (2007). Inactivation of RASSF2A by promoter methylation correlates with lymph node metastasis in nasopharyngeal carcinoma. *Int J Cancer, 120*(1), 32-38.

Chapter 4

FosPeg® mediated photodynamic therapy with LED activation induced LMP1 protein expression in EBV positive C666-1 cell line

Manuscript was published:

WU RWK, CHU ESM, HUANG Z, XU CS, IP CW, YOW CMN. FosPeg® PDT alters the EBV miRNAs and LMP1 protein expression in EBV positive nasopharyngeal carcinoma cells. PhotoChem PhotoBio B. 127(5): 114-122, 2013.

An abstract was published:

WU RWK, CHU ESM, Huang Z, YOW CMN. FosPeg® mediated photodynamic therapy with LED activation induced LMP1 protein expression in EBV positive C666-1 cell line. The 14th world congress of the International Photodynamic Association. (IPA), Seoul, Republic of Korea, 28 May -31May, 2013.

4.1 Abstract

Nasopharyngeal carcinoma (NPC) is one of the top ten cancers highly prevalent in Hong Kong and Southern China. Epstein-Barr virus (EBV) infection contributes to the tumourigenesis of NPC through the expression of different viral proteins. Among these, latent membrane protein 1 (LMP1) is the major oncoprotein expressed by EBV. Foscan® (Biolitec AG), m-tetrahydroxyphenylchlorin (mTHPC)-based photosensitizing drug, has been used in the photodynamic therapy (PDT) for head and neck cancers. FosPeg® (Biolitec AG) is a new formulation of mTHPC encapsulated in PEGylated liposomes with optimized distribution properties. In this *in vitro* study, the potential of FosPeg® PDT on human EBV positive NPC cells (C666-1) and EBV negative cells (HK1 and CNE2) were investigated. Effects of FosPeg® PDT on the expression of EBV BART miRNAs (EBV miRNA BART 1-5p, BART 16, and BART 17-5p), LMP1 mRNA and proteins on C666-1 cells were also elucidated.

The killing efficacy of FosPeg®-PDT on NPC cells was determined by MTT assay after LED activation. Effects of FosPeg®-PDT on the expression of LMP1 mRNA and protein were examined by real time PCR and western blot analysis. FosPeg®-PDT demonstrated its antitumour effect on C666-1 cells in a drug and light dose dependent manner. LD_{30}, LD_{50} and LD_{70} were achieved by applying LED activation (3 J/cm^2) at 4 hour post incubated cells with 0.05 μg/ml, 0.07 μg/ml and 0.3 μg/ml FosPeg®, respectively. Up-regulation of both LMP1 mRNA and protein were obtained after FosPeg®-PDT in a dose dependent manner in C666-1 cells. Understanding the mechanism of FosPeg® PDT may help to develop an alternative treatment for NPC.

4.2 Introduction

Nasopharyngeal Carcinoma (NPC) is one of the top ten cancers highly prevalent in Southern China, especially in Hong Kong and Guangdong (Hong Kong Cancer Registry, 2011; Wei et al., 2011). NPC encompasses any squamous cell carcinoma arising in the epithelial lining of the nasopharynx, a tubular space situated at the base of the skull. Different from other head and neck cancers, NPC is strongly associated with Epstein-Barr virus (EBV). EBV is a herpes virus that infects over 90% of adult population worldwide (Tsao et al., 2012). It is known as the most potent transforming agent for human cells and is associated with a number of malignancies including Burkitt's lymphoma, nasopharyngeal carcinoma, T cell lymphomas, lung carcinoma and gastric carcinoma (Herrmann & Niedobitek, 2003; Pattle & Farrell, 2006). The tumourigenic potential of EBV is mainly related to a unique set of latent gene products including the latent membrane proteins (LMP1, LMP2A, LMP2B) and EBV-determined nuclear antigens (EBNA1 and EBNA2) (Tsao et al., 2012). Among these, LMP1 is the principal oncogene involved in the process of EBV-associated oncogenesis of NPC (Dawson et al., 2012; Lo et al., 2007). LMP1 abnormally activates a number of signaling pathways in NPC cells, including the nuclear factor kappa B (NF-kB) and mitogen-activated protein kinases (MAPK) pathways, and resulted in inhibiting apoptosis; inducing cell immortality; promoting cell proliferation; and influencing the cell invasion and metastasis (Lo et al., 2007; Tulalamba & Janvilisri, 2012). Interestingly, several studies revealed that transforming potential of LMP1 was dose-dependent (Deng et al., 2003).

EBV was the first human virus reported to encode micro-RNAs (miRNAs). miRNA is a class of 20-25-nucleotide non-coding RNA which could bind with their target mRNA, leading to inhibition of gene expression (Marquitz & Raab-Traub, 2012). EBV encoded miRNAs were found mainly in two clusters, which namelly as the BamHI-A rightward transcripts (BARTs) cluster 1 and 2. Recently, researchers have identified at least three BARTs cluster 1 miRNAs (ebv-miR-BART1-5p, 16 and 17-

5p) targeting the LMP1 gene and down regulating the LMP1 protein expression (He et al., 2012; Lo et al., 2012; Lo et al., 2007).

The conventional treatments for NPC are radiotherapy and chemotherapy (Razak et al., 2010; Tang et al., 2011). However, different complications were resulted after receiving them and were mainly caused by radiation toxicities, distant recurrence and development of multi-drug resistance phenotypes (Caponigro et al., 2010; Suarez et al., 2010). Alternative treatment is advisable to NPC as it is often inoperable because of its complex anatomical location (Brennan, 2006; Tao & Chan, 2007). In order to develop improved therapeutic strategies, Photodynamic therapy (PDT) shed light on the development of NPC treatment (Koon et al., 2010; Wu et al., 2006; Yow et al., 2009). As a potential powerful treatment for cancer, PDT could be applied solitary or in combination with chemotherapy, radiotherapy, or surgery.

Photodynamic therapy (PDT) is an evolving cancer treatment regimen with approval for application in USA, EU, Canada, Russia and Japan. PDT uses a combination of photosensitizing agents (PSs), visible light and molecular oxygen to selectively destroy the biological targets in tumour cells. None of these is individually toxic, but together they initiate photo-destruction to biological targets. Effectiveness of PDT depends on the tumour localizing photosensitizer, which absorbs light to produce reactive oxygen species (ROS) (Agostinis et al., 2011; Bredell et al., 2010; Robertson et al., 2009). Advanced development of light source could also enhance the PDT efficiency. The clinical efficacy of PDT depends on complex dosimetry, including total light dose, light exposure time, and light delivery mode. Light-emitting diodes (LEDs) is one of the alternative light sources with several advantages, such as relatively narrow spectral bandwidths, high fluency rates, small and cost-effective, simple to install, and a longer operational life (Agostinis et al., 2011; Robertson et al., 2009). A novel light source with light emitting diode (LED) has been setup by our group showing promising results in activation of the nano-photosensitizer hypocrellin in nasopharyngeal carcinoma cells (Bai et al., 2010).

FosPeg® (Biolitec AG) is the derivative of meta-tetra (hydroxyphenyl) chlorine (mTHPC) contained in PEGylated liposomes. mTHPC is a chlorine-like 2nd generation photosensitizer which has been shown to be highly effective in treating skin, prostate and pancreatic cancer (Senge, 2012; Senge & Brandt, 2011). However, the major drawback of mTHPC is related to its photochemical properties. The hydrophobicity of mTHPC leads to poor solubility in physiologically acceptable media and complicates its formulation, administration and bio-distribution. Thus the liposomal formulations using PEGylated liposomes as the nanocarriers to encapsulate mTHPC have been developed. The aim of using liposomes with long-circulating polyethylene glycol (PEG) as an improved delivery system is to enhance its therapeutic effects by solubilizing the photosensitizer at suitable concentration, increasing drug uptake as well as tumour eradication (Lassalle et al., 2009; Reshetov et al., 2012).

This study aims to investigate the photodynamic efficacy of FosPeg® - a new liposomal formulation of mTHPC in EBV positive and EBV negative NPC cell lines and to reveal the effect of FosPeg®-PDT on the expression of LMP1 at both molecular and protein levels.

4.3Materials and Methods

4.3.1. Materials

FosPeg® (1.5 mg mTHPC/ml) was kindly provided by Biolitec AG (Jena, Germany). FosPeg® stock solution (10 μg/ml) was prepared in miliQ water.

3-(4,5-dimethylthiazol-2-yl)-2,5-diphenyltetrazolium bromide (MTT) and propidium iodide (PI) were purchased from Sigma Chemical Co. (Sigma-Aldrich, St. Louis, MO, USA). Primary antibody for GAPDH protein was purchased from Abcam, Inc. Primary mouse anti-LMP1 antibody (CS1-4) was purchased from Dako (Glastrup, Denmark). Secondary anti-mouse antibody was purchased from Cell Signaling Technology, Inc. (Danvers, MA, USA).

NPC cells (3×10^4 cells/well) were seeded in 96-well tissue culture plates and incubated with 0.03-0.3 μg/ml FosPeg® for 4 hours. Cells then were irradiated with 0 –3 J/cm^2 of light emitting diode (LED) light as descripted in chapter 2.

4.3.2. Cell culture

EBV-positive NPC cell line (C666-1), an undifferentiated NPC cell line and EBV-negative NPC cell line (HK1), a highly differentiated NPC cell line were kindly provided by Anatomical and Cellular Pathology Department, The Chinese University of Hong Kong (Cheung et al., 1999; Huang et al., 1980). EBV-negative NPC cell line (CNE2), a poorly differentiated NPC cell line was purchased from Shanghai Biosis Biotechnology Co., Ltd. (Shanghai, China). The C666-1 cells were cultured in RPMI 1640 supplemented with 10% fetal bovine serum (FBS; Gibco BRL, Carlsbad, CA, USA), 1% glutamax and 1% antibiotics PSN (Gibco BRL, Carlsbad, CA, USA). The HK1 and CNE2 cells were cultured in RPMI-1640 supplemented with 10% fetal bovine serum (FBS; Gibco BRL, Carlsbad, CA, USA) and 1% antibiotics PS. Cells were grown at 37 ^{o}C in a humidified 5% CO_2 incubator.

4.3.3. Examination of intracellular drug uptake and localization

Sub-confluent NPC cells were incubated with FosPeg® (0.1 μg/ml) in dark for 1, 2, 4, 8 and 24 hours. Cells were then washed and re-suspended in PBS. Cellular uptake of FosPeg® was determined by flow cytometry (Cytomics FC500, Beckman Coulter) equipped with a 15 mW argon ion laser providing excitation light at 488 nm. Cell suspensions were excited and the fluorescence signal of drug uptake by the cells was detected by a photomultiplier tube with a 610 nm long-pass filter. A minimum of 10,000 cells per sample was analyzed in three independent experiments. The uptake of FosPeg® in terms of mTHPC fluorescence intensity at single-cell level was acquired (Wu et al., 2006).

To determine the intracellular localization of FosPeg®, cells were incubated with FosPeg® (1 μg/ml) for 4 hours in darkness followed by co-incubation with 100 nM MitoTracker Green (Molecular Probe, Invitrogen, Carlsbad, CA, USA) and LysoTracker Green (Molecular Probe, Invitrogen, Carlsbad, CA, USA) for 30 minutes at 37 ^{o}C with 5% CO_2. The MitoTracker Green and LysoTracker Green were two fluorescent probes used specifically for the identification of sub-cellular organelles of the mitochondria and lysosomes, respectively. Prior to the visualization, the excess probes were washed off and the image analysis was accomplished with a fluorescence microscope (EZ-C1, Nikon). The fluorescent images were captured with a magnification of 400x. All parameters were kept constant to ensure reliable comparison throughout the experiment. The imaging measurements were repeated at least six times and several hundred cells were observed. Coloicalisation analysis was performed by using software image J.

4.3.4. 3-(4,5-dimethylthiazol-2-yl)-2,5-diphenyltetrazolium bromide (MTT) assay

The NPC cells (3 x 10^4 cells/well) were seeded in 96 well plates for 24 hours and incubated with a range of 0.03 – 0.3μg/ml FosPeg® for 4 hours. Light irradiated cells were washed and further incubated for 24 hours. MTT (5 mg/ml) was added to

each well and incubated for 3 hours. Viable cells took up MTT and reduced it to form dark blue water insoluble formazan by the mitochondrial dehydrogenase. The ability to form formazan refers to the normal function of the mitochondria and is used for the study of cell viability. To lyse cells and dissolve formazan crystals, 100 µl of dimethyl sulfoxide (DMSO, 99.9%, Sigma-Aldrich, St. Louis, MO, USA) was added to each well and the optical density was measured at 570 nm using the spectrophotometer (Benchmark Plus, Bio-Rad). All results were presented in triplicate as the mean ± SD.

Cell viability was calculated as:

Cell viability (%) = (mean OD value of treated cells ÷ mean OD value of control cells) × 100%

4.3.5. Quantitative real-time PCR

Evaluation of EBV LMP1 mRNA

NPC cells (10^6 cells/dish) were either treated as dark control cells (0.3 µg/ml FosPeg® without light irradiation) or at the LD_{30}, LD_{50} and LD_{70} PDT doses. To evaluate the modulation of LMP1 mRNA expression levels, qPCR was performed using the ABI PRIME 7500 Sequence Detection System (ABI life technologies, Foster City, CA, USA). PCR primers and TaqMan probe used for targeting LMP1 mRNA were followed as Ryan *et al.* (2004) described: LMP1 (Forward 5-CAG TCA GGC AAG CCT ATG A-3; Reverse 5-CTG GTT CCG GTG GAG ATG A-3; Probe 5-(6FAM)GTC ATA GTA GCT TAG CTG AAC(TAMRA)-3) (ABI life technologies, Foster City, CA, USA). At 24 hours post-PDT, the cells were harvested and the total RNA was extracted using the High Pure RNA isolation kit (Roche, USA) according to the manufacturer's specifications. Concentration of RNA in extracted samples was measured by nanodrop ND-2000 spectrophotometer (Nanodrop Technologies Inc., Wilmington, DE, USA). The extracted RNA (2 µg) from each tested sample was synthesized to cDNA using Transcriptor First Strand cDNA Synthesis Kit (Roche, USA) according to the manufacturer's specifications.

For qPCR, 20 ng of cDNA was used for each reaction with a final volume of 20 μL, containing 200 nM primers and 100 nM probe. The cycling condition for PCR were 50 ^{o}C for 5 minutes, 95 ^{o}C for 10 minutes followed by 50 cycles each of 95 ^{o}C for 15 s and finally 60 ^{o}C for 1 minute. Each sample was run in triplicate and mean/standard deviation cycle threshold values were determined. Results were normalized with endogenous reference gene GAPDH. Calculation of the relative expression values (fold change or ($2^{-(\Delta\Delta Ct)}$)) of LMP1 gene was performed using the comparative threshold cycle (Ct) method.

Evaluation of EBV BART miRNAs

To evaluate the alteration of BART miRNAs after PDT treatment, qPCR was performed using the reagents and protocols of the TaqMan MicroRNA Reverse Transcription and TaqMan MicroRNA Assay kits (ABI life technologies, Foster City, CA, USA). Total RNA was extracted from pre- and post-PDT treated NPC cells with the mirVana™ miRNA Isolation Kit (ABI life technologies, Foster City, CA, USA). The quality and quantity of the extracted RNA was assessed by nanodrop. The total RNA isolated (10 ng) was reverse transcribed with specific stem-loop primers and the TaqMan MicroRNA Reverse Transcription kit. Stem-loop specific primers were specific to EBV miRNA BART 1-5p, BART 16, and BART 17-5p. The small cellular nuclear RNA RNU48 was used as the internal control for normalization as recommended by the manufacturer. For qPCR, the cycling conditions for PCR were 50 ^{o}C for 5 minutes, 95 ^{o}C for 10 minutes followed by 45 cycles each of 95 ^{o}C for 15 seconds and finally 60 ^{o}C for 1 minute. Each sample was run in triplicate and mean/standard deviation cycle threshold values were determined. Results were normalized with RNU48. Calculation of the relative expression values (fold change or ($2^{-(\Delta\Delta Ct)}$)) of all three EBV miRNA genes were performed using the comparative threshold cycle (Ct) method.

4.3.6. Western blot analysis

Whole cells were collected from both adherent and non-adherent floating cells and washed with ice-cold PBS and lysed in 0.2 ml lysis buffer (50 mM Tris-HCl, 150 mM NaCl, 1% Nonidet 40, 0.5% (w/v) Na-deoxycholate, 2 mM phenylmethylsulfonyl fluoride, 1x protease inhibitors). Supernatant collected from cell lysates was then removed by centrifugation at 14,000g for 30 minutes at 4 ^{o}C. An equal amount of protein was subjected to 10% sodium dodecyl sulphate polyacrylamide gel electrophoresis before blotting onto a polyvinylidene difluoride membrane (Amersham Pharmacia Biotech, Piscataway, NJ, USA). The membrane was blocked with 5% skimmed milk in tris-buffered saline with 0.05% Tween 20 (pH 7.6) for 1 hour at room temperature. After blocking, the membrane was probed with a LMP1-primary antibody at 4 ^{o}C overnight. After washing, the membrane was incubated with a secondary anti-mouse antibody coupled to horseradish peroxidase (Amersham and Pharmacia Biotech) for 1 hour at room temperature. The antibody-antigen binding was then detected using an ECL chemiluminescence detection system according to the manufacturer's instructions and visualized by Bio-Rad Chemi Doc™ EQ densitometer (Bio-Rad laboratories, USA). The intensities of the protein bands were normalized and compared by Bio-Rad Quantity One software (Bio-Rad laboratories, USA).

4.3.7. Statistical analysis

All data were processed and presented by GraphPad Prism (Version 5.01) (GraphPad Software, Inc.). Mean and standard deviation (SD) were used to present data and all graphical error bars were represented in SD. Quantitative data from three independent experiments were used for analysis of the cell cycle progression, qPCR and western blotting. One-way analyze of variance (ANOVA) followed by Dunnett correction or two-way ANOVA followed by Bonferroni's correction post-hoc test was used to analyze differences between groups by the software (GraphPad Prism Version 5.01). Correlation between the expression of LMP1 miRNA, mRNA and proteins were analysed using Pearson correlation test. A P-value of less than 0.05 was considered as significant different.

4.4 Results

4.4.1 Intracellular accumulation FosPeg® in NPC cells

The cellular localization of photosensitizer is one of the important factors affecting PDT efficiency. The cellular accumulation of FosPeg® in C666-1, HK1 and CNE2 cells with different incubation times of drug (0.1 μg/ml, 1–24 hours) were determined by flow cytometry. Figure 4.1 summarized the kinetics of cellular accumulation of FosPeg® and showed a rise for up to 24 hours of incubation. The uptake kinetic pattern of FosPeg® in HK1 cells and CNE2 cells were similar, whereas more FosPeg® uptake was obtained after 8 hours of incubation in C666-1 cells. The data showed that 4 hour incubation demonstrated similar intracellular uptake concentration of FosPeg® in both EBV positive and EBV negative cells and thus a 4 hour drug incubation was selected for all subsequent experiments.

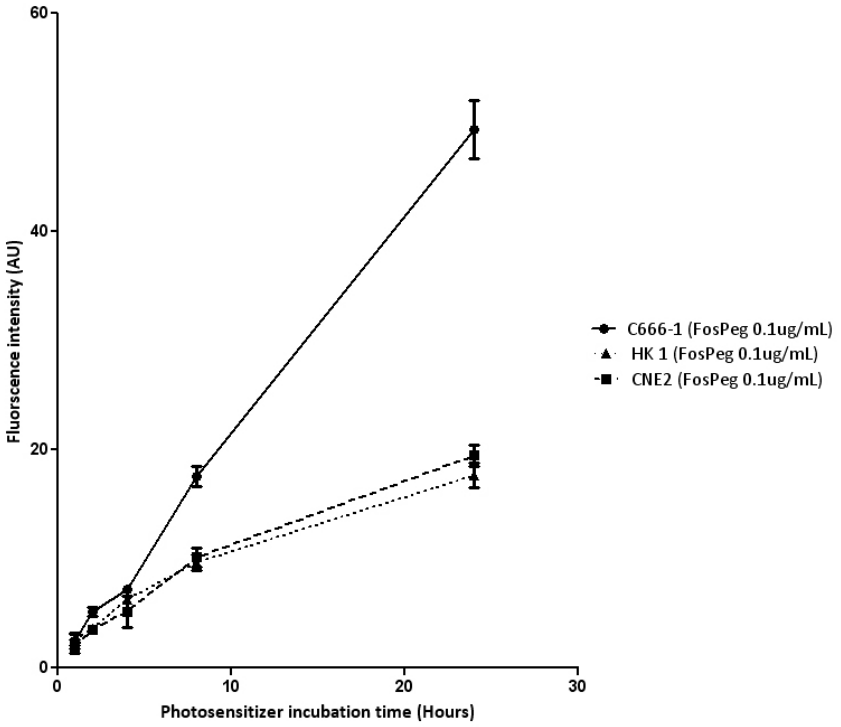

Figure 4.1 Kinetics of cellular FosPeg® accumulation in NPC cells.
The fluorescence intensity represents the cellular FosPeg® content (relative). Error bars (SD) were obtained from 3 to 6 independent experiments.

4.4.2 Intracellular localization of FosPeg® by fluorescence microscopy analysis

After being incubated with 1 μg/mL FosPeg® for 4 hours, the fluorescence images of NPC cells were acquired using the fluorescence microscope. The green fluorescence of MitoTracker Green and LysoTracker Green in cells indicated the position of the mitochondria and lysozyme while the red fluorescence represented the location of FosPeg®. By overlapping the images of FosPeg® and MitoTracker/LysoTracker, the yellow fluorescence demonstrated the subcellular distribution of FosPeg® with Mito/Lyso tracker. The coloicalisation analysis was performed by using the software image J. As shown in Figure 4.2, the diffused cytoplasmic distribution of FosPeg® in C666-1, HK1 and CNE2 cells were mainly localized at the mitochondria regions. There was no obvious difference in intracellular localization of FosPeg® in EBV positive and EBV negative cells.

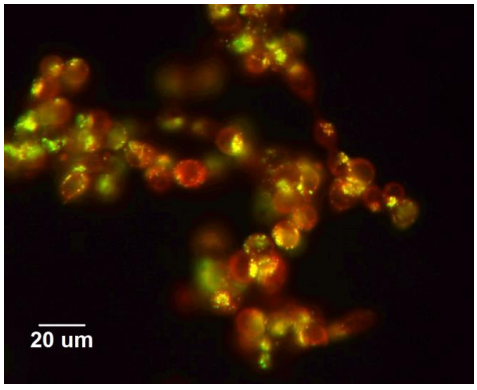

a. FosPeg® treated C666-1 cells labeled with lysosome probe (fluorescent green colour). Localization of FosPeg® was indicated as fluorescent red colour. R=0.614±0.045.

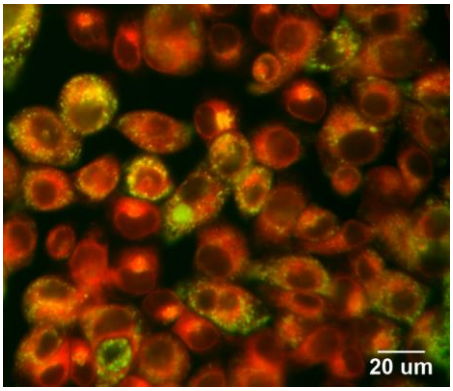

b. FosPeg® treated HK1 cells labeled with lysosome probe (fluorescent green colour). Localization of FosPeg® was indicated as fluorescent red colour. R=0.55±0.058.

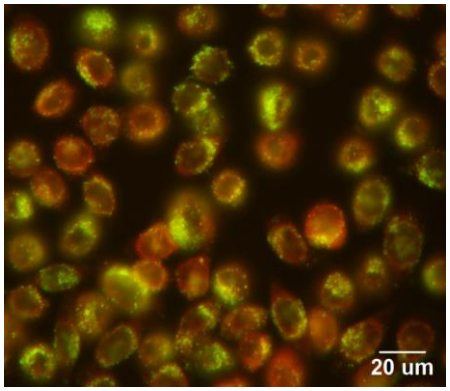

c. FosPeg® treated CNE2 cells labeled with lysosome probe (fluorescent green colour). Localization of FosPeg® was indicated as fluorescent red colour. R=0.598±0.049.

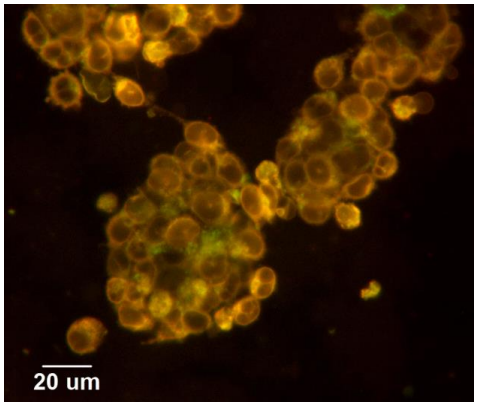

d. FosPeg® treated C666-1 cells labeled with mitochondrial probe (fluorescent green colour). Localization of FosPeg® was indicated as fluorescent red colour. R=0.765±0.044.

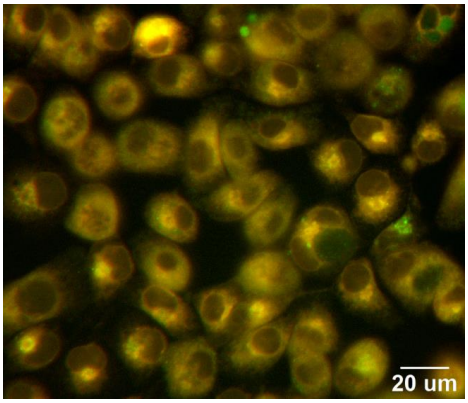

e. FosPeg® treated HK1 cells labeled with mitochondrial probe (fluorescent green colour). Localization of FosPeg® was indicated as fluorescent red colour. R=0.861±0.058.

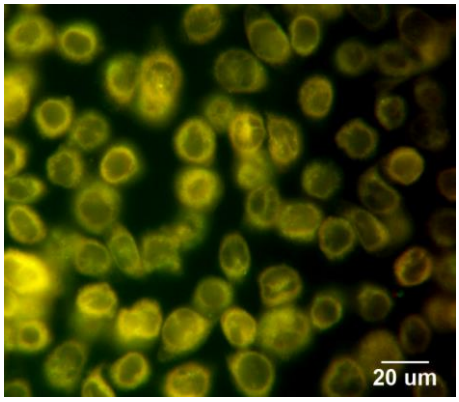

f. FosPeg® treated CNE2 cells labeled with mitochondrial probe (fluorescent green colour). Localization of FosPeg® was indicated as fluorescent red colour. R=0.843±0.061.

Figure 4.2 Intracellular localization of FosPeg® in NPC cells.

Fluorescence images were acquired from a fluorescence microscope after incubating with FosPeg® (1 μg/ml) for 4 h (x400). Red fluorescence represents the location of FosPeg®, green fluorescence the region of lysosome or mitochondria, and yellow fluorescence represent their overlay. (a, d) FosPeg® loaded C666-1 cells; (b, e) FosPeg® loaded HK-1 cells; (c, f) FosPeg® loaded CNE2 cells. coloicalisation analysiswas performed by using software image J.

4.4.3 Phototoxicity of FosPeg® PDT in NPC cells

MTT assay was used to evaluate the phototoxicity of FosPeg®-PDT on C666-1, HK-1 and CNE2 cells. The results of FosPeg®-PDT mediated cytotoxicity were presented in Figure 4.3. Within the range of FosPeg® concentration at 0.03 to 0.3 μg/ml, the cytotoxic effect of FosPeg® on C666-1 cells, HK-1 cells and CNE2 cells increased progressively with the light dose of 3 J/cm^2. The effect of drugs alone (dark toxicity) and light irradiation alone were negligible (data not shown). For all three tested cell lines, LD_{30} and LD_{50} were obtained at 0.05 μg/ml and 0.07 μg/ml FosPeg®, respectively. LD_{70} was obtained at 0.125 μg/ml, 0.2 μg/ml and 0.3 μg/ml FosPeg® on CNE2 cells, HK-1 cells and C666-1 cells, respectively. The results showed that the FosPeg®-PDT mediated cytotoxicity were positively related to the drug concentrations in all three tested cell lines. From the cytotoxicity data, LD_{30}, LD_{50} and LD_{70} at 3 J/cm^2 were selected for subsequent experiments.

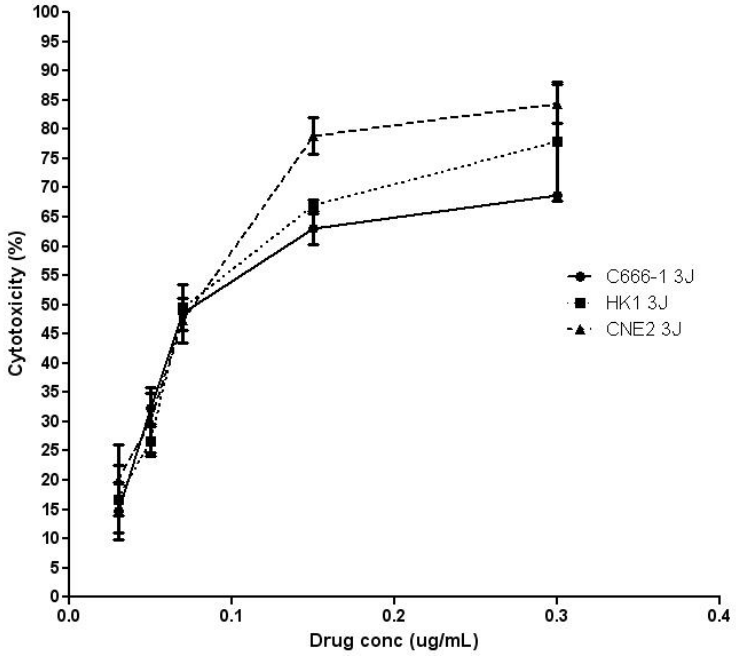

Figure 4.3 Phototoxicity of FosPeg® on NPC cells.
Cells were incubated with FosPeg® of different concentrations for 4 h, and then irradiated with light of 3 J/cm^2. The percentage of cytotoxicity was measured by MTT assay. Error bars (S.D.) were from 3 to 6 independent experiments.

4.4.4 Quantitative Evaluation of EBV LMP1 related microRNAs and mRNA

LMP1 is the principal onco-protein contributes to NPC tumourigenesis. It activates the NF-kB and MAPK signaling pathways through the C-terminal activation regions (CART regions). The effect of FosPeg® mediated PDT to LMP1 mRNA and EBV encoded miRNA expression were evaluated by qPCR. LMP1 mRNA was found only expressed in C666-1 cells but not in HK1 cells and CNE2 cells. Figure 4.4 shows the effect of FosPeg®-PDT treatment to LMP1 mRNA expression in C666-1 cells. Up to 8-fold increase in LMP1 mRNA expression was obtained after FosPeg® mediated PDT at LD_{70}. The effect of FosPeg® treatment to LMP1 mRNA expression was dose-dependent.

The expression of three selected EBV-miRNAs (*ebv-miR-BART1-5p, 16* and *17-5p*) were examined after FosPeg® mediated PDT. Figure 4.5 shows the effect of FosPeg®-PDT treatment to EBV-miRNAs expression in C666-1 cells. Up to 40% decrease of EBV-miR-BART was obtained after FosPeg® mediated PDT at LD_{70} and was dose-dependent.

The consequence of the decrease in *ebv-miR-BART1-5p, 16 and 17-5p* is the up-regulation of LMP1 mRNA. Increase in the expression of LMP1 mRNA significantly enhanced the LMP1 protein expression in FosPeg®-PDT treated C666-1 cells. Figure 4.6 shows the LMP1 protein expression pattern in C666-1 cells, HK-1 cells and CNE2 cells. Only C666-1 cells showed expression of LMP1 protein. Up-regulation of LMP1 protein with 40% increase was found after FosPeg®-PDT treatment at LD_{70} and it was in a dose dependent manner.

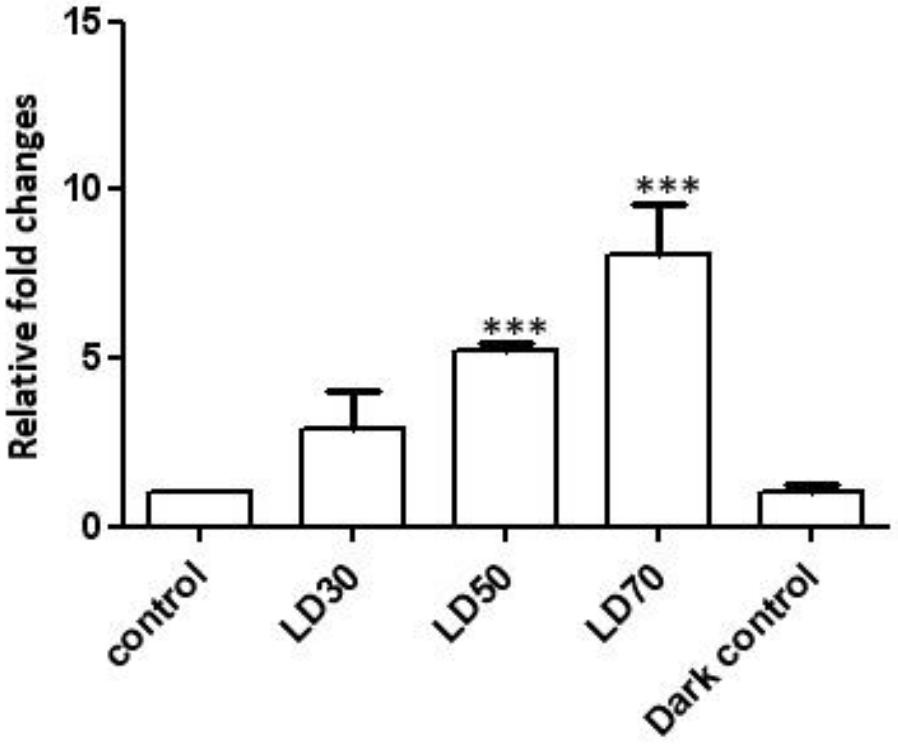

Figure 4.4 Effect of FosPeg® mediated PDT on LMP1 mRNA gene expression in C666-1 cells.

A 8-fold increase in LMP1 mRNA expression was obtained after FosPeg® mediated PDT at LD_{70}. Total RNA was extracted and converted to cDNA from control and PDT treated cells for the detection of LMP1 mRNA expression by TaqMan qPCR. mRNA amounts was normalized with GAPDH. Significant differences between treatment and control groups were analyzed by one-way ANOVA and followed by Dunnett's post-tests (*: $p<0.05$, **: $p<0.01$, ***: $p<0.001$).

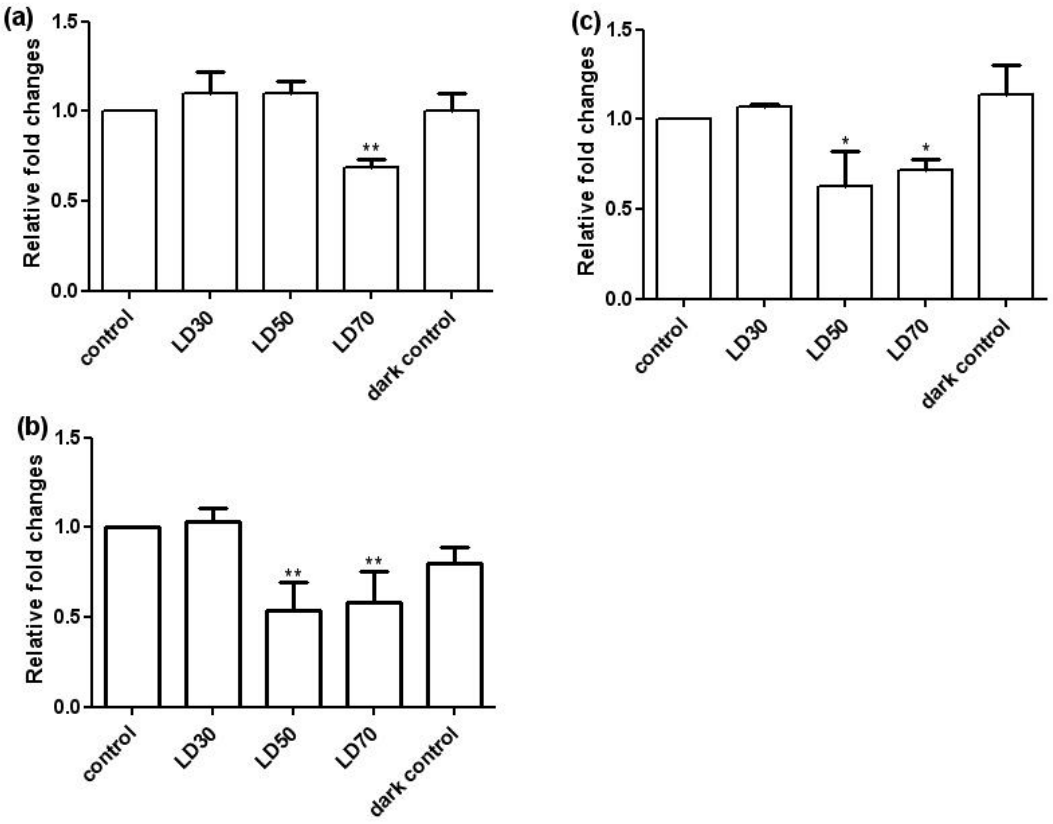

Figure 4.5 Effect of FosPeg® mediated PDT on EBV-miRNAs expression in C666-1 cells.

(a) EBV-miR-BART 1-5p; (b) EBV miR-BART 16; (c) EBV miR-BART 17-5p. A decrease in EBV-miR-BART 1-5p, EBV miR-BART 16 and EBV miR-BART 17-5p were obtained after FosPeg® mediated PDT at LD_{70}. Total RNA was extracted and converted to cDNA from control and PDT treated cells for the detection of EBV-miRNAs by qPCR. mRNA amounts was normalized with GAPDH. Significant differences between treatment and control groups were analyzed by one-way ANOVA and followed by Dunnett's post-tests (*: $p<0.05$, **: $p<0.01$, ***: $p<0.001$).

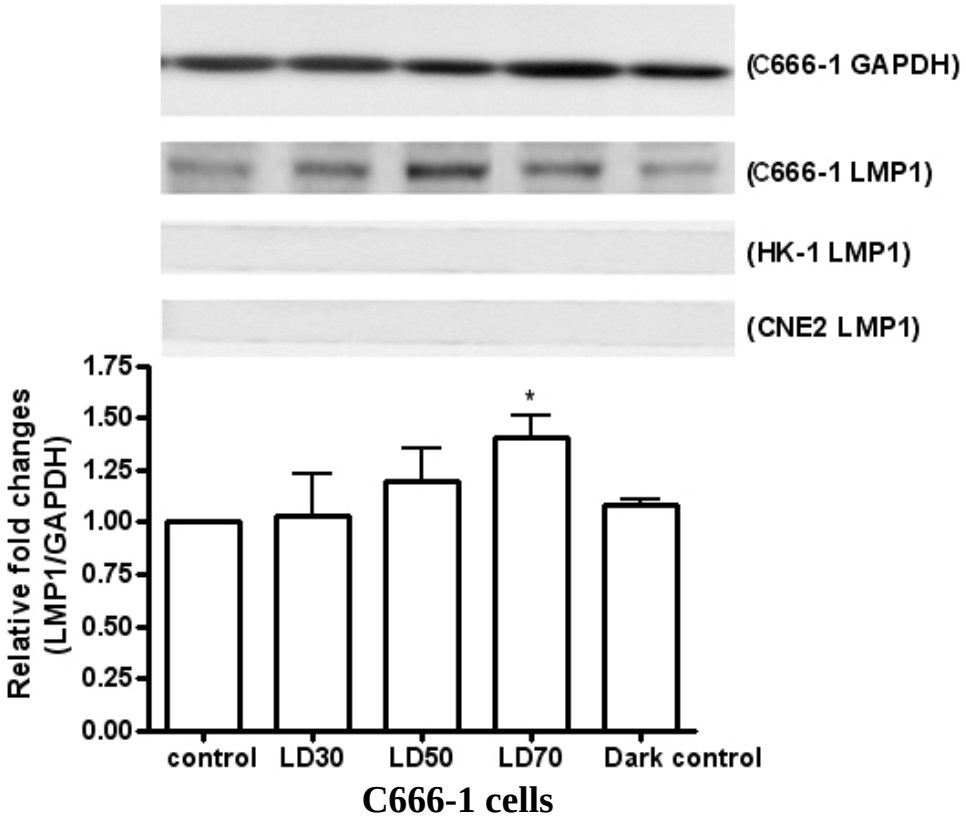

Figure 4.6 Effect of FosPeg® mediated PDT on the LMP1 protein expression in C666-1 cells.

A 40% increase of LMP1 protein expression was obtained after FosPeg® mediated PDT at LD_{70}. Total cellular proteins were extracted from control and PDT treated cells for the detection of LMP1 protein by western blot analysis Protein amount was normalized with GAPDH. Significant differences between treatment and control groups were analyzed by one-way ANOVA and followed by Dunnett's post-tests (* $p<0.05$, ** $p<0.01$, *** $p<0.001$).

4.5 Discussion

This is the first report to reveal the effect of FosPeg® mediated PDT on EBV positive and EBV negative NPC cells and its effect to EBV-miRNAs, LMP1 mRNA and LMP1 protein expression *in vitro*.

PDT is an evolving cancer treatment regimen and approved for use in USA, EU, Canada, Russia and Japan (Bredell et al., 2010). Different studies demonstrated the potential of PDT as cancer treatment. Lai and his colleagues showed that PDT has an immuno-enhancing effect in NPC patients by increasing natural killer cells and interleukin-2 (Lai et al., 1997). Our group also demonstrated promising outcomes from a number of *in vitro* studies concerning the PDT effect using several PSs including hypericin, mTHPC, merocyanine 540, 5-ALA and H-ALA on NPC/HK1, NPC/CNE1 and NPC/CNE2 cells (Bai et al., 2011; Wu et al., 2006; Yow et al., 2009; Yow et al., 2000a; Yow et al., 2000b; Yow et al., 2000c). All these findings suggested that PDT should be one of the best choices over the conventional cancer therapies for NPC.

PDT uses a combination of photosensitizing agents (PS), visible light and molecular oxygen to selectively destroy the biological targets. PDT efficacy depends on the tumour localizing photosensitizer, which absorbs light to produce reactive oxygen species (ROS) to destroy the biological targets (Robertson et al., 2009). Therefore, studying the localization and the biological targets of PS become very important to understand the mechanism of cellular destruction in tumours. In this study, FosPeg®, the liposomal encapsulated formulation of mTHPC has been studied to address the following in EBV positive and EBV negative NPC cell line models: (a) uptake kinetics and subcellular localization; (b) the photocytotoxic effect; (c) effect on EBV related biological targets, including EBV-miRNA BART 1-5p, BART 16, BART 17-5p, LMP1 mRNA and LMP1 protein; and (d) the mode of cell death.

FosPeg® (Biolitec AG) is the derivative of meta-tetra (hydroxyphenyl) chlorine (mTHPC) contained in PEGylated liposomes. The aim of using liposomes with long-circulating polyethylene glycol (PEG) as carriers and delivery systems is to improve its therapeutic effects by solubilizing the photosensitizer at suitable concentration, increasing drug uptake, shorter drug-light interval, higher tumour-to-skin ratio, with substantially decrease in forming aggregates in plasma as well as tumour eradication (Hallewin et al., 2008; Lassalle et al., 2009; Senge, 2012). The liposomal encapsulated formulation of FosPeg® provides a nanoscale drug delivery system to overcome the highly hydrophobic properties of mTHPC and optimizes the distribution and bioavailability of mTHPC (de Visscher et al., 2011). Buchholz et al. reported that the maximal tumour fluorescence intensity of FosPeg® could be nearly twice higher than Foscan®, with consequence of lower drug dose and shorter incubation time required for generalized photosensitivity in patients. As a result, the drug-light interval could be reduced. A much higher tumour-to-skin ratio was also obtained by applying FosPeg® in spontaneous feline squamous carcinoma. In general, the PEGylated photosensitizers could penetrate tumour vessels easily and be retained in tumour cells as tumour lacks functional lymphatic system to return the extracasated macromolecules. The study from Sherifa et al. also illustrated that FosPeg® produced less skin photosensitivity and higher tumour accumulation compared to Foscan®. Nevertheless, no complication was observed during injection of FosPeg®. All these results support the hypothesis that using PEGylated liposomes as photosensitizer nanocarriers could have advantages over the ordinarily formula Foscan®(Petri, et al., 2012; Senge, 2012; Sherifa et al., 2012).

Our study demonstrated that the accumulation of FosPeg® in C666-1 cells, HK1 cells and CNE2 cells were continued to rise up at 24 hours incubation (see Figure 4.1). The uptake kinetic pattern of FosPeg® on C666-1 cells, HK1 cells and CNE2 cells were similar in short incubation time, while a more effective FosPeg® uptake was obtained after 8 hour drug incubation time for C666-1 cells. Nevertheless, 4 hours of incubation provided a similar intracellular drug uptake concentration of

FosPeg® among all tested cell lines and thus was selected for all subsequent *in vitro* experiments.

The mitochondrion is one of the common organelles where photosensitizer localized. Photo-destruction of mitochondria could induce apoptosis (Buytaert et al., 2007; Hilf, 2007; Yow et al., 2009). Our group previously demonstrated that mTHPC possessed a strong phototoxicity toward human NPC cells which might be attributed to severe damage to the mitochondria during mTHPC photosensitization (Yow et al., 2009; Yow et al., 2007). This study further confirmed the finding by identifying FosPeg® intracellular localization. FosPeg® was dominantly localized in the mitochondria of C666-1, HK1 and CNE2 NPC cells. Images obtained by fluorescence microscopy indicated that most of the FosPeg® was localized in the mitochondria rather than in the lysosomes (see Figure 4.2) in all three tested cell lines, suggesting that apoptosis followed by mitochondrial photo-toxicity could be the primary cause of cell destruction.

A promising anti-tumour effect of FosPeg® on NPC cells were obtained with effective drug uptake and localization. MTT method was applied to evaluate the cytotoxic effect of FosPeg® PDT to C666-1 cells, HK1 cells and CNE2 cells. With a range of FosPeg® concentration (0.03 – 0.3 μg/ml), photo-cytotoxic effect of FosPeg® on C666-1 cells, HK-1 cells and CNE2 cells increased progressively with the light dose treatment (3 J/cm^2). LD_{70} of CNE2 cells, HK-1 cells and C666-1 cells was 0.125 μg/ml, 0.2 μg/ml and 0.3 μg/ml FosPeg®, respectively (see Figure 4.3). Compared with our previous study, FosPeg® showed a nearly 10 fold decrease in drug dose required to achieve similar phototoxic effects on CNE2 cells and HK1 cells (0.4-0.8μg/ml, 5-40J/cm^2) (Yow et al., 2000).

In order to study the effect of FosPeg®-PDT on EBV infected NPC cells, the expression level of EBV encoded microRNAs, LMP1 mRNA and protein were evaluated. LMP1 is one of the principal EBV encoded genes expressed in NPC

which contributes to the tumourigenesis (Dawson et al., 2012; Zheng et al., 2007). LMP1 protein activates a number of signaling pathways including NF-kB, MAPK and Janus Kinase/Signal Transducer and Activator of Transcription (JAK/STAT) pathways. LMP1-induced signal pathways can be attributed to four functions, i.e. inhibition of apoptosis; induction of cell immortality; promotion of cell proliferation, and influence of cell invasion and metastasis (Li et al., 2007; Lo et al., 2007). Interestingly, transforming potential of LMP1 is dose-dependent. A number of studies showed that low levels of LMP1 induced cell growth and promoted cell survival while high levels of LMP1 suppressed cell growth and sensitized to apoptosis. The study of Deng et al. illustrated that increased in LMP1 expression could trigger cell cycle arrest through activation of NF-kB and AP-1 protein in NPC cell line (Deng et al., 2003). Yoshizaki et al. (2012) also reported that high level of p53 expression was correlated with high LMP1 level. All these data revealed the importance of LMP1 protein level in NPC pathogenesis and the maintenance of the tumour cell properties. The expression of EBV encoded microRNA is one of the strategies applied by EBV to maintain a low level of LMP1 protein in EBV transfected cells. At least three EBV encoded miRNAs were identified to target LMP1 gene and down regulate the LMP1 protein expression, including EBV-miR-BART1-5p, 16 and 17-5p (Lo et al., 2012; Lo et al., 2007).

Similar finding was obtained in this study. It was found that LMP1 mRNA and protein only expressed in EBV positive C666-1 cells but not in EBV negative HK1 cells and CNE2 cells at pre- and post- PDT treatment. FosPeg® mediated PDT could significantly up-regulate LMP1 mRNA and protein expression in C666-1 cells and was in a dose dependent manner. This suggested that the expression of LMP1 mRNA and protein was correlated with the presence of virus. Quantitative measurement of EBV-miR-BART1-5p, 16 and 17-5p expression was performed by qPCR. The expression levels of all three tested microRNAs in C666-1 cells were suppressed significantly after FosPeg®-PDT treatment and were in a dose dependent manner. All these results suggested that FosPeg®-mediated PDT altered the

expression of LMP1 protein leading to an increased sensitivity to apoptosis in C666-1 cells. All the evidence shown in this study supports the hypothesis that LMP1 is one of the major contributors to NPC tumourigenesis and could be one of the therapeutic targets and biomarkers for NPC treatment. Additional information on the effect of FosPeg®-mediated PDT on LMP1 induced signal transductions is needed to reveal in cell death mechanism.

In summary, our findings confirmed that FosPeg® is effective to both EBV positive and EBV negative NPC. Down regulation of EBV-miRNAs BART 1-5p, BART 16 and BART 17-5p significantly increased the expression of LMP1 mRNA and protein in EBV positive C666-1 cell line. EBV-miRNAs, LMP1 mRNA and LMP1 protein could be potential therapeutic markers for EBV positive NPC cells. Understanding the mechanism of FosPeg®-PDT may shed light on enhanced strategic development.

4.6 Acknowledgments

We thank Dr. Kwok-Wai Lo from Anatomical and Cellular Pathology Department, The Chinese University of Hong Kong for providing NPC/C666-1 cells and NPC/HK1 cells, Biolitec for photosensitizer FosPeg®.

4.7 References

Agostinis P, Berg K, Cengel KA, Foster TH, Girotti AW, Gollnick SO, Golab J. (2011) Photodynamic therapy of cancer: an update. *CA Cancer J Clin, 61*(4), 250-281.

Bai DQ, Xia X, Yow CMN, Chu ESM, Xu C. (2011) Hypocrellin B-encapsulated nanoparticle-mediated rev-caspase-3 gene transfection and photodynamic therapy on tumor cells. *Eur J Pharmacol, 650*(2-3), 496-500.

Bai DQ, Yow CMN, Tan Y, Chu ESM, Xu CS. (2010) Photodynamic action of LED-activated nanoscale photosensitizer in nasopharyngeal carcinoma cells. *Laser Physics, 20*(2), 7.

Bredell MG, Besic E, Maake C, Walt H. (2010) The application and challenges of clinical PD-PDT in the head and neck region: a short review. *J Photochem Photobiol B, 101*(3), 185-190.

Brennan B. (2006) Nasopharyngeal carcinoma. *Orphanet J Rare Dis, 1*, 23.

Buytaert E, Dewaele M, Agostinis P. (2007) Molecular effectors of multiple cell death pathways initiated by photodynamic therapy. *Biochim Biophys Acta, 1776*(1), 86-107.

Caponigro F, Longo F, Ionna F, Perri F. (2010) Treatment approaches to nasopharyngeal carcinoma: a review. *Anticancer Drugs, 21*(5), 471-477.

Cheung ST, Huang DP, Hui ABY, Lo K, Ko C, Tsang YS, Lee JCK. (1999) Nasopharyngeal carcinoma cell line (C666-1) consistently harbouring Epstein-Barr virus. *International Journal of Cancer, 83*, 6.

D'Hallewin MA, Kochetkov D, Viry-Babel Y, Leroux A, Werkmeister E, Dumas D, Bezdetnaya L. (2008) Photodynamic therapy with intratumoral administration of Lipid-Based mTHPC in a model of breast cancer recurrence. *Lasers Surg Med, 40*(8), 543-549.

Dawson CW, Port RJ, Young LS. (2012) The role of the EBV-encoded latent membrane proteins LMP1 and LMP2 in the pathogenesis of nasopharyngeal carcinoma (NPC). *Semin Cancer Biol., 22*(2), 144-153.

de Visscher SA, Kascakova S, de Bruijn HS, van den Heuvel A, Amelink A, Sterenborg HJ, Witjes MJ. (2011) Fluorescence localization and kinetics of mTHPC and liposomal formulations of mTHPC in the window-chamber tumor model. *Lasers Surg Med, 43*(6), 528-536.

Deng L, Yang J, Zhao XR, Deng XY, Zeng L, Gu HH, Cao Y. (2003) Cells in G2/M phase increased in human nasopharyngeal carcinoma cell line by EBV-LMP1 through activation of NF-κB and AP-1. *Cell Res, 13*(3), 8.

He ML, Luo MX, Lin MC, Kung HF. (2012) MicroRNAs: potential diagnostic markers and therapeutic targets for EBV-associated nasopharyngeal carcinoma. *Biochim Biophys Acta, 1825*(1), 1-10.

Herrmann K, Niedobitek G. (2003) Epstein-Barr virus-associated carcinomas: facts and fiction. *J Pathol., 199*(2), 140-145.

Hilf R. (2007) Mitochondria are targets of photodynamic therapy. *J Bioenerg Biomembr, 39*(1), 85-89.

Hospital Authority: Hong Kong Cancer Registry. (2011). from http://www3.ha.org.hk/cancereg/Statistics.html

Huang DP, Ho JH, Poon YF, Chew EC, Saw D, Lui M, Lau WH. (1980) Establishment of a cell line (NPC/HK1) from a differentiated squamous carcinoma of the nasopharynx. *Int J Cancer, 26*(2), 127-132.

Koon HK, Lo KW, Leung KN, Lung ML, Chang CC, Wong RN, Mak NK. (2010) Photodynamic therapy-mediated modulation of inflammatory cytokine production by Epstein-Barr virus-infected nasopharyngeal carcinoma cells. *Cellular & Molecular Immunology, 7*(4), 323-326.

Lai JP, Tao ZD, Xiao JY, Zhao SP, Tian YQ. (1997) Effect of photodynamic therapy on selected laboratory values of patients with nasopharyngeal carcinoma. *Ann Otol Rhinol Laryngol, 106*(8), 680-682.

Lassalle HP, Dumas D, Grafe S, D'Hallewin MA, Guillemin F, Bezdetnaya L. (2009) Correlation between in vivo pharmacokinetics, intratumoral distribution and photodynamic efficiency of liposomal mTHPC. *J Control Release, 134*(2), 118-124.

Li L, Guo L, Tao Y, Zhou S, Wang Z, Luo W, Cao Y. (2007) Latent membrane protein 1 of Epstein-Barr virus regulates p53 phosphorylation through MAP kinases. *Cancer Lett., 255*(2), 219-231.

Lo AK, Dawson CW, Jin DY, Lo KW. (2012) The pathological roles of BART miRNAs in nasopharyngeal carcinoma. *J Pathol, 227*(4), 392-403.

Lo AK, To KF, Lo KW, Lung RW, Hui JW, Liao G, Hayward SD. (2007) Modulation of LMP1 protein expression by EBV-encoded microRNAs. *Proc Natl Acad Sci U S A., 104*(41), 16164-16169.

Marquitz AR, Raab-Traub N. (2012) The role of miRNAs and EBV BARTs in NPC. *Semin Cancer Biol., 22*(2), 166-172.

Pattle SB, Farrell PJ. (2006) The role of Epstein-Barr virus in cancer. *Expert Opin Biol Ther., 6*(11), 1193-1205.

Petri A, Yova D, Alexandratou E, Kyriazi M, Rallis M. (2012) Comparative characterization of the cellular uptake and photodynamic efficiency of Foscan® and Fospeg in a human prostate cancer cell line. *Photodiagnosis Photodyn Ther, 9*(4), 344-354.

Razak AR, Siu LL, Liu FF, Ito E, O'Sullivan B, Chan K. (2010) Nasopharyngeal carcinoma: the next challenges. *Eur J Cancer, 46*(11), 1967-1978.

Reshetov V, Zorin V, Siupa A, D'Hallewin MA, Guillemin F, Bezdetnaya L. (2012) Interaction of liposomal formulations of meta-tetra(hydroxyphenyl)chlorin (temoporfin) with serum proteins: protein binding and liposome destruction. *Photochem Photobiol, 88*(5), 1256-1264.

Robertson CA, Evans DH, Abrahamse H. (2009) Photodynamic therapy (PDT): a short review on cellular mechanisms and cancer research applications for PDT. *J Photochem Photobiol B, 96*(1), 1-8.

Ryan JL, Fan H, Glaser SL, Schichman SA, Raab-Traub N, Gulley ML (2004) Epstein-Barr virus quantitation by real time PCR targeting multiple gene segments: a novel approach to screen for the virus in paraffin-embedded tissue and plasma. *J Mol Diagn*. 6(4), 378-85.

Senge MO. (2012) mTHPC--a drug on its way from second to third generation photosensitizer? *Photodiagnosis Photodyn Ther, 9*(2), 170-179.

Senge MO, Brandt JC. (2011) Temoporfin (Foscan®, 5,10,15,20-tetra(m-hydroxyphenyl)chlorin)--a second-generation photosensitizer. *Photochem Photobiol, 87*(6), 1240-1296.

Sherifa G, Saad Zaghloul MA, Elsayed OF, Rueck A, Steiner R, Abdelaziz AI, Abdel-Kader MH. (2012) Functional characterization of Fospeg, and its impact on cell cycle upon PDT of Huh7 hepatocellular carcinoma cell model. *Photodiagnosis Photodyn Ther*. 10(1), 87-94.

Suarez C, Rodrigo JP, Rinaldo A, Langendijk JA, Shaha AR, Ferlito A. (2010) Current treatment options for recurrent nasopharyngeal cancer. *Eur Arch Otorhinolaryngol, 267*(12), 1811-1824.

Tang F, Xie C, Huang D, Wu Y, Zeng M, Yi L, Sun L. (2011) Novel potential markers of nasopharyngeal carcinoma for diagnosis and therapy. *Clin Biochem, 44*(8-9), 711-718.

Tao Q, Chan AT. (2007) Nasopharyngeal carcinoma: molecular pathogenesis and therapeutic developments. *Expert Rev Mol Med, 9*(12), 1-24.

Tsao SW, Tsang CM, Pang PS, Zhang G, Chen H, Lo KW. (2012) The biology of EBV infection in human epithelial cells. *Semin Cancer Biol., 22*(2), 137-143.

Tulalamba W, Janvilisri T. (2012) Nasopharyngeal carcinoma signaling pathway: an update on molecular biomarkers. *Int J Cell Biol. , 2012*, 594681.

Wei KR, Xu Y, Liu J, Zhang WJ, Liang ZH. (2011) Histopathological Classification of Nasopharyngeal Carcinoma. *Asian Pac J Cancer Prev., 12*, 7.

Wu RWK, Chu ESM, Yow CMN, Chen JY. (2006) Photodynamic effects on nasopharyngeal carcinoma (NPC) cells with 5-aminolevulinic acid or its hexyl ester. *Cancer Lett., 242*(1), 112-119.

Yoshizaki T, Ito M, Murono S, Wakisaka N, Kondo S, Endo K. (2012) Current understanding and management of nasopharyngeal carcinoma. *Auris Nasus Larynx, 39*(2), 137-144.

Yow CMN, Chen JY, Mak NK, Cheung NH, Leung AW. (2000a) Cellular uptake, subcellular localization and photodamaging effect of temoporfin (mTHPC) in nasopharyngeal carcinoma cells: comparison with hematoporphyrin derivative. *Cancer Lett, 157*(2), 123-131.

Yow CMN, Mak NK, Leung AW, Huang Z. (2009) Induction of early apoptosis in human nasopharyngeal carcinoma cells by mTHPC-mediated photocytotoxicity. *Photodiagnosis Photodyn Ther, 6*(2), 122-127.

Yow CMN, Mak NK, Szeto S, Chen JY, Lee YL, Cheung NH, Leung AW. (2000b) Photocytotoxic and DNA damaging effect of temoporfin (mTHPC) and merocyanine 540 (MC540) on nasopharyngeal carcinoma cell. *Toxicology Letters, 115*(1), 53-61.

Yow CMN, Chen JY, Mak NK, Cheung NH, Leung AWN. (2000c) Cellular uptake, subcellular localization and photodamaging effect of Temopor®n (mTHPC) in nasopharyngeal carcinoma cells:comparison with hematoporphyrin derivative. *Cancer Lett, 157*, 9.

Yow CMN, Leung AWN, Huang Z. (2007) mTHPC-photodynamic therapy induced apoptosis in nasopharyngeal carcinoma cells. *Optics in Health Care and Biomedical Optics III, 6826*, 68261P-68261P-68266.

Zheng H, Li LL, Hu DS, Deng XY, Cao Y. (2007) Role of Epstein-Barr virus encoded latent membrane protein 1 in the carcinogenesis of nasopharyngeal carcinoma. *Cellular & Molecular Immunology, 4*(3), 185-196.

Chapter 5

Effect of FosPeg®-PDT on the modulation of MAPK signaling proteins in undifferentiated NPC cells/C666-1, poorly differentiated NPC cells/CNE2 and well differentiated NPC cells/HK1

Abstracts were presented:

WU RWK, CHU ESM, IP CW, HUANG Z, YOW CMN. FosPeg® mediated photocytotoxicity down-regulates the expression of Epidermal Growth Factor Receptor (EGFR) and Vascular Endothelial Growth Factor (VEGF) in EBV positive nasopharyngeal carcinoma cell line (C666-1)." 1st Singapore Pathology Conference, 19-20 October, 2012. Pp. 70.

WU RWK, HUANG Z, YOW CMN. FosPeg® mediated photocytotoxicity suppresses cancer cell growth through down-regulation of MEK pathways." Photodiagnosis and Photodynamic Therapy, 8(2): 188, 2011.

5.1 Abstract

Mitogen-activated protein kinase (MAPK) signaling pathways are some of the major signaling pathways triggered by Epstein-Barr virus (EBV) in nasopharyngeal carcinoma (NPC) cells. Latest findings reported that photosensitizers localized in mitochondria resulted in modulation of MAPK signaling pathways.

FosPeg® is a new formulation of mTHPC encapsulated in PEGylated liposomes with optimized distribution properties. In our previous publication, we reported that FosPeg® localized in mitochondria. This chapter focused on the effect of FosPeg®-PDT on the epidermal growth factor receptor (EGFR) signaling proteins; MAPK signaling proteins, and their downstream proteins such as telomerase, NF-kB and Vascular endothelial growth factor (VEGF).

Results showed that at LD_{70}, FosPeg®-PDT elicited down-regulation of different signaling proteins, including EGFR signaling proteins (EGFR and Raf); MAPK signaling proteins (p38, JNK, ERK) and their downstream proteins (telomerase and VEGF) in all three NPC cell lines. Our study indicated that EGFR signaling pathways; MAPK signaling pathways, and their downstream signal proteins were modulated by FosPeg®-PDT, leading to inhibition of cell proliferation and cell motility.

Our study provided the first evidence for the role of FosPeg®-PDT on modulation of MAPK signaling proteins and their downstream effectors in NPC cells. *In vivo* studies of FosPeg® are worth examined for the benefit of PDT applications in EBV induced cancers.

5.2 Introduction

The localization of photosensitizer is important to PDT treatment as the singlet oxygen and reactive oxygen species (ROS) being generated only work on a narrow distance range (de Visscher et al., 2013Green et al., 2013; Kushibiki et al., 2013; Shirasu et al., 2013). The preferential localization of photosensitizers in cells was vital for the determination of the mode of cell death and the alteration of corresponding signaling pathways (Agostinis et al., 2011; Robertson et al., 2009).

Our publication (section 4.4.1) showed that the photosensitizer FosPeg® was selectively localized in mitochondria. A number of studies demonstrated that photosensitizers localized in mitochondria would induce apoptotic cell destruction (Chen et al., 2011; Devi et al., 2013; Dougherty et al., 1998; Miki et al., 2013; Wang et al., 2012; Yow et al., 2009). Studies also reported that photosensitizers localized in mitochondria resulted in alteration of mitogen-activated protein kinase (MAPK) signaling pathways (Bui-Xuan et al., 2010; Ji et al., 2010).

Figure 5.1 summarized the MAPK signaling pathways involved in NPC tumourigenesis and proposed protein targets by FosPeg®-PDT. The MAPK signaling proteins are a chain of proteins in cells that communicate a signal from cell surface receptor to the nucleus by phosphorylation. Signals transmitted by a cascade of kinases, including the extracellular signal-regulated kinase (ERK), c-Jun N-terminal kinase (JNK) and p38 MAPK (p38). Their importance in nasopharyngeal carcinoma (NPC) development has been proved (Darling and Cook, 2014; Dent 2014; Sui et al., 2014; Wu et al., 2011).

Phosphorylation of ERK in NPC cells is via the EGFR/Raf/ERK cascade, resulted in deregulation of cell proliferation (Kung et al., 2011; Lo et al., 2013; Wu & Li et al., 2009). Phosphorylation of JNK and p38 in NPC cells is LMP1 dependent, resulted in activation of transcription factor NF-kB. NF-kB regulated a large number of genes transcription, such as telomerase, angiogenic factors (e.g. VEGF)

and matrix metalloproteases (MMP) (Chung et al., 2013; Deng et al., 2003; Murono et al., 2001; Zheng et al., 2007). Telomerase is an enzyme actively lengthens telomere in tumour cells, leading to cell immortality.

Here in this chapter, the study aimed to determine the effect of FosPeg®-PDT on the EGFR signaling proteins; MAPK signaling proteins, and their downstream proteins in three NPC cell lines.

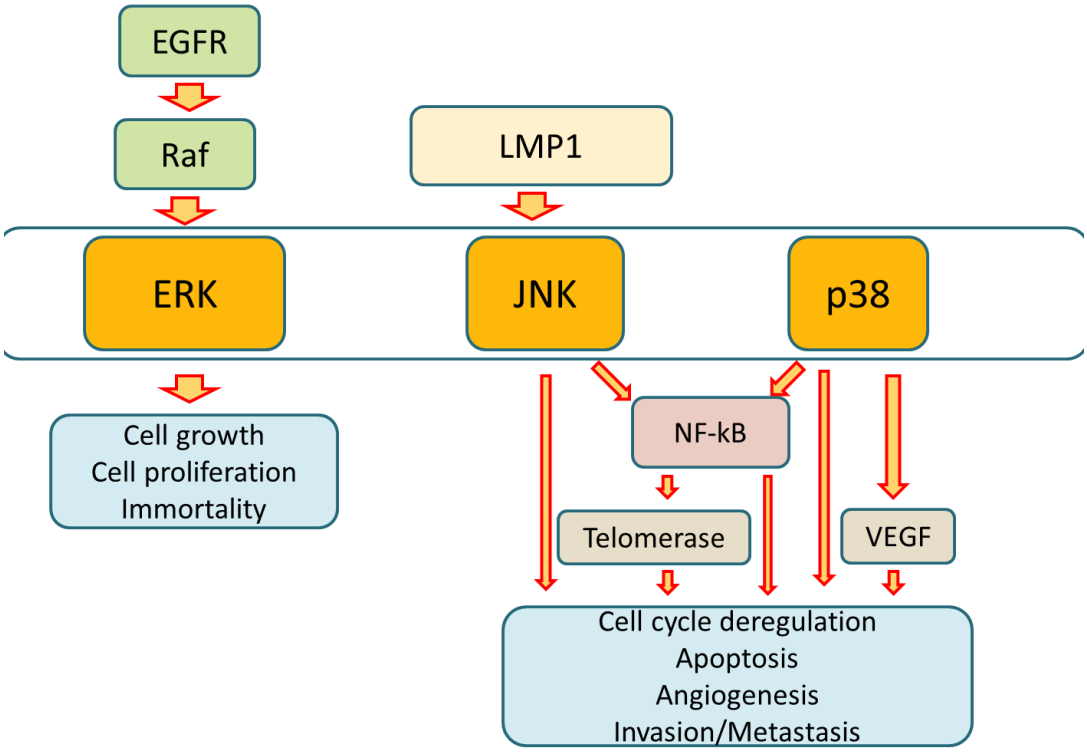

Figure 5.1 MAPK signaling pathways and their downstream effector proteins.

5.3 Methodology

5.3.1 Materials

FosPeg® (1.5 mg mTHPC/ml) was kindly provided by Biolitec AG (Germany). FosPeg® stock solution (10 μg/ml) was prepared in miliQ water. Primary antibodies for p38 and JNK were purchased from Cell Signaling Technology, Inc. (Danvers, MA). Primary antibodies for phospho-p38, phospho-JNK, ERK and phospho-ERK were purchased from BD transduction, Inc. Primary antibodies for EGFR, phospho-EGFR, VEGF and Raf, were purchased from Santa Cruz Biotech, Inc. Primary antibodies for telomerase and GAPDH were purchased from Abcam, Inc. Secondary anti-mouse, anti-goat and anti-rabbit antibodies coupled to horseradish peroxidase were purchased from Cell Signaling Technology, Inc.

5.3.2 The effect of FosPeg®-PDT on MAPK signal pathways and their down-stream proteins in NPC cells

In order to elucidate the intracellular signal transduction pathways triggered by FosPeg®-PDT in EBV positive and EBV negative cells, Western blot analysis was applied specifically for three major members of the MAP-kinase family, namely p38, ERK, and JNK. Whole cell lysates collected from both adherent and non-adherent floating cells were washed with ice-cold PBS and lysed in 0.2 ml lysis buffer (50 mM Tris-HCl, 150 mM NaCl, 1% Nonidet 40, 0.5% (w/v) Na-deoxycholate, 2 mM phenylmethylsulfonyl fluoride, 1x protease inhibitors). Supernatant was collected from lysates by centrifugation at 14,000g for 30 minutes at 4 ^{o}C. An equal amount of protein was subjected to 10% sodium dodecyl sulphate polyacrylamide gel electrophoresis before blotting onto a polyvinylidene difluoride membrane (Amersham Pharmacia Biotech, Piscataway, NJ). The membrane was blocked with 5% skimmed milk in tris-buffered saline with 0.05% Tween 20 (pH 7.6) for 1 hour at room temperature. After blocking, the membrane was probed with specific-primary antibodies at 4 ^{o}C overnight. After washing, the membrane was incubated with a secondary antibody coupled to horseradish peroxidase (Amersham and

Pharmacia Biotech) for 1 hour at room temperature. The antibody-antigen binding was then detected using an ECL chemiluminescence detection system according to the manufacturer's instructions and visualized by Bio-Rad Chemi Doc™ EQ densitometer (Bio-Rad laboratories, USA). The intensities of the protein bands were normalized and compared by Bio-Rad Quantity One software (Bio-Rad laboratories, USA).

5.3.3 Cell cycle and DNA content analysis

Cell cycle phase distribution was analyzed by flow cytometry with propidium iodide (PI) staining. NPC cells (5×10^5 cells/dish) were cultured and synchronized in RPMI-1640 without FBS for 24 hours. At 4, 24, 48 and 72 hours post-PDT, treated cells were harvested, washed and suspended in PBS. Cells were fixed with ice cold 80% ethanol overnight at -20 °C. Fixed cells were washed twice with PBS, then re-suspended in PBS containing PI staining solution (10 µg/ml PI, 10 mg/ml RNase A and triton X-100) followed by incubation at 37 °C for 30 minutes. For each sample, 10,000 events in triplicate were counted by Cytomics FC500 (Beckman Coulter). The data were analyzed by the FlowJo Software (Version 5.7.2) to estimate the proportion of the cell cycle phases in form of the cell number against DNA content histograms. The debris and doublet were gated out and excluded by the software.

5.3.4 Cell motility analysis

The cell migration was determined by wound-healing assay. The NPC cells (3×10^4 cells/well) were seeded in 96-well plates overnight at 37°C with 5% CO_2. After the cells reached confluent, a wound was made with a 200 µl pipette tip. The detached cells and debris were removed and washed with PBS. The cells were then treated with FosPeg® at LD_{50}; control and dark controls were included. The closure of the wound by migrating cells was determined at 24 hours post-PDT using a Leica inverted-phase contrast microscope (Leica DMI 4000B) coupled with a CCD camera and quantified by NIH Image Software. The dose-dependent effect of the PSs on wounded NPC cells was as a migration rate compared with the untreated

cells as the control. Distance of cell migration was estimated by subtracting the length between the lesion edges at 24 hours from this distance measured at 0 hours.

5.3.5 Statistical analysis

All data were processed and presented by GraphPad Prism (GraphPad Software, Inc.). Mean and standard deviation (SD) were used to present data and all graphical error bars were represented in SD. Quantitative data from three independent experiments were used for analysis of the Western blotting, the cell cycle progression and wound healing assay. One-way analysis of variance (ANOVA) followed by Dunnett correction or two-way ANOVA followed by Bonferroni's correction post-hoc test was used to analyze differences between groups by the GraphPad Prism (GraphPad Software, Inc.). A P-value of less than 0.05 was considered as significant different.

5.4 Results

5.4.1 Effect of FosPeg®-PDT on EGFR signal proteins

The effect of FosPeg®-PDT on EGFR and Raf protein was measured by Western blot analysis. Figure 5.2 and 5.3 indicated that FosPeg®-PDT down-regulated EGFR and Raf protein in all three NPC cell lines. There was a 0.5-fold decrease of EGFR obtained in both C666-1 and CNE2 cells while a 0.4-fold decrease of EGFR was obtained in HK1 cells at LD_{70}. A 0.5-fold, 0.7-fold and 0.6-fold decrease of Raf protein was obtained in C666-1 cells, CNE2 cells and HK1 cells at LD_{70}, respectively. However, the expression of pEGFR was obtained only in C666-1 cells and CNE2 cells but not in HK-1 cells. Result indicated that the phorphorylation site of EGFR protein in HK1 cells may not at regions Tyr1173. Figure 5.2 shows a 0.3-fold and 0.7-fold decrease of pEGFR protein in C666-1 cells and CNE2 cells at LD_{70}, respectively. All these results confirmed that FosPeg® mediated PDT suppressed EGFR signaling pathways.

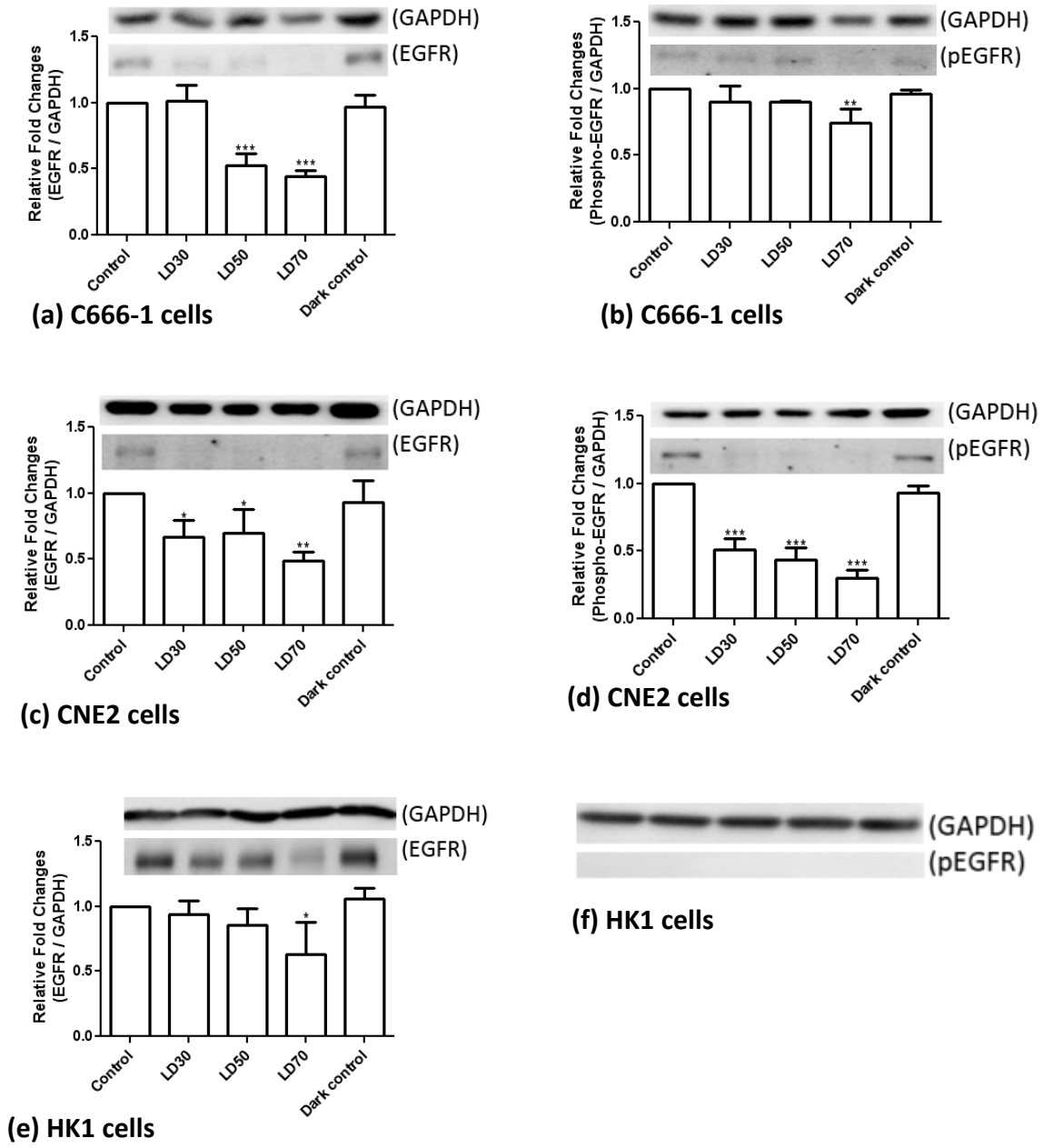

Fig 5.2 Effect of FosPeg® mediated PDT on the EGFR and phospho-EGFR (pEGFR) protein expression in C666-1 cells, HK1 cells and CNE2 cells.

Total cellular protein was extracted from control and PDT treated cells for the detection of JNK and phospho-JNK protein by Western blot analysis. Protein amounts were normalized with GAPDH.

EGFR and phospho-EGFR protein expressed by C666-1 cells (fig a & b); EGFR and phospho-EGFR protein expressed by CNE2 cells (fig c & d); EGFR protein expressed by HK1 cells (fig. e). Phosphor-EGFR protein was not expressed in HK1 cells (fig. f). Significant differences between treatment and control groups were analyzed by one-way ANOVA and followed by Dunnett's post-tests (* $p<0.05$, ** $p<0.01$, *** $p<0.001$).

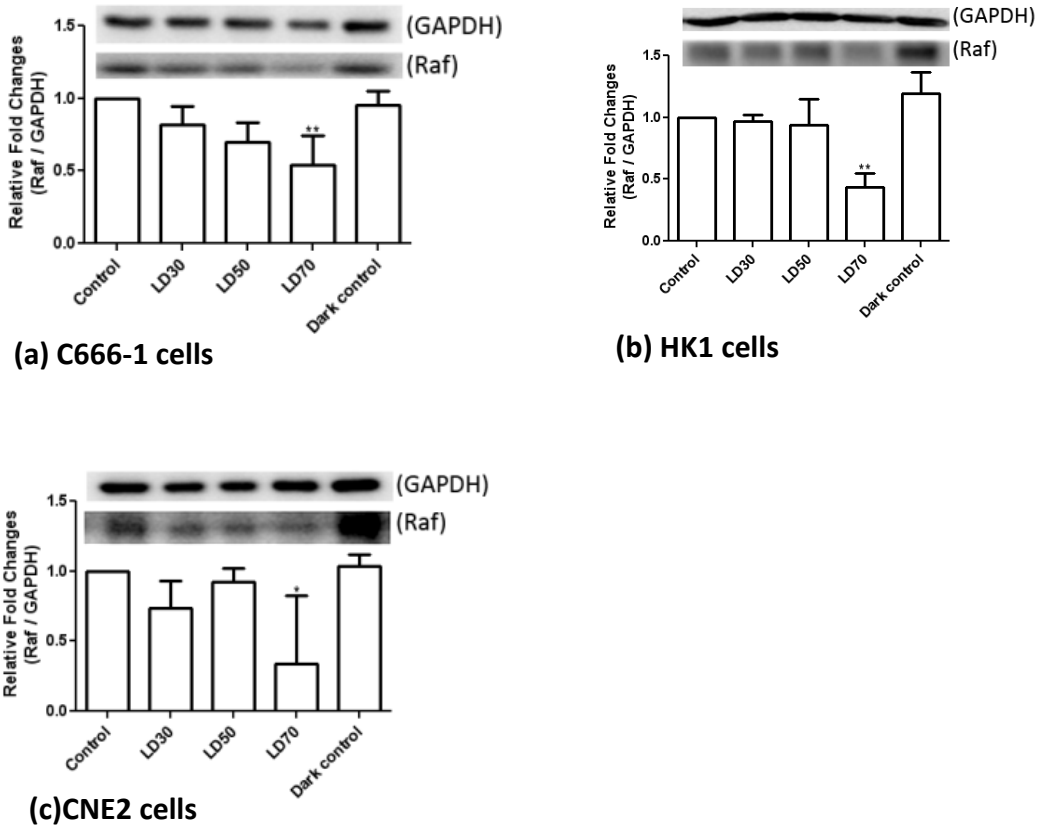

Fig 5.3 Effect of FosPeg® mediated PDT on the Raf protein expression in C666-1 cells, HK1 cells and CNE2 cells.

Total cellular protein was extracted from control and PDT treated cells for the detection of Raf protein by Western blot analysis. Protein amounts were normalized with GAPDH. Figure a – c showed Raf proteins expression in C666-1 cells, HK1 cells and CNE2 cells, respectively. Significant difference between treatment and control groups were analyzed by one-way ANOVA and followed by Dunnett's post-tests (* $p<0.05$, ** $p<0.01$).

5.4.2 Effect of FosPeg® PDT on MAPK signaling proteins

We presented in Chapter 4 that FosPeg® localized in mitochondria in all three NPC cell lines. We also reported that FosPeg®-PDT suppressed EGFR signaling proteins. Taken together, it is suggested that FosPeg®-PDT could alter MAPK signaling proteins. Hence in this section, the responses of MAPK proteins (ERK, JNK, p38) to FosPeg®-PDT were elucidated.

Total ERK and phosphorylated ERK; total JNK and phosphorylated JNK; total p38 and phosphorylated p38 proteins were found to be expressed in all three NPC cell lines. In comparison to control cells and dark control cells with FosPeg®-PDT treated cells, FosPeg® mediated PDT down-regulated MAPK signaling proteins was in drug-dose and light-dependent manners ($P<0.05$).

Figure 5.4 indicated a 0.3-fold, 0.7-fold and 0.5-fold decrease of ERK signaling protein in C666-1 cells, HK1 cells and CNE2 cells, respectively. Figure 5.4 also indicated a 0.4-fold, 0.5-fold and 0.5-fold decrease of pERK signaling protein in C666-1 cells, HK1 cells and CNE2 cells, respectively. Figure 5.5 indicated a 0.3-fold, 0.7-fold and 0.3-fold decrease of JNK signaling protein in C666-1 cells, HK1 cells and CNE2 cells, respectively. Figure 5.5 also indicated a 0.4-fold, 0.2-fold and 0.2-fold decrease of pJNK signaling protein in C666-1 cells, HK1 cells and CNE2 cells, respectively. Figure 5.6 indicated a 0.4-fold, 0.7-fold and 0.5-fold decrease of p38 signaling protein in C666-1 cells, HK1 cells and CNE2 cells, respectively. Figure 5.6 also indicated a 0.2-fold, 0.3-fold and 0.5-fold decrease of p-p38 signaling protein in C666-1 cells, HK1 cells and CNE2 cells, respectively. These results confirmed that FosPeg® mediated PDT down-regulated ERK, JNK and p38 protein, but this varied in different NPC cell lines.

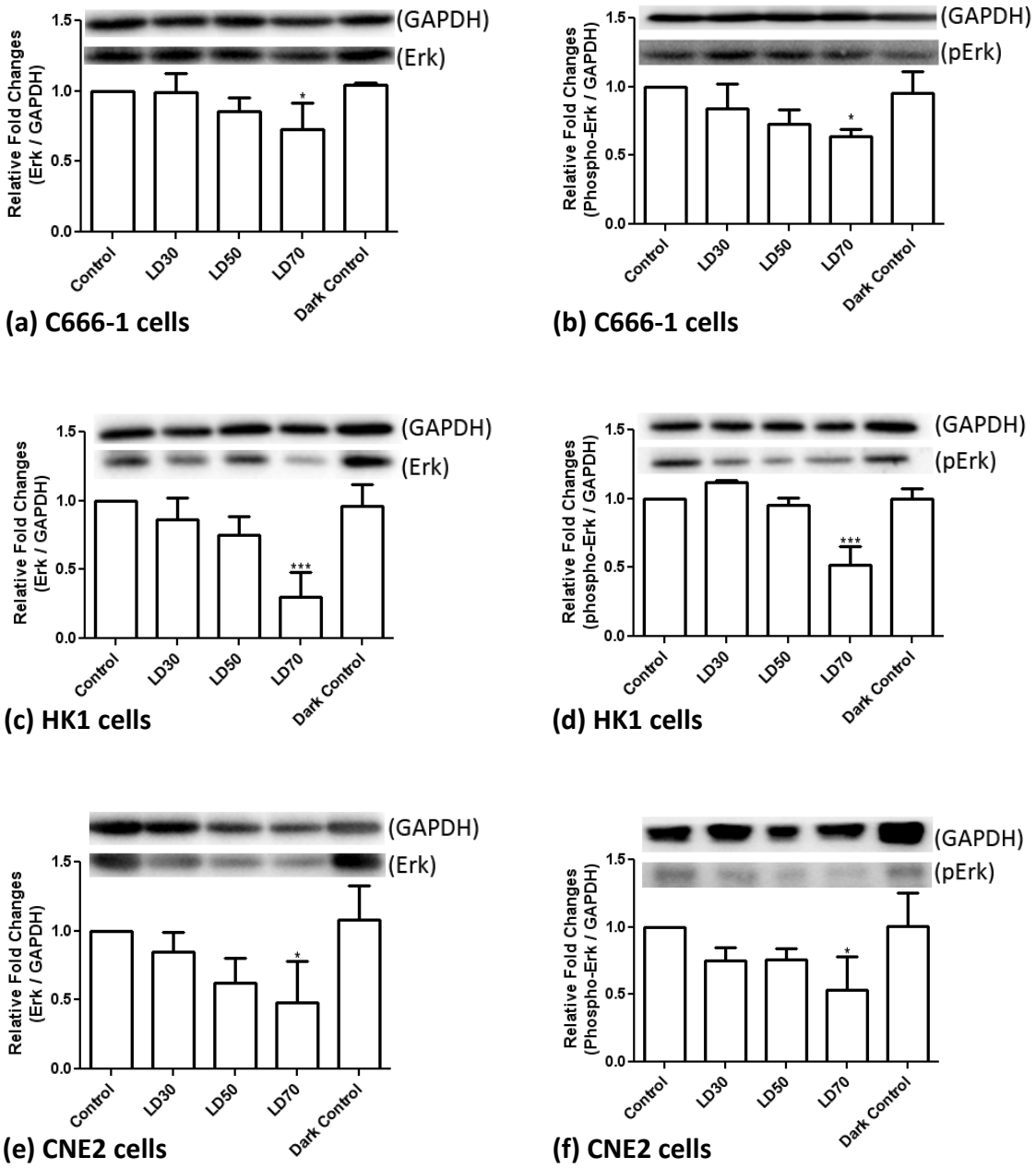

Fig 5.4 Effect of FosPeg® mediated PDT on the ERK and phospho-ERK (pERK) protein expression in C666-1 cells, HK1 cells and CNE2 cells.

Total cellular proteins were extracted from control and PDT treated cells for the detection of ERK and phospho-ERK protein by Western blot analysis. Protein amounts were normalized with GAPDH.

ERK and phospho-ERK proteins expressed by C666-1 cells (a & b); ERK and phospho-ERK proteins expressed by HK1 cells (c & d); ERK and phospho-ERK proteins expressed by CNE2 cells (e & f).

Significant differences between treatment and control groups were analyzed by one-way ANOVA and followed by Dunnett's post-tests (*: $p<0.05$, ***: $p<0.001$).

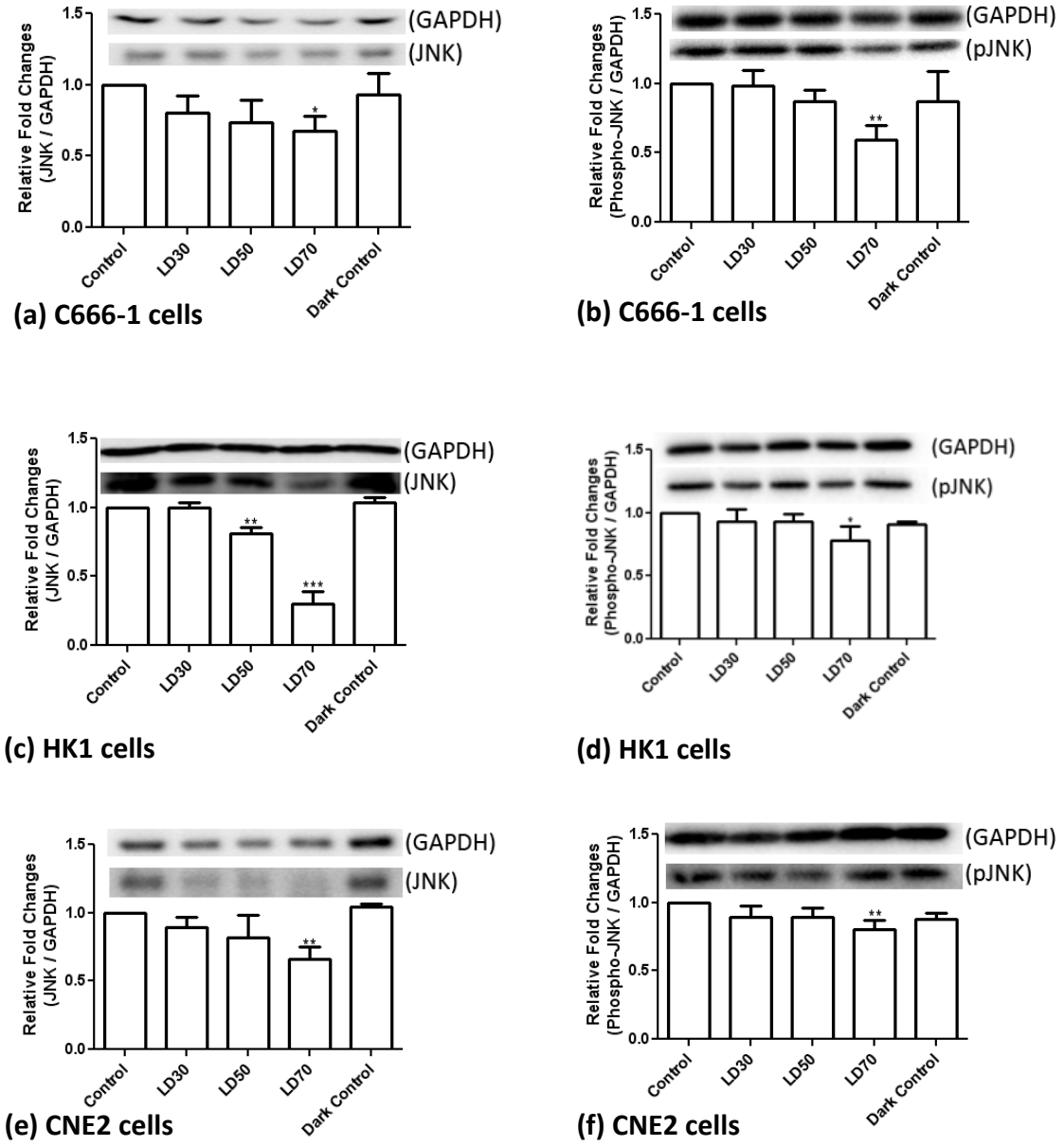

Fig 5.5 Effect of FosPeg® mediated PDT on the JNK and phospho-JNK protein expression in C666-1 cells, HK1 cells and CNE2 cells.

Total cellular proteins were extracted from control and PDT treated cells for the detection of JNK and phospho-JNK protein by Western blot analysis. Protein amounts were normalized with GAPDH.

JNK and phospho-JNK protein expressed by C666-1 cells (a & b); JNK and phospho-JNK proteins expressed by HK1 cells (c & d); JNK and phospho-JNK proteins expressed by CNE2 cells (e & f). Significant differences between treatment and control groups were analyzed by one-way ANOVA and followed by Dunnett's post-tests (* $p<0.05$, ** $p<0.01$, *** $p<0.001$).

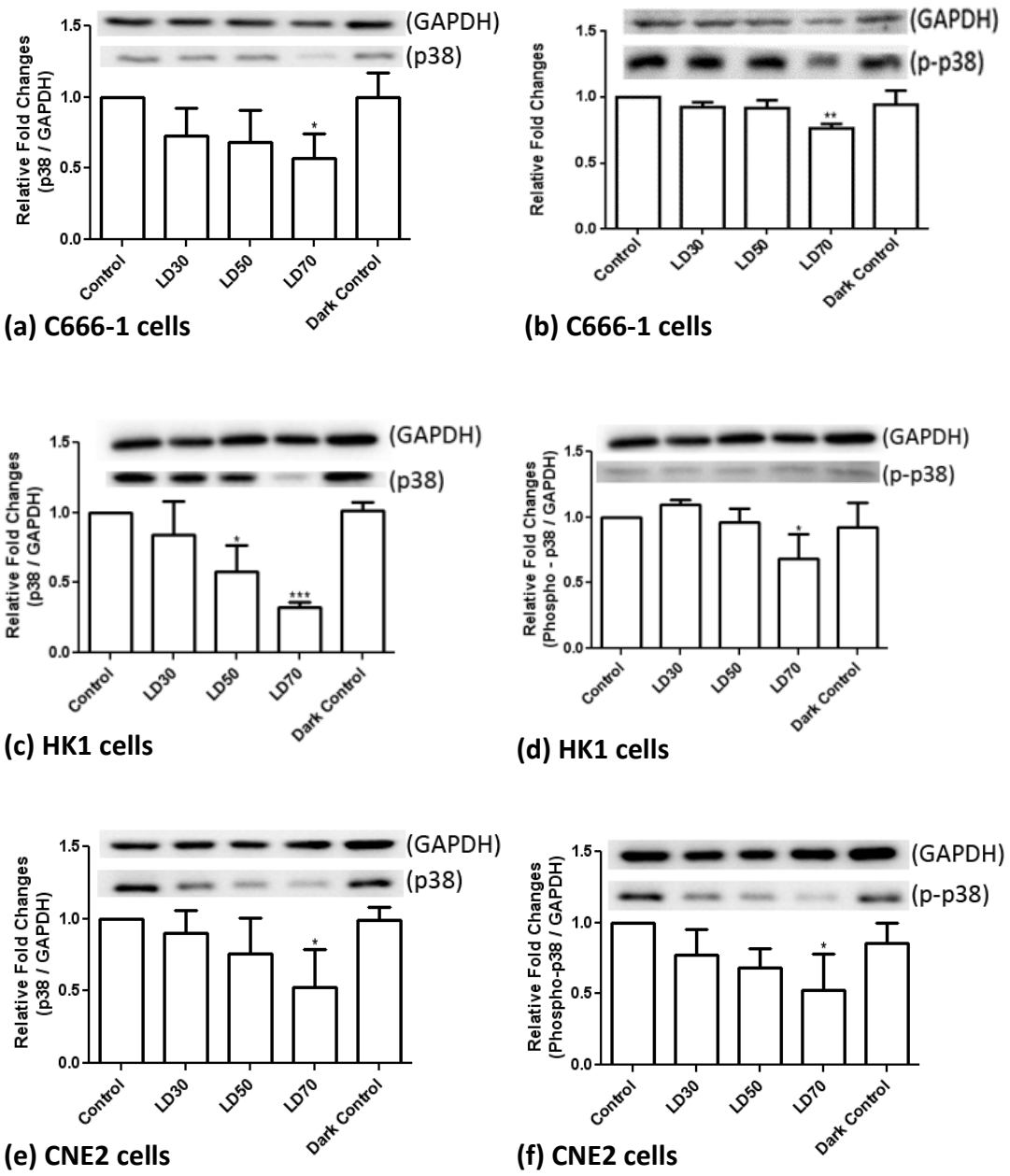

Fig 5.6 Effect of FosPeg® mediated PDT on the p38 and phospho-p38 protein expression in C666-1 cells, HK1 cells and CNE2 cells.

Total cellular proteins were extracted from control and PDT treated cells for the detection of p38 and phospho-p38 protein by Western blot analysis. Protein amounts were normalized with GAPDH. p38 and phospho-p38 proteins expressed by C666-1 cells (a & b); p38 and phospho-p38 proteins expressed by HK1 cells (c & d); p38 and phospho-p38 proteins expressed by CNE2 cells (e & f). Significant differences between treatment and control groups were analyzed by one-way ANOVA and followed by Dunnett's post-tests (*: $p<0.05$, ***: $p<0.001$).

5.4.3 Effect of FosPeg®-PDT on down-stream proteins of MAPK signaling pathway

Down-regulation of MAPK signaling proteins responded to FosPeg®-PDT may alter the expression of MAPK signaling pathway down-stream proteins. Thus the effect of FosPeg®-PDT on telomerase, VEGF, and NF-kB (down-stream proteins of MAPK signal pathways) were measured by Western blot analysis.

Figure 5.7 indicated that at LD_{70}, a significant down-regulation of telomerase was obtained in C666-1 cells ($P<0.05$). Figure 5.8 indicates that VEGF was only expressed in C666-1 cells. A significant decrease in VEGF was obtained at LD_{70} in C666-1 cells ($P<0.05$). However, Figure 5.9 indicates that the expression of NF-kB protein was not affected by FosPeg®-PDT. The expression of NF-kB protein may be overwhelmed by the oxidative stress caused by FosPeg®-PDT or other LMP1 signals present in NPC cells (Lavogna and Harhaj, 2012; Chung et al., 2013; Price et al., 2012). All these results confirmed that FosPeg® mediated PDT suppressed EGFR signaling proteins; MAPK signaling proteins and their down-stream proteins.

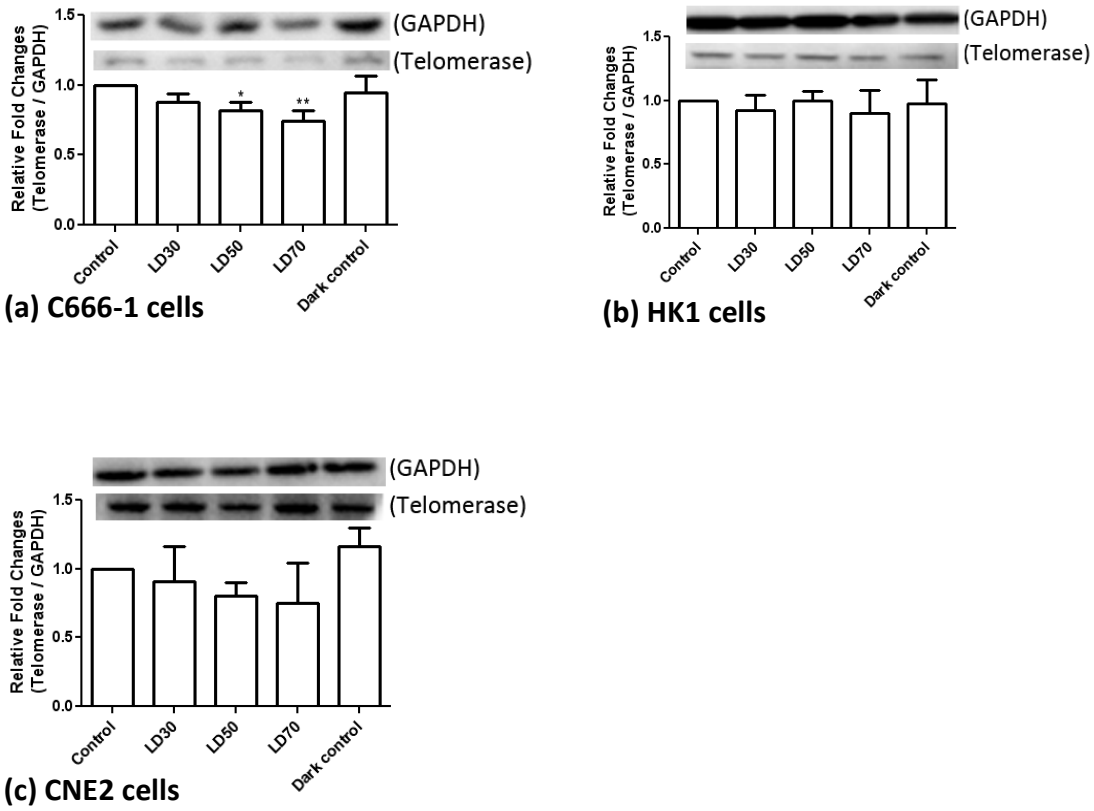

Fig 5.7 Effect of FosPeg® mediated PDT on the telomerase expression in C666-1 cells, HK1 cells and CNE2 cells.

Total cellular protein was extracted from control and PDT treated cells for the detection of telomerase protein by Western blot analysis. Protein amounts were normalized with GAPDH. Figure a – c shows Telomerase expression in C666-1 cells, HK1 cells and CNE2 cells, respectively. Significant differences between treatment and control groups were analyzed by one-way ANOVA and followed by Dunnett's post-tests (* $p<0.05$, ** $p<0.01$).

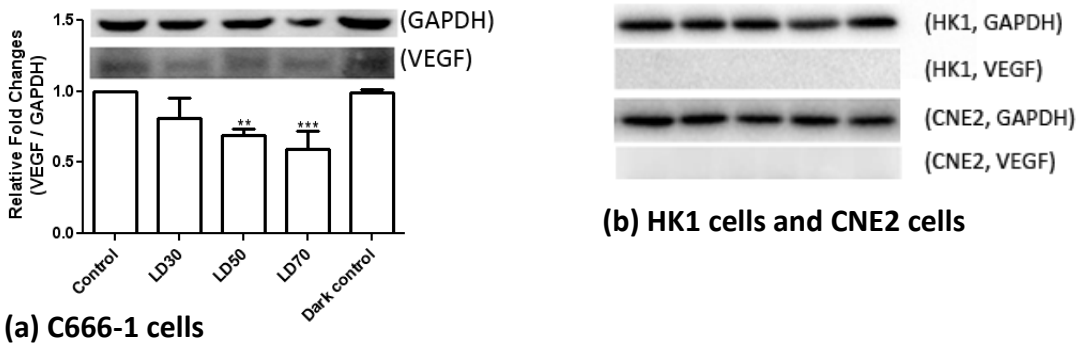

Fig 5.8 Effect of FosPeg® mediated PDT on the VEGF protein expression in C666-1 cells, HK1 cells and CNE2 cells.

Total cellular protein was extracted from control and PDT treated cells for the detection of VEGF protein by Western blot analysis. Protein amounts were normalized with GAPDH.

VEGF protein expressed by C666-1 cells (a); VEGF protein was not expressed by HK1 cells and CNE2 cells (b). Significant differences between treatment and control groups were analyzed by one-way ANOVA and followed by Dunnett's post-tests (* $p<0.05$, ** $p<0.01$, *** $p<0.001$).

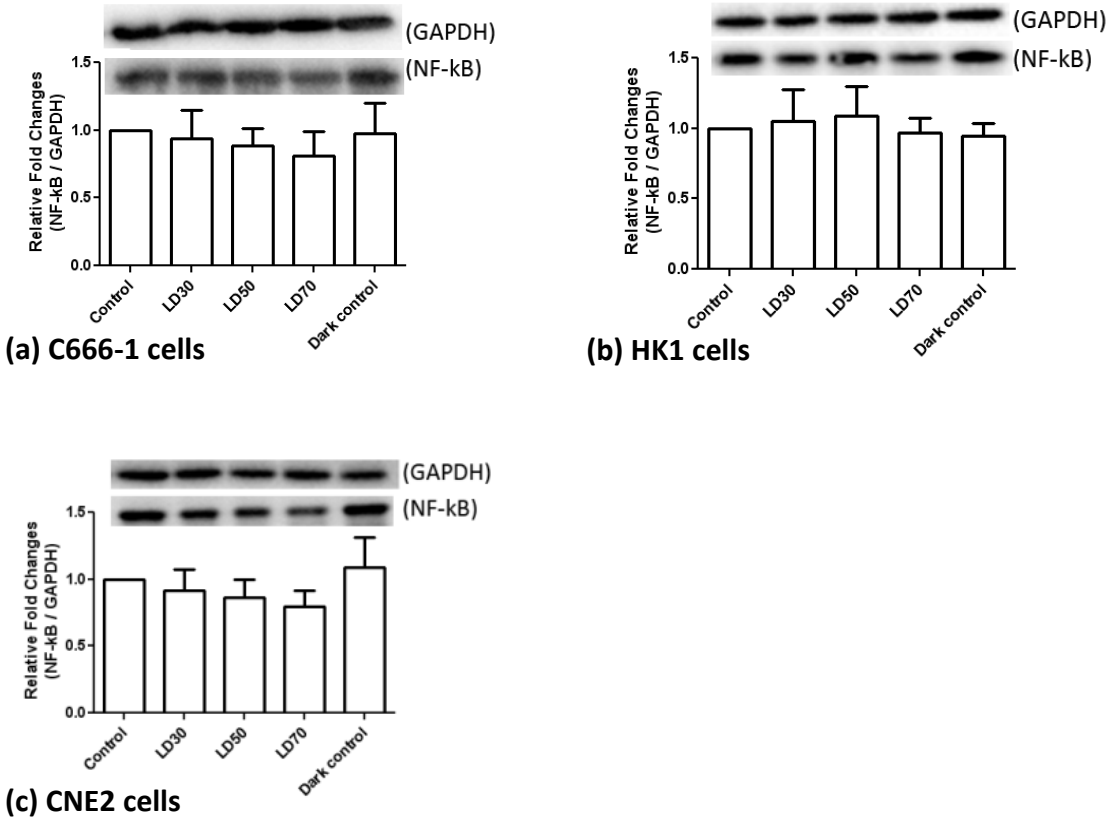

Fig 5.9 Effect of FosPeg® mediated PDT on the NF-kB protein expression in C666-1 cells, HK1 cells and CNE2 cells.

Total cellular protein was extracted from control and PDT treated cells for the detection of NF-kB protein by Western blot analysis. Protein amounts were normalized with GAPDH. Figure a – c showed NF-kB protein expression in C666-1 cells, HK1 cells and CNE2 cells respectively. Significant differences between treatment and control groups were analyzed by one-way ANOVA and followed by Dunnett's post-tests (* $p<0.05$, ** $p<0.01$, *** $p<0.001$).

5.4.4 FosPeg®-PDT induced cell cycle and DNA content change in NPC cells

It was suggested that alteration of MAPK signaling proteins regulated cell cycle. Thus alteration of cell cycle phase distribution mediated by FosPeg® was determined by flow cytometric analysis.

In Table 5.1, data showed that FosPeg®-PDT demonstrated a time dependent cell cycle arrest in all three NPC cell lines. Representative data were shown in Figure 5.10. The sub-G1, G1/G0, S and G2 phases were represented as (A), (B), (C) and (D) in the histograms, respectively.

Table 5.1 represented the time-dependent cell cycle regulated by FosPeg®-PDT on C666-1 cells, HK1 cells and CNE2 cells, respectively. For C666-1 cells, CNE2 cells and HK1 cells at LD_{50}, a significant increase in percentage of sub-G1 phase cells were obtained at 72 hours post FosPeg®-PDT, with 62.6%, 12.7% and 13.6% C666-1 cells, CNE2 cells and HK1 cells undergoing apoptosis, respectively ($p<0.05$).

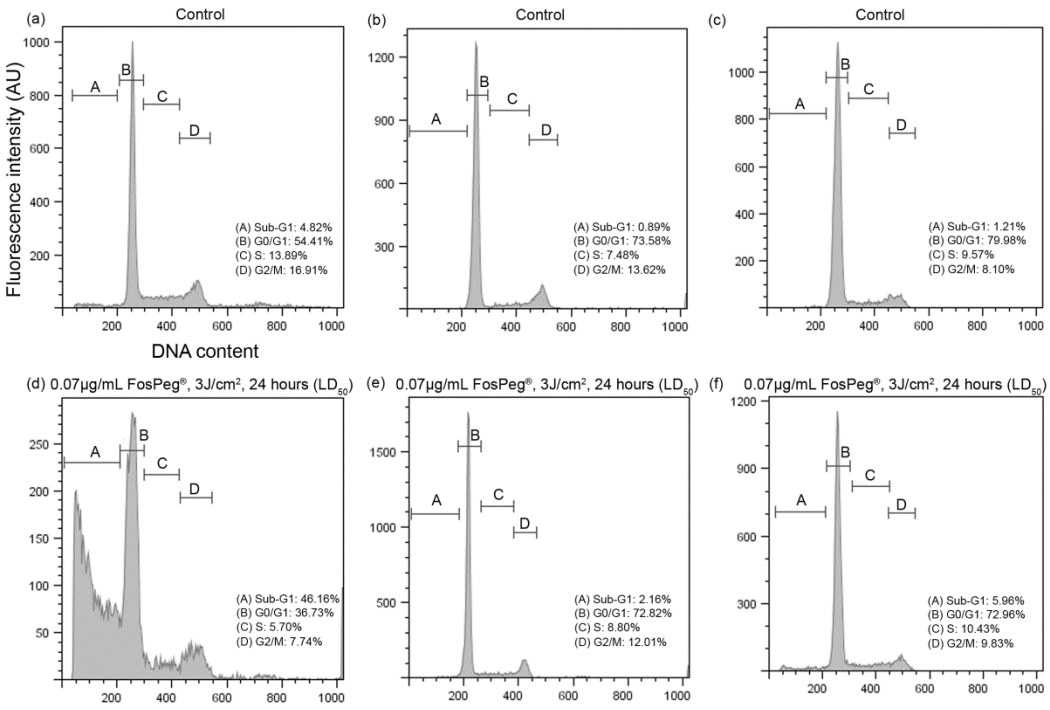

Figure 5.10 Flow cytometric analysis for effect of FosPeg®-PDT on cell cycle distribution in NPC cells 24 h after treatment at LD_{50}.
Representative data were shown in (a, d) C666-1 cells; (b, e) HK1 cells; (c, f) CNE2 cells.

Table 5.1 Flow cytometric analysis for time-effect of FosPeg®-PDT on cell cycle distribution in NPC cells 4-72 hours after treatment at LD_{50}.

C666-1 cells	Control	4 hours	24 hours	48 hours	72 hours
Sub-G1	4.40 ± 0.45%	3.91 ± 1.33%	**47.01 ± 2.03%*** **	51.46 ± 8.80%***	**62.62 ± 12.06%*** **
G0/G1	54.03 ± 0.39%	59.74 ± 1.97%	29.97 ± 8.36%***	25.68 ± 10.91%***	21.69 ± 6.89%***
S	15.23 ± 1.48%	14.32 ± 1.72%	9.96 ± 5.41%	16.57 ± 8.76%	8.61 ± 3.75%
G2/M	17.45 ± 1.24%	19.93 ± 2.42%	7.02 ± 1.45%	3.72 ± 2.62%***	3.82 ± 3.32%**
HK1 cells	**Control**	**4 hours**	**24 hours**	**48 hours**	**72 hours**
Sub-G1	1.01 ± 0.36%	0.83 ± 0.25%	3.60 ± 2.65%	9.43 ± 2.71%*	**13.64 ± 5.34%*** **
G0/G1	70.51 ± 3.73%	80.05 ± 1.61%	76.57 ± 3.85%	69.88 ± 2.05%	67.10 ± 7.84%
S	8.48 ± 2.39%	8.76 ± 1.64%	8.36 ± 1.18%	8.64 ± 0.44%	9.10 ± 0.61%
G2/M	13.61 ± 0.71%	10.69 ± 0.58%	12.24 ± 2.24%	11.27 ± 0.42%	9.50 ± 3.04%
CNE2 cells	**Control**	**4 hours**	**24 hours**	**48 hours**	**72 hours**
Sub-G1	1.36 ± 0.26%	1.13 ± 0.54%	6.08 ± 0.97%	6.52 ± 0.37%	**12.74 ± 5.76%** **
G0/G1	77.53 ± 6.78%	65.48 ± 3.01%	73.03 ± 1.05%	78.98 ± 1.95%	64.04 ± 3.91%***
S	12.40 ± 8.66%	12.48 ± 2.75%	10.74 ± 0.74%	5.55 ± 2.49%	15.6 ± 2.47%
G2/M	7.66 ± 0.66%	13.32 ± 1.12%	8.89 ± 1.00%	8.25 ± 0.54%	6.62 ± 2.02%

(a) C666-1 cells; (b) HK1 cells; (c) CNE2 cells. The cell percentages at different cell cycle phases expressed as mean±S.D. of three independent experiments. Significant difference between treatment and control groups were analyzed by two-way ANOVA and followed by Bonferroni's post-tests (* $p<0.05$, ** $p<0.01$, *** $p<0.001$).

5.4.5 FosPeg®-PDT reduced cell motility

Given the impact of MAPK signal proteins on the cell motility, scratch/wound healing assay was performed on FosPeg®-PDT treated cells (LD_{50}). Figure 5.11 indicated that FosPeg®-PDT treated cells reduced cell migration rate in all three NPC cell lines.

After 24 hours, the controls of HK1 cells and CNE2 cells showed a complete closure of the wounded area. A 66% closure of the wounded area was obtained in C666-1 control cells after 48 hours. The migration rate of FosPeg®-PDT treated C666-1 cells, HK1 cells and CNE2 cells were 0%, 8% and 60% respectively.

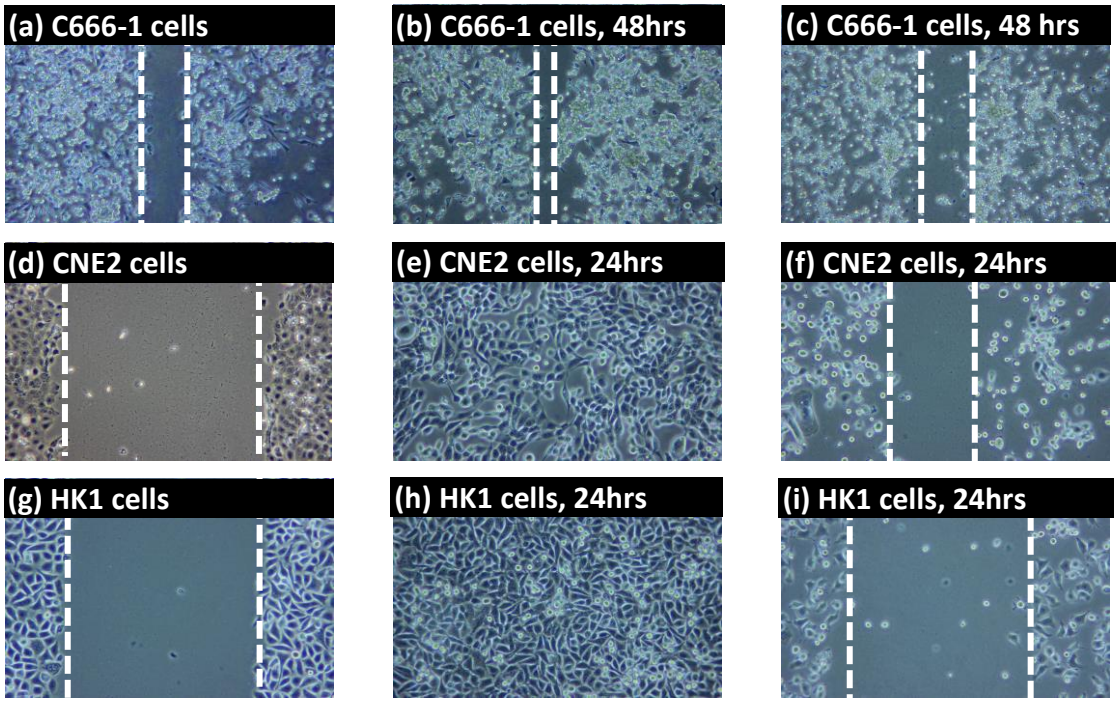

Fig 5.11 Effect of FosPeg® mediated PDT on cell migration in C666-1 cells, HK1 cells and CNE2 cells.

Figure a, b & c represent C666-1 control cells, C666-1 control cells (48 hours after scratch) and C666-1 cells (LD_{50} FosPeg® PDT treated cells, 48 hours after scratch);

Figure d, e & f represent CNE2 control cells, CNE2 control cells (24 hours after scratch) and CNE2 cells (LD_{50} FosPeg® PDT treated cells, 24 hours after scratch);

Figure g, h & I represent HK1 control cells, HK1 control cells (24 hours after scratch) and HK1 cells (LD_{50} FosPeg® PDT treated cells, 24 hours after scratch).

5.5 Discussion

As a 3rd generation photosensitizer, FosPeg® showed an improved PDT efficacy over mTHPC *in vitro* (Bovis et al., 2012; Buchholz et al., 2005; Compagnin et al., 2011; de Visscher et al., 2011; Hallewin et al., 2008; Lassalle et al., 2009; Maeda et al., 2000; Pegaz et al., 2006). According to chapter 4, it was confirmed that mitochondria were the major target site of FosPeg® PDT in NPC cells regardless of cell differentiation status.

Studies reported that PDT localized in mitochondria inhibited the expression of EGFR signaling protein. Hwang et al. (2013) reported that photosensitizers carboplatin and radachlorin targeted to mitochondria in head and neck cancer cells (AMC-HN3), resulted in alteration of EGFR expression. Tsai et al. (2009) reported that 5-ALA localized in mitochondria supress the EGFR expression level in lung cancer cells, melanoma cells and breast carcinoma cells via reduction of EGFR mRNA expression. Hence the effect of FosPeg®-PDT on EGFR signaling proteins was measured in this study.

Our results illustrated that EGFR and its down-stream Raf protein were consistently expressed in all three NPC cell lines. Down-regulation of EGFR and Raf protein was resulted in all three NPC cell lines after FosPeg®-PDT. Similar results were observed in various studies. Tsai et al. (2009) reported that 5-ALA-PDT down-regulated the protein level of EGFR in lung adenocarcinoma cells and melanoma cells. The reduction of EGFR was correlated with reduced invasiveness. Wong et al. (2003) also reported that 5-ALA- and Photofrin-PDT down-regulated EGFR expression in FaDu cells and lung fibroblasts. Ahmad et al. (2001) reported that PDT down-regulated EGFR expression in human squamous carcinoma A431 cells. Bhuvaneswari et al. (2009) also reported that combination therapies of PDT and EGFR inhibitors inhibited tumour growth effectively in the bladder tumour xenograft model.

EGFR is an oncoprotein involved in cell proliferation. Phosphorylation of EGFR signaling protein activated transcription factors via MAPK signaling pathways that modulate different cellular responses, such as the cell cycle, cell proliferation, inhibition of apoptosis, and angiogenesis (Yang et al., 2012). Studies also reported that photosensitizers localized in mitochondria resulted in alteration of MAPK signaling pathways (Bui-Xuan et al., 2010; Ji et al., 2010). Taken together, the effect of FosPeg®-PDT on MAPK signaling proteins were elucidated.

The signal transduction pathways triggered by PDT treatment varied with the cell type and photosensitizer employed (Oleinick, et al., 2002; Wu et al., 2011; Yow, et al., 2006). Studies showed that up-regulation of MAPK signaling pathways played a vital role in NPC development (Chan 2010; Dawson et al., 2012; Tsao et al., 2012).

ERKs are constitutively expressed in NPC cells, which regulated a diverse range of cellular functions, such as cell growth and development (Kerkhoff & Rapp, 1998; Zhang et al., 2007). Phosphorylation of ERK via the EGFR cascade activated NF-kB, stimulated angiogenesis, cell migration and invasion (Downward, 2003; Roberts & Der, 2007; Yu et al., 2013). Up-regulation of JNK was also observed in NPC cells, resulted in cell cycle deregulation via increased p53 phosphorylation (Eliopoulos & Young, 1998; Tsai et al., 2006). The p38 protein was also constitutively expressed in NPC cells, which regulated a wide range of cellular functions, including the self-sufficiency of growth signals, angiogenesis, metastasis, regulation of the cell cycle, and protection against apoptosis (Chen et al., 2010; Roux & Blenis, 2004).

Inhibition of MAPK signaling protein expression could be one of the therapeutic approaches to eliminate NPC cells. Our data confirmed that FosPeg®-PDT significantly down-regulated the expression of ERK, JNK and p38 proteins at LD_{70} in all three NPC cells, resulted in apoptotic cell death ($P<0.05$). The MAPK signaling pathways downstream proteins, including telomerase and VEGF, were also down-regulated by FosPeg®-PDT at LD_{70}. Our finding was echoed with other

studies, indicating the vital role of MAPK and their down-stream proteins in NPC cell elimination. Chan et al. (2009) reported that inhibition of p38 expression enhanced hypericin-PDT efficacy in HK1 cells, resulted in apoptotic cell death. It was also reported that inhibition of p38 protein enhanced the therapeutic efficacy in NPC cells (Chen et al., 2010). Deng et al. (2011) reported that down-regulation of ERK protein expression in CNE2 cells by microRNA resulted in tumour growth suppression.

However, our data indicated that the expression of NF-kB protein was not affected by FosPeg®-PDT. The down-regulation of NF-kB protein via regulation of MAPK signaling proteins may be overwhelmed by the oxidative stress caused by FosPeg®-PDT or other LMP1 signals present in NPC cells (Lavogna and Harhaj, 2012; Chung et al., 2013; Price et al., 2012). It was well document that NF-kB is sensitive to the cellular oxidative stress (Ryter and Gomer, 1993; Piret et al., 1995; Rapozzi et al., 2011). Studies also illustrated that ROS generated by PDT lead to NF-kB activation, resulted in regulation of the inflammatory response, cell proliferation, apoptosis and angiogenesis (Matroule et al., 2006; Coupienne et al., 2010).

To sum up, FosPeg®-PDT is an effective treatment option for both EBV positive and EBV negative NPC cells *in vitro*. All the evidence shown in this study supports the hypothesis that MAPK signaling proteins could be one of the therapeutic targets and biomarkers for FosPeg®-PDT NPC treatment (Figure 5.12). Continuing work in this field will further elucidate the action mechanisms mediated by FosPeg®-PDT, in turn, as an alternative treatment complementary to radiation therapy with minimized adverse effects. However, there remains a need for well-designed, randomized, controlled trials in order to allow PDT to become a part of mainstream clinical practice.

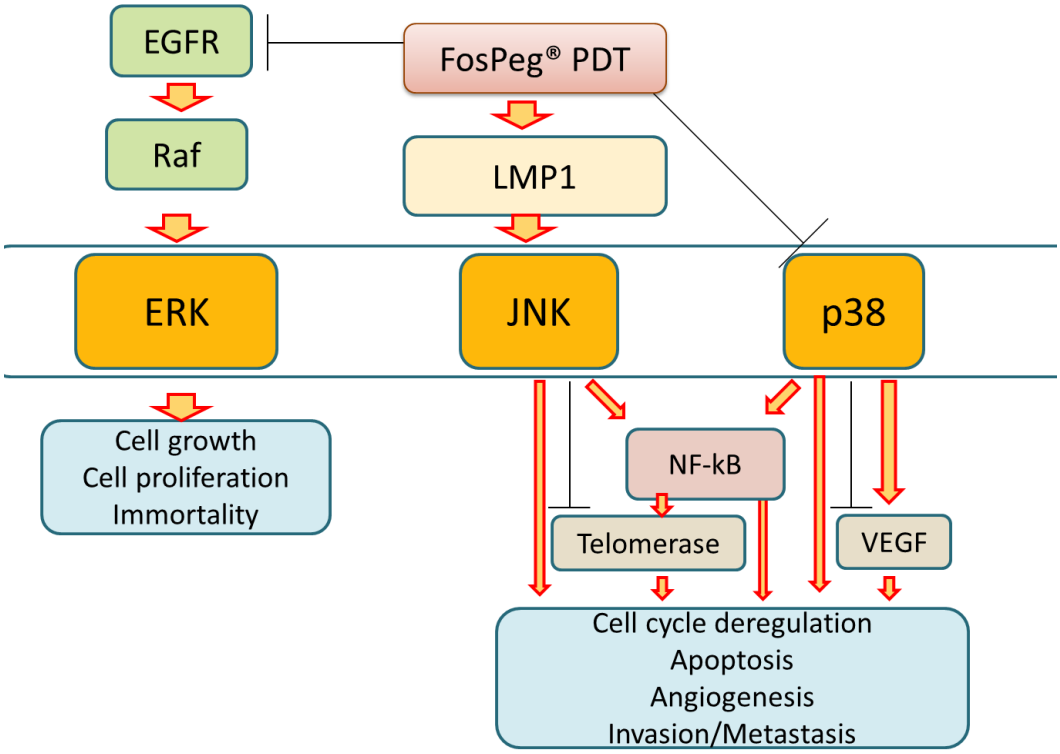

Fig 5.12 Diagram indicated inhibitory effect of FosPeg® mediated PDT on MAPK signaling proteins and their down-stream proteins.
→ Stimulatory effect. ⊣ Inhibitory effect.

5.6 References

Ahmad N, Kalka K, Mukhtar H. (2001) In vitro and in vivo inhibition of epidermal growth factor receptor-tyrosine kinase pathway by photodynamic therapy. *Oncogene*. 20(18), 2314-7.

Agostinis P, Berg K, Cengel KA, Foster TH, Girotti AW, Gollnick SO, Hahn SM, Hamblin MR, Juzeniene A, Kessel D, Korbelik M, Moan J, Mroz P, Nowis D, Piette J, Wilson BC, Golab J (2011) Photodynamic theray of cancer: An update. *CA Cancer J Clin*. 61(4), 250-81.

Bhuvaneswari R, Gan YY, Soo KC, Olivo M. (2009) Targeting EGFR with photodynamic therapy in combination with Erbitux enhances in vivo bladder tumor response. *Mol Cance*r. 8, 94.

Bovis MJ, Woodhams JH, Loizidou M, Scheglmann D, Bown SG, Macrobert AJ. (2012) Improved in vivo delivery of m-THPC via pegylated liposomes for use in photodynamic therapy. *J Control Release, 157*(2), 196-205.

Buchholz J, Kaser-Hotz B, Khan T, Rohrer Bley C, Melzer K, Schwendener RA, Walt H. (2005) Optimizing photodynamic therapy: in vivo pharmacokinetics of liposomal meta-(tetrahydroxyphenyl)chlorin in feline squamous cell carcinoma. *Clin Cancer Res, 11*(20), 7538-7544.

Bui-Xuan NH, Tang PM, Wong CK, Fung KP. (2010) Photo-activated pheophorbide-a, an active component of Scutellaria barbata, enhances apoptosis via the suppression of ERK-mediated autophagy in the estrogen receptor-negative human breast adenocarcinoma cells MDA-MB-231. *J Ethnopharmacol*. 131(1), 95-103.

Chan AT. (2010) Nasopharygneal carcinoma. *Ann Oncol*. 21(7), 308-12.

Chan PS, Koon HK, Wu ZG, Wong RN, Lung ML, Chang CK, Mak NK. (2009) Role of p38 MAPKs in hypericin photodynamic therapy-induced apoptosis of nasopharyngeal carcinoma cells. *Photochem Photobiol, 85*(5), 1207-1217.

Chen X, Zhao P, Chen F, Li L, Luo R. (2011) Effect and mechanism of 5-aminolevulinic acid-mediated photodynamic therapy in esophageal cancer. *Lasers Med Sci, 26*(1), 69-78.

Chen CC, Chen LC, Liang Y, Tsang NM, Chang YS. (2010) Epstein-Barr virus latent membrane protein 1 induces the chemotherapeutic target, thymidine phosphorylase, via NF-kappaB and p38MAPK pathways. *Cell signal*. 22(7): 1132-42.

Compagnin C, Moret F, Celotti L, Miotto G, Woodhams JH, MacRobert AJ, Reddi E. (2011) Meta-tetra(hydroxyphenyl)chlorin-loaded liposomes sterically stabilised with poly(ethylene glycol) of different length and density: characterisation, in vitro cellular uptake and phototoxicity. *Photochem Photobiol Sci, 10*(11), 1751-1759.

Coupienne I, Piette J, Bontems S. (2010) How to monitor NF-kappaB activation after photodynamic therapy. *Methods Mol Biol*. 635, 79-95.

Chung GT, Lou WP, Chow C, To KF, Choy KW, Leung AW, Tong CY, Yuem JW, Ko CW< Yip TT, Busson P, Lo KW. (2013) Consitutive activation of distinct NF-kB signals in EBV-associated nasopharyngeal carcinoma. *J Pathol*. 231(3), 311-22.

D'Hallewin MA, Kochetkov D, Viry-Babel Y, Leroux A, Werkmeister E, Dumas D, Bezdetnaya L. (2008) Photodynamic therapy with intratumoral administration of Lipid-Based mTHPC in a model of breast cancer recurrence. *Lasers Surg Med, 40*(8), 543-549.

Darling NJ and Cook SJ. (2014) The role of MAPK signalling pathways in the response to endoplasmic reticulum stress. *Biochim Biophys Acta*. http://dx.doi.org/10.1016/j.bbamcr.2014.01.009

Dawson CW, Port RJ, Young LS. (2012) The role of the EBV-encoded latent membrane proteins LMP1 and LMP2 in the pathogenesis ofnasopharyngeal carcinoma (NPC). *Semin Cancer Biol*. 22(2), 144-53.

de Visscher SA, Dijkstra PU, Tan IB, Roodenburg JL, Witjes MJ. (2013) mTHPC mediated photodynamic therapy (PDT) of squamous cell carcinoma in the head and neck: a systematic review. *Oral Oncol*. 49(3), 192-210.

de Visscher SA, Kascakova S, de Bruijn HS, van den Heuvel A, Amelink A, Sterenborg HJ, Witjes MJ. (2011) Fluorescence localization and kinetics of mTHPC and liposomal formulations of mTHPC in the window-chamber tumor model. *Lasers Surg Med, 43*(6), 528-536.

Dent P. (2014) Crosstalk between ERK, AKT, and cell survival. *Cancer Biol Ther*. 15(3), 245-46.

Deng L, Yang J, Zhao XR, Deng XY, Zeng L, Gu HH, Cao Y. (2003) Cells in G2/M phase increased in human nasopharyngeal carcinoma cell line by EBV-LMP1 through activation of NF-kappaB and AP-1. *Cell Res, 13*(3), 187-194.

Deng M, Tang H, Zhou M, Xiong W, Zheng Y, Ye Q, Zeng X, Liao Q, Guo X, Li X, Ma J, Li G. (2011) miR-216b suppresses tumor growth and invasion by targeting KRAS in nasopharyngeal carcinoma. *J Cell Sci*. 124(Pt17): 2997-3005.

Devi DG, Cibin TR, Abraham A. (2013) Bis (3,5-diiodo-2,4,6-trihydroxyphenyl) squaraine photodynamic therapy induices in vivo tumor ablation by triggering cytochrome dependent mitochondria mediated apoptosis. *Photodiagnosis Photodyn Ther*. 10(4), 510-7.

Dougherty TJ, Gomer CJ, Henderson BW, Jori G, Kessel D, Korbelik M, Peng Q. (1998) Photodynamic Therapy. *J Natl Cancer Inst, 90*(12), 17.

Downward J. (2003) Targeting RAS signalling pathways in cancer therapy. *Nat Rev Cancer, 3*(1), 11-22.

Eliopoulos AG, Young LS. (1998) Activation of the cJun N-terminal kinase (JNK) pathway by the Epstein-Barr virus-encoded latent membrane protein 1 (LMP1). *Oncogene, 16*(13), 1731-1742.

Green B, Cobb AR, Hopper C. (2013) Photodynamic therapy in the management of lesions of the head and neck. *Br J Oral Maxillofac Surg*. 51(4), 283-7.

Hwang H, Biswas R, Chung PS, Ahn JC. (2013) Modulation of EGFR and ROS induced cytochrome c release by combination of photodynamic therapy and carboplatin in human cultured head and neck cancer cells and tumor xenograft in nude mice. *J Photochem Photobiol B*. 128, 70-7.

Ji HT, Chien LT, Lin YH, Chien HF, Chen CT. (2010) 5-ALA mediated photodynamic therapy induces autophagic cell death via AMP-activated protein kinase. *Mol Cancer*. 9: 91.

Kerkhoff E, Rapp UR. (1998) Cell cycle targets of Ras/Raf signalling. *Oncogene, 17*(11 Reviews), 1457-1462.

Kim JH, Kim WS, Park C. (2013) Epstein-Barr virus latent membrane protein 1 increases genomic instability through Egr-1-mediated up-regulation of activation-induced cytidine deaminase in B-cell lymphoma. *Leuk Lymphoma*. 54(9), 2035-40.

Kung CP, Meckes DG, Raab-Traub N. (2011). Epstein-Barr virus LMP1 activates EGFR, STAT3, and ERK through effects on PKCdelta. *J Virol, 85*(9), 4399-4408.

Kushibiki T, Hirasawa T, Okawa S, Ishihara M. (2013) Responses of cancer cells induced by photodynamic therapy. *J Healthc Eng*. 4(1), 87-108.

Lassalle HP, Dumas D, Grafe S, D'Hallewin MA, Guillemin F, Bezdetnaya L. (2009) Correlation between in vivo pharmacokinetics, intratumoral distribution and photodynamic efficiency of liposomal mTHPC. *J Control Release, 134*(2), 118-124.

Lavorgna A, Harhaj EW. (2012) EBV LMP1: New and shared pathways to NF-kB activation. *Proc NAtl Acad Sci USA*. 109(7), 2188-9.

Liu MG, Wang RR, Chen XF, Zhang FK, Cui XY, Chen J. (2011) Differential roles of ERK, JNK and p38 MAPK in pain-related spatial and temporal enhancement of synaptic responses in the hippocampal formation of rats: multi-electrode array recordings. *Brain Res, 1382*, 57-69.

Lo AK, Lo KW, Ko CW, Young LS, Dawson CW. (2013) Inhibition of the LKB1-AMPK Pathway by the Epstein-Barr Virus-encoded LMP1 Promotes Proliferation and Transformation of Human Nasopharyngeal Epithelial Cells. *J Pathol*. 230(3), 336-346.

Maeda H, Wu J, Sawa T, Matsumura Y, Hori K. (2000) Tumor vascular permeability and the EPR effect in macromolecular therapeutics: a review. *J Control Release, 65*(1-2), 271-284.

Matroule JY, Volanti C, Piette J. (2006) NF-kappaB in photodynamic therapy: discrepancies of a master regulator. *Photochem Photobiol*. 82(5), 1241-6.

Miki Y, Akimoto J, Yokoyama S, Homma T, Tsutsumi M, Haraoka J, Hirano K, Beppu M. (2013) Photodynamic therapy in combination with talaporfin sodium induces mitochondrial apoptotic cell death accompanied with necrosis in glioma cells. *Biol Pharm Bull*. 36(2), 215-21.

Murono S, Inoue H, Tanabe T, Joab I, Yoshizaki T, Furukawa M, Pagano JS. (2001) Induction of cyclooxygenase-2 by Epstein-Barr virus latent membrane protein 1 is involved in vascular endothelial growth factor production in nasopharyngeal carcinoma cells. *Proc Natl Acad Sci U S A, 98*(12), 6905-6910.

Oleinick NL, Morris RL, Belichenko I. (2002) The role of apoptosis in response to photodynamic therapy: what, where, why, and how. *Photochem Photobiol Sci, 1*(1), 1-21.

Pegaz B, Debefve E, Ballini JP, Wagnieres G, Spaniol S, Albrecht V, Konan-Kouakou YN. (2006) Photothrombic activity of m-THPC-loaded liposomal formulations: pre-clinical assessment on chick chorioallantoic membrane model. *Eur J Pharm Sci*, *28*(1-2), 134-140.

Piret B, Legrand-Poels S, Sappey C, Piette J. (1995) NF-kappa B transcription factor and human immunodeficiency virus type 1 (HIV-1) activation by methylene blue photosensitization. *Eur. J. Biochem*. 228, 447-455.

Price AM, Tourigny JP, Forte E, Salinas RE, Dave SS, Luftig MA. (2012) Analysis of Epstein-Barr virus-regulated host gene expression changes through primary B-cell outgrowth reveals delayed kinetics of latent membrane protein 1-mediated NF-κB activation. *J Virol*. 86(20), 11096-106.

Rapozzi V, Umezawa K, Xodo LE. (2011) Role of NF-kB/Snail/RKIP loop in the response of tumor cells to photodynamic therapy. *Lasers Surg Med*. 43(7), 575-85.

Roberts PJ, Der CJ. (2007) Targeting the Raf-MEK-ERK mitogen-activated protein kinase cascade for the treatment of cancer. *Oncogene, 26*(22), 3291-3310.

Robertson CA, Evans DH, Abrahamse H. (2009) Photodynamic therapy (PDT): a short review on cellular mechanisms and cancer research applications for PDT. *J Photochem Photobiol B*. 96(1), 1-8.

Roux PP, Blenis J. (2004) ERK and p38 MAPK-activated protein kinases: a family of protein kinases with diverse biological functions. *Microbiol Mol Biol Rev, 68*(2), 320-344.

Ryter SW and Gomer CJ. (1993) Nuclear factor jappa B binding activity in mouse L1210 cells following Photofrin II-mediated photosensitization. *Photochem. Photobiol*. 58, 753-756.

Shirasu N, Nam SO, Kuroki M. (2013) Tumor-targeted photodynamic therapy. *Anticancer Res*. 33(7), 2823-31.

Sui X, Kong N, Ye L, Han W, Zhou J, Zhang Q, He C, Pan H. (2014) p38 and JNK MAPK pathways control the balance of apoptosis and autophagy in response to chemotherapeutic agents. *Cancer Lett*. 344(2), 174-9.

Tsai CL, Li HP, Lu YJ, Hsueh C, Liang Y, Chen CL, Chang YS. (2006) Activation of DNA methyltransferase 1 by EBV LMP1 Involves c-Jun NH(2)-terminal kinase signaling. *Cancer Res, 66*(24), 11668-11676.

Tsai T, Ji HT, Chiang PC, Chou RH, Chang WS, Chen CT. (2009) ALA-PDT results in phenotypic changes and decreased cellular invasion in surviving cancer cells. *Lasers Surg Med*. 41(4), 305-15.

Tsao SW, Tsang CM, Pang PS, Zhang G, Chen H, Lo KW. (2012) The biology of EBV infection in human epithelial cells. *Semin Cancer Biol*. 22(2), 137-43.

Wang CY, Wng X, Wang Y, Zhou T, Bai Y, Li YC, Huang B. (2012) Photosensitization of phycocyanin extracted from Microcystis in human hepatocellular carcinoma cells: implication of mitochondria-dependent apoptosis. *J Photochem Photobiol B*. 117, 70-9.

Wong TW, Tracy E, Oseroff AR, Baumann H. (2003) Photodynamic therapy mediates immediate loss of cellular responsiveness to cytokines and growth factors. *Cancer Res*. 63(13), 3812-8.

Wu M, Li X, Li X, Li G. (2009) Signaling Transduction Network Mediated by Tumor Suppressor/Susceptibility Genes in NPC. *Curr Genomics, 10*(4), 216-222.

Wu RWK, Yow CMN, Wong CK, Lam YH. (2011) Photodynamic therapy (PDT) - Initiation of apoptosis via activation of stress-activated p38 MAPK and JNK signal pathway in H460 cell lines. *Photodiagnosis Photodyn Ther, 8*(3), 254-263.

Yang PW, Hung MC, Hsieh CY,Tung EC, Wang YH, Tsai JC, Lee JM. (2012) The effects of Photofrin-mediated photodynamic therapy on the modulation of EGFR in esophageal squamous cell carcinoma cells. *Lasers Med Sci*. 28(2), 605-14.

Yow CMN, Mak NK, Leung AW, Huang Z. (2009) Induction of early apoptosis in human nasopharyngeal carcinoma cells by mTHPC-mediated photocytotoxicity. *Photodiagnosis Photodyn Ther, 6*(2), 122-127.

Yu PH, Chou SF, Chen CL, Hung H, Lai CY, Yang PM, Jeng YM, Liaw SF, Kuo HH, Hsu HC, Chen JY, Wang WB. (2013) Upregulatio of endocan by Epstein-barr virus latent membrane protein 1 and its clinical significance in nasopharyngeal carcinoma. *PLoS One*. 8(12), e82254.

Zhang J, Bowden GT. (2012) Activation of p38 MAP kinase and JNK pathways by UVA irradiation. *Photochem Photobiol Sci, 11*(1), 54-61.

Zhang Z, Sun D, Van do N, Tang A, Hu L, Huang G. (2007) Inactivation of RASSF2A by promoter methylation correlates with lymph node metastasis in nasopharyngeal carcinoma. *Int J Cancer, 120*(1), 32-38.

Zheng G, Chen J, Stefflova K, Jarvi M, Li H, Wilson BC. (2007) Photodynamic molecular beacon as an activatable photosensitizer based on protease-controlled singlet oxygen quenching and activation. *Proc Natl Acad Sci U S A, 104*(21), 8989-8994.

Chapter 6

Effects of FosPeg®-PDT on *MDR1* expressing in NPC cells

6.1 Abstract

Multidrug resistance is the major obstacle to chemotherapy in tumour patients. The term multidrug resistance (MDR) refers to the ability of cancer cells to develop cross resistance to a range of anti-tumour drugs which are structurally and functionally unrelated. Recent studies illustrated the importance of ABC membrane transporters as one of the leading mechanisms of MDR in cancer cells. Among these, P-glycoprotein (P-gp) is the best studied mechanisms of MDR phenotype in photodynamic therapy (PDT) treated cells.

In this *in vitro* study, the expression of *MDR1* gene and its product, P-gp on human undifferentiated, poorly differentiated and well differentiated human nasopharyngeal carcinoma (NPC) cells were investigated at pre and post FosPeg® photoactivation via flow cytometry and Western blotting analysis. The influence of P-gp efflux activity on FosPeg® was also examined via flow cytometry.

Regardless the differentiation status, all the three NPC cell lines express P-gp protein. Results indicated that FosPeg® photoactivation heighten the expression of *MDR1* gene and P-gp transporter at LD_{70}. 4-fold to >10-fold increase of MDR gene and 1-fold to 2-fold increase of P-gp protein expression were obtained on NPC cells after FosPeg® mediated-PDT. Interestingly, FosPeg® itself is not the substrate of P-gp transporter protein and no efflux of FosPeg® through P-gp was observed in all three tested NPC cell lines. Thus the PDT efficiency was not affected even FosPeg® mediated PDT induced *MDR1* gene and P-gp protein expression in NPC cells.

FosPeg®-PDT could be a potential therapeutic approach for MDR cancer patients. Understanding the mechanism of FosPeg® on development of drug resistance properties may help to develop better treatment strategies for NPC.

6.2 Introduction

Multidrug resistance is the major obstacle to chemotherapy in tumour patients. The term multidrug resistance (MDR) refers to the ability of cancer cells being developed to cross resists with a range of anti-tumour drugs which are structurally and functionally unrelated. Development of resistant cells after conventional chemotherapy is a major concern for oncologists, which may affect the therapeutic efficacy. The ability of tumour cells to efflux a wide variety of chemotherapeutics limited the choices of chemo-drugs by the clinicians. Resistance of tumours to chemotherapies depends on the influence to uptake, transport and metabolism of the drug. The phenomenon of MDR could be achieved by the following mechanisms: increase drug efflux from the cells via the adenosine triphosphate binding cassette transporters (ABC); inactivation of drugs via detoxifying enzymes; and defective apoptotic pathways (Stavrovskaya, 2000; Szakacset et al., 2006). Among these, over-expression of the transporter protein that actively pumps out chemo-drugs or photosensitizers admitted is the major cause of drug resistance. These plasma membrane glycoproteins include P-glycoprotein (P-gp/ABCB1), multidrug resistance associated protein (MRP1/ABCC1) and breast cancer resistance protein (BCRP/ABCG2).

Multi-drug resistance (*MDR1*) transporter, P-glycoprotein (P-gp) is one of the transporter proteins over-expressed in resistant tumours. Recent studies indicated that P-gp is the most typical ATP-dependent drug efflux pump contributed to multidrug resistance in cancer cells. P-gp/MDR transporter protein is the best-characterized mechanism of MDR in tumour (Eichhorn & Efferth, 2012; Gottesman & Ling, 2006; Lespine et al., 2012; Szakacs et al., 2006; Tredan et al., 2007). Studies also revealed that the expression of P-gp was correlated with poor survival rates in recurrent or metastatic nasopharyngeal carcinoma (NPC) patients (Chen et al., 2001; Hsu et al., 2002). Increased expression of P-gp was frequently seen in NPC drug-resistant cancer cell lines. Ji's study demonstrated an increase in P-gp expression in NPC/CNE1 cell line after radiotherapy (Ji et al., 2013). The increased

expression of P-gp was associated with various stimuli including anticancer drugs and oxidative stress (Lin et al., 2001; Mo et al., 2012; Schrenk et al., 2001; Su et al., 1998; Yamane et al., 1998).

Since there was considerable growth of PDT in the past two decades, researchers have raised their concern on drug resistance to photosensitizers. Among these, P-gp is the well-studied mechanism of MDR phenotype in PDT treated cells (Aszalos, 2007; Solazzo et al., 2006). Pre-clinical and clinical data published in the past two decades indicated that tumour cells resistant to some photosensitizers did affect the efficacy and choices of PDT to cancer patients. Patients with different tumours, such as head and neck and liver carcinoma were affected (Capella & Capella, 2003; Moan & Peng, 2003; Robey et al., 2005). Controversially, studies indicated that some photosensitizers were able to inhibit the expression of P-gp in various cancers, such as uterine carcinoma and hepatocellular carcinoma (Chu et al., 2008; Tang et al., 2009). mTHPC-PDT was being investigated as a potential drug candidate against multi-drug resistant breast tumours with promising results (Teiten et al., 2001). Study also indicated that mTHPC mediated PDT did not induce resistance to subsequent cycles of PDT (Hornung et al., 1998). However, the exact mechanism for overcoming resistance is not fully understood.

In view of limited information related to the interaction between FosPeg® and P-gp/*MDR1* transporter proteins, we therefore have systemically examined whether FosPeg® is a P-gp substrate and determined its effects on the drug resistant properties by examined *MDR1* and P-gp protein expression in three NPC cell lines. Expression of *MDR1* mRNA and P-gp protein after FosPeg® mediated PDT treatment together with the functional role of P-gp efflux properties on FosPeg® were carried out.

6.3 Methodology

6.3.1 Quantitation of *MDR1* mRNA expression by real-time RT-PCR

NPC cells ($1x10^6$ cells/dish) were either treated as dark control cells (0.3μg/ml FosPeg® without light irradiation) or at the following lethal doses of FosPeg® and LED light dose. For C666-1 cells, LD_{30} (0.05μg/ml, 3 J/cm^2) and LD_{70} (0.30μg/ml, 3 J/cm^2) were applied for subsequent experiments. For HK1 cells, LD_{30} (0.05μg/ml, 3J/cm^2) and LD_{70} (0.25μg/ml, 3 J/cm^2) were used. For CNE2 cells, LD_{30} (0.05μg/ml, 3J/cm^2) and LD_{70} (0.125μg/ml, 3 J/cm^2) were used. At 24 hours post-PDT, the cells were harvested and the total cellular RNA was extracted using the High Pure RNA isolation kits (Roche, USA) according to the manufacturer's specifications. Concentration of RNA in extracted samples was measured by nanodrop ND-2000 spectros photometer (Nanodrop Technologies Inc., Wilmington, DE, USA). The extracted RNA (2 μg) from each tested sample was synthesized to cDNA using Transcriptor First Strand cDNA Synthesis Kit (Roche, USA). Transcript of the human *MDR1* gene was quantitatively measured by Real-Time PCR using an Applied Biosystems (ABI) 7500HT-SDS instrument (Foster City, CA). The primers and probe set for the assay were purchased from Applied Biosystems as "Taqman Gene Expression Assays®" for *MDR1* transcript, which spans intron 23 and generate a 110 bp amplicon. For qPCR, 20 ng of cDNA was used for each reaction with a final volume of 20 μL, containing 200 nM primers and 100 nM probe. The cycling conditions for PCR were 50 ^oC for 5 minutes, 95 ^oC for 10 minutes followed by 50 cycles each of 95 ^oC for 15 s and 60 ^oC for 1 minute. Each sample was run in triplicate and mean/standard deviation cycle threshold values were determined. Results were normalized with endogenous reference gene GAPDH. Calculation of the relative expression values (fold change or ($2^{-(\Delta\Delta Ct)}$)) of all genes was performed using the comparative threshold cycle (Ct) method.

6.3.2 Flow cytometric analysis of the P-glycoprotein expression modulation mediated by FosPeg® PDT

The untreated control and FosPeg® treated NPC cells at LD_{50} and LD_{70} were harvested at 24 hours post-PDT. The cells were trypsinized and washed twice with PBS. Then, the cells were re-suspended in 100μL PBS and stained with 20μL of PE-conjugated P-glycoprotein monoclonal antibody CD243 (Immunotech; Beckman Coulter, USA) for 30 minutes at room temperature. Each sample with 10,000 events/counts was analyzed by flow cytometry. The fluorescent intensity was proportional to the P-gp expression on the cell surface.

6.3.3 Determination of *MDR1*/P-gp efflux transporter function in FosPeg® treated NPC cells by flow cytometric analysis

NPC cells (1×10^6 cells/dish) were seeded in 35mm culture dishes with 5% CO_2 at 37˚C overnight. Cells were either incubated in serum free medium with Rhodamine123 (5μM), a P-gp substrate (Sigma, St Louis MO), for 30 minutes or incubated in serum free medium with FosPeg® (0.3 μg/ml). After washed with PBS, cells were incubated in fresh medium and allowed to efflux for up to four hours. Then, these cells were incubated in fresh medium and allowed to efflux for four hours in the presence or absence of 100μM verapamil as a P-gp inhibitor (Sigma, St Louis MO). All the treated cells were harvested, washed, and analyzed by flow cytometry as described above.

6.3.4 Statistical analysis

All data were processed and presented using GraphPad Prism (Version 5.01) (GraphPad Software, Inc.). Mean and standard deviation (SD) were used to present data and all graphical error bars were represented in SD. Quantitative data from three independent experiments were used for analysis of the qPCR and flow cytometric assay. One-way analysis of variance (ANOVA) followed by Dunnett correction or Student's t test was used to analyze differences between groups by the GraphPad Prism (GraphPad Software, Inc.). A P-value of less than 0.05 was considered as significant different.

6.4 Results

6.4.1 Effect of FosPeg®-PDT on *MDR1* mRNA expression

In order to determine whether photoactivation of FosPeg® modulated multi-drug resistance transporter function, *MDR1* transcript expression was measured. Our initial data indicated that all three tested NPC cell lines expressed *MDR1* mRNA (Figure 6.1). A significant increase in *MDR1* mRNA expression was obtained at LD_{70} in both C666-1 cells and HK1 cells (4.5-fold and 12.4-fold increase respectively, $P<0.05$). We observed a 2.2-fold increase at LD_{50} and 4.5 fold increase at LD_{70} in C666-1 cells; a 3-fold increase at LD_{50} and 12.4-fold increase at LD_{70} in HK1 cells; and a 5.3-fold increase at LD_{50} and 4.7-fold increase at LD_{70} in CNE2 cells (Figure 6.1 a-c).

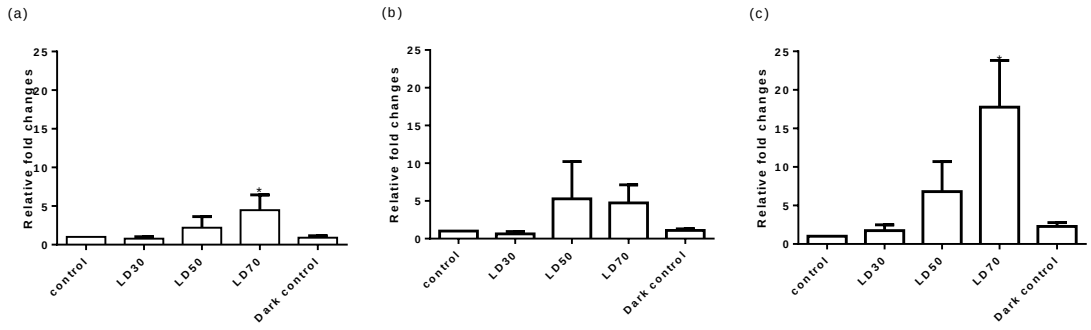

Figure 6.1 *MDR1* mRNA levels with photoactivated FosPeg® at pre- and post-treatment C666-1, CNE2 and HK1 cells were treated with FosPeg® at LD_{30}, LD_{50}, and LD_{70} (a: C666-1 cells; b: CNE2 cells; c: HK1 cells).

The *MDR1* mRNA levels in the control and treated cells were measured using Real-time PCR 24 hours post-PDT as described in the materials and methods. Total RNA was extracted and converted to cDNA from control and PDT treated cells for the detection of *MDR1* mRNA expression by TaqMan qPCR. Housekeeping gene GAPDH was used as control to normalize the mRNA amounts in different treatment. Up-regulation of *MDR1* mRNA expression was obtained at LD_{70} at all three tested cell lines. There were statistically significant changes in C666-1 cells and HK1 cells at LD_{70} FosPeg® mediated PDT. Significant differences between treatment and control groups were analyzed by one-way ANOVA and followed by Dunnett's post-tests (*: $p<0.05$, **: $p<0.01$, ***: $p<0.001$).

6.4.2 Effects of FosPeg®-PDT on *MDR1*/P-gp protein expression

The expression of P-gp/*MDR1* protein was measured by flow cytometry to determine whether photoactivatvation of FosPeg® up-regulated the expression of multi-drug resistance transporter protein P-gp. The following 4 conditions were selected for the follow-up protein expression assay including control, dark control, LD_{50} and LD_{70}. NPC cells stained with PE-conjugated P-glycoprotein monoclonal antibody CD243 were examined by flow cytometry. As shown in figure 6.2 and Table 6.1, increased expression of P-gp protein was obtained after FosPeg® incubation. A significant increase in P-gp expression was obtained in both C666-1 and HK1 cells when treated with FosPeg® (LD_{70}). A slight increase of P-gp expression was also obtained in both C666-1 and HK1 cells when treated with FosPeg® in dark, indicated that FosPeg® alone may induced P-gp protein expression. This increased expression of P-gp protein induced by FosPeg® was evident by the increase in the number of cells with a high P-gp surface expression at LD_{70}. To further investigate the effects of increased *MDR1* gene expression to P-gp activity, a P-gp/*MDR1* efflux transporter assay was carried out.

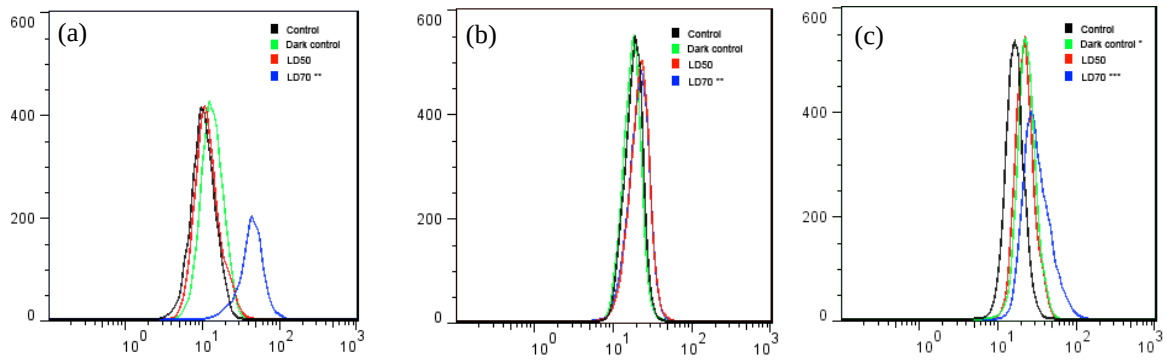

Figure 6.2 P-gp/*MDR1* protein levels before and after treatment with photoactivated FosPeg®.

C666-1, CNE2 and HK1 cells were treated with FosPeg® at LD_{50}, and LD_{70} (a: C666-1 cells; b: CNE2 cells; c: HK1 cells). The control and treated cells were stained with PE-conjugated P-glycoprotein monoclonal antibody (CD243) for 20 minutes at 24 hours post-PDT followed by flow cytometric analysis (One-way ANOVA * $p<0.05$, ** $p<0.01$ and ***<0.001).

Table 6.1 Flow cytometric analysis for PE-conjugated P-glycoprotein monoclonal antibody CD243 expression on NPC cells.

	C666-1 cells	CNE2 cells	HK1 cells
Control	10.35 ± 1.49	19.31 ± 0.61	16.95 ± 1.06
LD50	11.32 ± 0.81	20.38 ± 0.91	22.02 ± 1.22
LD70	46.67 ± 1.91**	20.55 ± 0.60	29.81 ± 4.16***
Dark control	12.64 ± 1.18	17.10 ± 2.16	24.78 ± 1.20**

The fluorescence intensity of cells at different conditions expressed as mean±S.D. of three independent experiments. Significant difference between treatment and control groups were analyzed by one-way ANOVA and followed by Dunnett's post-tests (*: $p<0.05$, **: $p<0.01$, ***: $p<0.001$).

6.4.3 Effect of *MDR1*/P-gp efflux transporter on FosPeg® accumulation in NPC

cells

In order to determine whether FosPeg® is a P-gp substrate, we evaluated its levels in the proposed cells in the presence of a validated P-gp inhibitor, verapamil. Verapamil was applied at a concentration (100μM) known to effectively inhibit P-gp function. The following conditions were being tested: 1) incubation with Rhodamine 123 (Rho123) for 30 minutes, then allowed for up to 4 hours efflux; 2) incubation with FosPeg® for 4 hours, then allowed for up to 4 hours efflux in the absence of verapamil; 3) incubation with FosPeg® for 4 hours, then allowed for up to 4 hours efflux in the presence of verapamil; 4) control cells only. A significant efflux of Rho123 was observed in all three NPC cell lines in a time-dependent manner (Figure 6.3 and Table 6.2). This was evidenced by the decreased fluorescent intensity after 4 hour efflux. All data pointed out that an active P-gp function was identified in the tested NPC cell lines. Data also indicated that FosPeg® is not the substrate of P-gp. In the FosPeg® treated group, no significant changes of fluorescence intensity were observed after 4 hour efflux in the presence or in the absence of verapamil. All these data suggested that FosPeg® induced P-gp expression but itself was not a P-gp substrate in the C666-1 cells, CNE2 cells and HK1 cells.

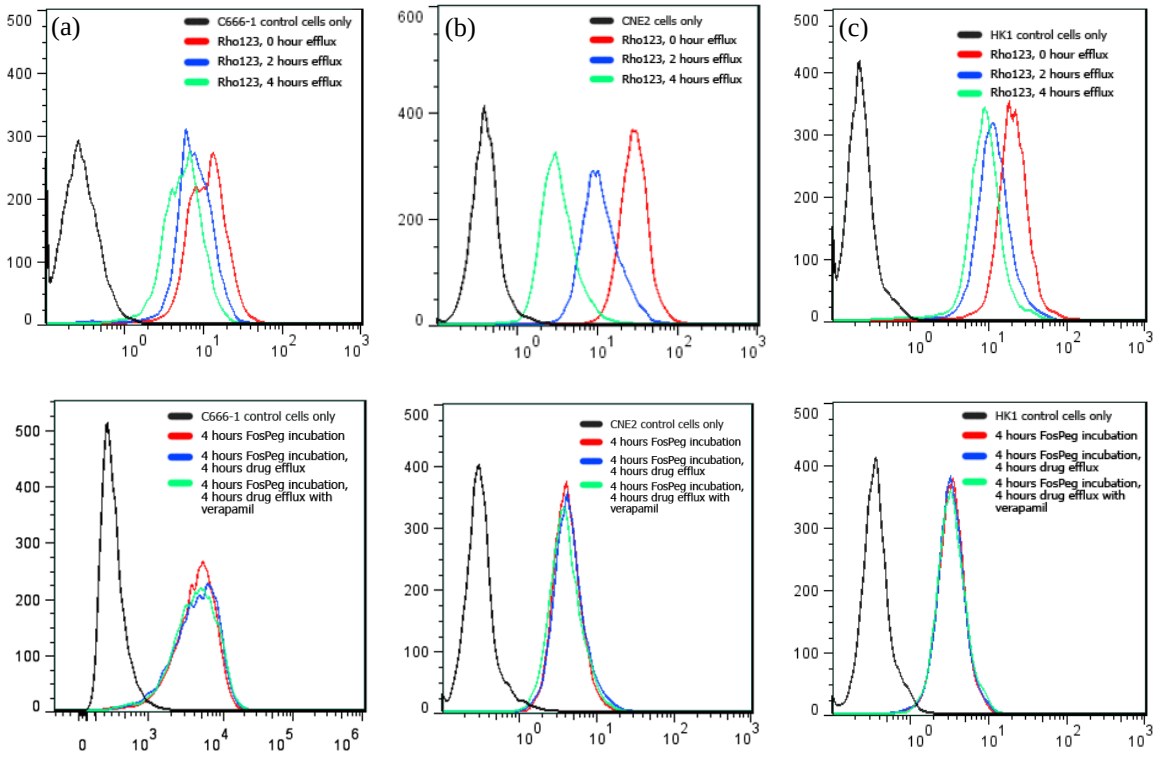

Figure 6.3 P-gp efflux activity in C666-1cells, CNE2 cells and HK1 cells.
The C666-1 cells, CNE2 cells and HK1 cells were incubated with either 5μM Rhodamine123 for 30 minutes or with 0.07μg/ml FosPeg® for 4 hours to allow for uptake (a: C666-1 cells; b: CNE2 cells; c: HK1 cells). Rho123 or FosPeg® was allowed to be efflux out of the cells for up to 4 hours. Intracellular fluorescent intensities were measured by flow cytometry in both the Rhodamine123 treated cells and the FosPeg® treated cells after 4 hours efflux time in the presence or absence of verapamil (100μM).

Table 6.2 Flow cytometric analysis for Rho123/FosPeg® efflux on NPC cells.

	C666-1 cells	CNE2 cells	HK1 cells
Control	0.26 ± 0.01	0.38 ± 0.01	0.28 ± 0.04
Rho123 0h efflux	38.90 ± 1.57	25.57 ± 1.25	21.58 ± 0.76
Rho123 2h efflux	26.32 ± 1.59**	8.13 ± 2.44***	12.3 ± 0.46****
Rho123 4h efflux	19.38 ± 4.39***	5.88 ± 2.96***	9.74 ± 0.54****
FosPeg® 0h efflux	3.76 ± 0.42	4.14 ± 0.07	3.38 ± 0.02
FosPeg® 4h efflux	4.02 ± 0.06	4.51 ± 0.14	3.38 ± 0.05
FosPeg® 4h efflux with verapamil	3.9 ± 0.21	4.34 ± 0.30	3.47 ± 0.07

The fluorescence intensity of cells at different conditions expressed as mean±S.D. of three independent experiments. Significant difference between treatment and control groups were analyzed by one-way ANOVA and followed by Dunnett's post-test (** p<0.01, *** p<0.001, ****p,0.0001).

6.5 Discussion

This is the first study aim at studying the effect of FosPeg®-PDT to P-gp function modulation in NPC cells. To evaluate the potential effect of FosPeg®-PDT as a long term treatment for nasopharyngeal carcinoma, the effects of FosPeg®-PDT on *MDR1* transcript and protein levels in three NPC cell lines were examined. There are only few articles revealed the correlation of multidrug resistance protein expression on EBV infected NPC cells. A few studies demonstrated that P-gp and MRP1 were found to be expressed in NPC cells but at different levels (Larbcharoensub et al., 2008; Tsuzuki et al., 1998). This study found that photoactivation of intracellular FosPeg® resulted in activation of *MDR1* mRNA levels in all three NPC cell lines. The significant effect of FosPeg® on *MDR1* gene expression was observed at high dose (LD_{70}) in all three NPC cells ($P<0.05$). Compare to the photoactivated FosPeg®, however, FosPeg® itself could also trigger P-gp expression. A slightly increased of P-gp expression was obtained in both C666-1 and HK1 cells when treated with FosPeg® in dark indicated that FosPeg® alone could also stimulate P-gp protein expression. Taken together, results indicated that photosensitizer FosPeg® induced P-gp transporter protein expression at LD_{70}. With substantial P-gp expression detected in all three NPC cells, drug efflux functional assay was then performed. The drug efflux functional assay was used to evaluate the effect of increased *MDR1* gene expression and P-gp protein expression to P-gp activity, especially on the efflux of photosensitizer FosPeg®.

P-gp transporter activity was constantly detected in C666-1, HK1 and CNE2 cells, which evidenced by the efflux of Rhodamine 123, a substrate of P-gp. For up to 4 hours efflux time, a continuously efflux of Rhodamine 123 was detected in all three NPC cell lines in a time-dependent manner (Figure 6.3). Interestingly, FosPeg® itself appeared not to be a substrate of P-gp. No efflux of FosPeg® was detected in all three NPC cells for up to 4 hours efflux time. Results were in-line with Teiten's finding (Teiten et al., 2001). By using MCF-7/DXR human breast cancer cells (with P–gp expression), Teiten demonstrated that the mTHPC-induced cytotoxicity was

not modified by the presence of P-gp inhibitors SDZ-PSC-833. Our finding proved that mTHPC based photosenstizer FosPeg® is not the substrate of P-gp transporters. Compared with the constant efflux of Rho123, similar concentration of intracellular FosPeg® was detected after 4 hour efflux time in the presence or absence of verapamil. Results indicated that FosPeg® is not the substrate of P-gp transporters (Figure 6.3). Thus FosPeg® could be used ideally as a combined therapy together with chemo-drugs and P-gp inhibitors for drug resistance patients. Given that the *MDR1* effects appeared to increase with drug dose, it is possible to initiate the multiple photoactivation process with lower FosPeg® dose in cancer cells in order to minimize the FosPeg® induced *MDR1* effects. Regarding the limited recognition of FosPeg® to P-gp transporters, sufficient intracellular FosPeg® levels were reached to provide reasonable potency against highly resistant human nasopharyngeal carcinoma cells with P-gp over-expression phenotype. ABCG2 is another type of transporter proteins that contribute to drug resistance properties. Robey et al. (2005) revealed the effect of ABCG2- mediated transporter proteins on a range of photosensitizers. The study concluded that ABCG2 should be a possible cause for cellular resistance to photodynamic therapy. On the contrary, photosensitizers with strong amphiphilic properties were not being affected. Selbo et al. (2012) reported that photosensitizers, such as meso-tetra(3-hydroxyphenyl)porphyrin (m-THPP) and meso-tetra(3-hydroxyphenyl)chlorin (m-THPC, Foscan) were not substrates of ABCG2. These echoed with our findings as no FosPeg® was effluxed out 4 hours after drug addition in all three NPC cell lines.

Our mechanistic studies suggested that the photosensitizer FosPeg® played a significant role in overcoming resistant tumours with P-gp transporter protein over-expression. FosPeg®-PDT could be used to overcome *MDR1*-related cancer drug resistance, which is evidenced by this study. Yet the expression of other transporter proteins in NPC cells and their interaction with FosPeg® remain to be determined.

In summary, this study found that FosPeg® mediated PDT induced up regulation of *MDR1* gene transcript and P-gp proteins. However, the FosPeg® mediated PDT efficacy was independent to the P-gp transporters function. Our results suggested that FosPeg® mediated PDT could be one of the novel treatments for P-gp mediated resistant cells.

6.6 References

Aszalos A. (2007) Drug-drug interactions affected by the transporter protein, P-glycoprotein (ABCB1, MDR1) I. Preclinical aspects. *Drug Discov Today, 12*(19-20), 833-837.

Capella MA, Capella LS. (2003) A light in multidrug resistance: photodynamic treatment of multidrug-resistant tumors. *J Biomed Sci, 10*(4), 361-366.

Chen CL, Sheen TS, Lou IU, Huang AC. (2001) Expression of multidrug resistance 1 and glutathione-S-transferase-Pi protein in nasopharyngeal carcinoma. *Hum Pathol, 32*(11), 1240-1244.

Chu ESM, Yow CMN, Shi M, Ho RJ. (2008) Effects of photoactivated 5-aminolevulinic acid hexyl ester on MDR1 over-expressing human uterine sarcoma cells. *Toxicol Lett, 181*(1), 7-12.

Eichhorn T, Efferth T. (2012) P-glycoprotein and its inhibition in tumors by phytochemicals derived from Chinese herbs. *J Ethnopharmacol, 141*(2), 557-570.

Gottesman MM, Ling V. (2006) The molecular basis of multidrug resistance in cancer: the early years of P-glycoprotein research. *FEBS Lett, 580*(4), 998-1009.

Hornung R, Walt H, Crompton NE, Keefe KA, Jentsch B, Perewusnyk G, Kochli OR. (1998) m-THPC-mediated photodynamic therapy (PDT) does not induce resistance to chemotherapy, radiotherapy or PDT on human breast cancer cells in vitro. *Photochem Photobiol, 68*(4), 569-574.

Hsu CH, Chen CL, Hong RL, Chen KL, Lin JF, Cheng AL. (2002) Prognostic value of multidrug resistance 1, glutathione-S-transferase-pi and p53 in advanced nasopharyngeal carcinoma treated with systemic chemotherapy. *Oncology, 62*(4), 305-312.

Ji XN, Yang F, Sui XM, Wang FG, Ge RG, Quan XL, Wang RY. (2013) Effect of fractionated irradiation on the expression of multidrug resistance genes in the CNE1 human nasopharyngeal carcinoma cell line. *Mol Med Rep, 7*(1), 187-194.

Larbcharoensub N, Leopairat J, Sirachainan E, Narkwong L, Bhongmakapat T, Rasmeepaisarn K, Janvilisri T. (2008) Association between multidrug resistance-associated protein 1 and poor prognosis in patients with nasopharyngeal carcinoma treated with radiotherapy and concurrent chemotherapy. *Hum Pathol, 39*(6), 837-845.

Lespine A, Ménez C, Bourguinat C, Prichard RK. (2012) P-glycoproteins and other multidrug resistance transporters in the pharmacology of anthelmintics: Prospects for reversing transport-dependent anthelmintic resistance. *International Journal for Parasitology: Drugs and Drug Resistance, 2*, 58-75.

Lin-Lee YC, Tatebe S, Savaraj N, Ishikawa T, Tien KM. (2001) Differential sensitivities of the MRP gene family and gamma-glutamylcysteine synthetase to prooxidants in human colorectal carcinoma cell lines with different p53 status. *Biochem Pharmacol, 61*(5), 555-563.

Mo W, Liu JY, Zhang JT. (2012) Biochemistry and Pharmacology of Human ABCC1/MRP1 and Its Role in Detoxification and in Multidrug Resistance of Cancer Chemotherapy. 371-404.

Moan J, Peng Q. (2003) An outline of the hundred-year history of PDT. *Anticancer Res, 23*(5A), 3591-3600.

Robey RW, Steadman K, Polgar O, Bates SE. (2005) ABCG2-mediated transport of photosensitizers: potential impact on photodynamic therapy. *Cancer Biol Ther, 4*(2), 187-194.

Schrenk D, Baus PR, Ermel N, Klein C, Vorderstemann B, Kauffmann HM. (2001) Up-regulation of transporters of the MRP family by drugs and toxins. *Toxicol Lett, 120*(1-3), 51-57.

Selbo PK, Weyergang A, Eng MS, Bostad M, Maelandsmo GM, Hogset A, Berg K. (2012) Strongly amphiphilic photosensitizers are not substrates of the cancer stem cell marker ABCG2 and provides specific and efficient light-triggered drug delivery of an EGFR-targeted cytotoxic drug. *J Control Release, 159*(2), 197-203.

Solazzo M, Fantappie O, Lasagna N, Sassoli C, Nosi D, Mazzanti R. (2006) P-gp localization in mitochondria and its functional characterization in multiple drug-resistant cell lines. *Exp Cell Res, 312*(20), 4070-4078.

Stavrovskaya AA. (2000) Cellular mechanisms of multidrug resistance of tumor cells. *Biochemistry (Mosc), 65*(1), 95-106.

Su GM, Davey MW, Davey RA. (1998) Induction of broad drug resistance in small cell lung cancer cells and its reversal by paclitaxel. *Int J Cancer, 76*(5), 702-708.

Szakacs G, Paterson JK, Ludwig JA, Booth-Genthe C, Gottesman MM. (2006) Targeting multidrug resistance in cancer. *Nat Rev Drug Discov, 5*(3), 219-234.

Tang PM, Zhang DM, Xuan NH, Tsui SK, Waye MM, Kong SK, Fung KP. (2009) Photodynamic therapy inhibits P-glycoprotein mediated multidrug resistance via JNK activation in human hepatocellular carcinoma using the photosensitizer pheophorbide a. *Mol Cancer, 8*, 56.

Teiten MH, Bezdetnaya L, Merlin JL, Bour-Dill C, Pauly ME, Dicato M, Guillemin F. (2001) Effect of meta-tetra(hydroxyphenyl)chlorin (mTHPC)-mediated photodynamic therapy on sensitive and multidrug-resistant human breast cancer cells. *J Photochem Photobiol B, 62*(3), 146-152.

Tredan O, Galmarini CM, Patel K, Tannock IF. (2007) Drug resistance and the solid tumor microenvironment. *J Natl Cancer Inst, 99*(19), 1441-1454.

Tsuzuki H, Fujieda S, Sunaga H, Sugimoto C, Tanaka N, Saito H. (1998) Expression of multidrug resistance-associated protein (MRP) in head and neck squamous cell carcinoma. *Cancer Lett, 126*(1), 89-95.

Yamane Y, Furuichi M, Song R, Van NT, Mulcahy RT, Ishikawa T, Kuo MT. (1998) Expression of multidrug resistance protein/GS-X pump and gamma-glutamylcysteine synthetase genes is regulated by oxidative stress. *J Biol Chem, 273*(47), 31075-31085.

Chapter 7

Summary of Findings and Further Investigations

7.1 Summary of findings

In summary, this study was the first report to demonstrate the therapeutic potential of H-ALA and FosPeg®-PDT on EBV positive undifferentiated NPC cells/C666-1, EBV negative poorly differentiated NPC cells/CNE2 and EBV negative well differentiated NPC cells/HK1.

The photodynamic efficacy of H-ALA-PDT in the NPC cells was compared and reported in Chapters 2 and 3 in detail. The findings presented in Chapter 2 indicated that H-ALA offered a more effective treatment for undifferentiated NPC cells/C666-1 and poorly differentiated NPC cells/CNE2 than the well differentiated NPC cells/HK1. The PDT dosage of FosPeg® required to achieve LD_{50} in CNE2 was lower than that of C666-1 (2-fold) and HK1 cells (167.8-fold).

A more in-depth investigation of H-ALA-PDT effect on NPC cells has been carried out in both chapters 2 and 3, including the regulation of cell cycle, modulation of EBV LMP1 protein and modulation of MAPK signaling proteins. Our findings indicated H-ALA-PDT up-regulated EBV LMP1 protein expression in C666-1 cells, which suggested that LMP1 protein was a therapeutic target of H-ALA-PDT in NPC cells. Besides, down-regulation of EGFR, ERK and p38 signaling proteins were elucidated, thereby triggering apoptotic cell death in all three NPC cell lines.

FosPeg®-PDT efficacy and antitumour mechanisms were elucidated in Chapters 4 to 6. Our findings illustrated the interaction between FosPeg® mediated PDT and EBV encoded miRNAs. Down-regulation of EBV-miRNAs (EBV-miR-BART 1-5p, EBV miR-BART 16 and EBV miR-BART 17-5p) followed by the up-regulation of EBV LMP1 mRNA and protein were observed after FosPeg® mediated PDT. Results confirmed that LMP1 mRNA and protein were the potential therapeutic targets of FosPeg®-PDT in NPC cells.

The findings presented in Chapters 4 and 5 also indicated that FosPeg® offered a more effective treatment for NPC cells/HK1 and NPC cells/CNE2 than that for NPC cells/C666-1 cells. The PDT dosage of FosPeg® required to achieve LD_{70} in HK1 was lower than that of CNE2 (1.6 fold) and C666-1 cells (2.4 fold). Results illustrated that FosPeg® was localized in mitochondria; thereby triggering apoptotic cell death with the down-regulation of EGFR/MAPK signaling proteins. The cell motility was reduced in all three tested NPC cell lines in response to FosPeg®-PDT.

The findings presented in Chapter 6 demonstrated the up-regulation of MDR1 mRNA and P-gp transporter protein in all three NPC cell lines. However, FosPeg® itself is not a substrate of the P-gp transporter proteins. Results indicated that FosPeg®-PDT could be a potential therapeutic approach towards cancer patients with P-gp mediated drug resistance properties.

It is encouraging that this study yielded new dimensions of PDT intervention for EBV positive and EBV negative NPC cells. This study described the PDT efficacy of two improved 3rd generation photosensitizers, namely H-ALA and FosPeg®, on three NPC cell lines. Evaluation of the PDT effects on EBV microRNAs, mRNA and LMP1 protein provided new insights for identification of the possible therapeutic targets and prognostic markers. The study of PDT effect on MAPK signal pathways offered better understanding in PDT responses and identified possible protein targets for further investigation. The study of FosPeg®-PDT effect on MDR1 transporter protein generated better understanding of the causes of PDT resistance. Through elucidating the relationship between the regulation of EBV LMP1 protein, MAPK signaling pathways and MDR1 transporter protein, a new therapeutic strategy could be developed to improve PDT efficacy. Additional *in vivo* studies and clinical trials must be undertaken with H-ALA- and FosPeg®-PDT for the development of this innovative technique. Its efficacy and its safety over the conventional cancer treatments remain to be explored.

7.2 Further investigations

This study revealed the photodynamic effect of H-ALA/FosPeg® to one of the principal oncoprotein LMP1. In NPC, EBV expression is restricted to a subset of latent transcripts. Other than the latent membrane protein LMP1, EBV latent nuclear antigens EBNA1, the latent membrane protein LMP2A, as well as small noncoding RNAs BamHI A rightward transcripts (BARTs) are also consistently expressed in NPC cells (Marquitz & Raab-Traub, 2012). Several studies reported that LMP2A expression resulted in transformation of epithelial cell lines to anchorage independence tumour cells through activation of Syk, PI3K/Akt, and Ras protein. LMP2A also provided pro-survival signals for the survival, colonization and invasion of NPC cells and B cells (Dawson et al., 2012; Lan et al., 2012; Shair et al., 2012). Various EBV encoded RNAs were found in NPC cells in additional to the LMP2A viral protein expression. These RNAs were referred as complementary strand transcripts (CSTs), BamHI A rightward transcripts (BARTs) or the BARF0 RNAs (Smith, 2001; Smith et al., 2000; Takada, 2012). The recent discovery of BART microRNAs (miRNA) has shed new light on the function of these transcripts. The number of EBV miRNAs made up of 23.2% of the total miRNAs in the biopsy samples in NPC patients, whereas only 0.1% EBV miRNAs was found in adjacent normal nasopharynx tissues (Chen et al., 2010). There were 44 EBV encoded miRNAs registered on the miRBase version 18. These potent gene regulators are thought to control a wide range of biological functions, including differentiation, cell growth and cancer development (Cosmopoulos et al., 2009; He et al., 2012; Lo et al., 2012; Marquitz & Raab-Traub, 2012; Zhao, et al., 2012). Recent studies also indicated interaction between human miRNAs and EBV expressed viral proteins. Du et al. (2011) reported that LMP1 and LMP2A expressed in nasopharyngeal carcinoma could up-regulate the expression of MiR-155, which was associated with N stage and poor prognosis of NPC patients. Thus further studies on the effect of FosPeg®-PDT to other EBV encoded miRNAs as well as human miRNA profiling is needed to further elucidate the mechanisms in NPC tumour destruction.

Further investigation on the effect of FosPeg®-PDT to MAPK singaling proteins using gene knockout cell models is also needed to further elucidate the mechanisms in NPC tumour destruction. Our data showed a down-regulation of MAPK signaling proteins after FosPeg®-PDT. Yet the correlation between modulation of MAPK signaling proteins and cancer cell death was not provided in this study. Using cells models which MAPK signalling proteins are knocked-out could help to illustrate the relationship between modulation of MAPK signaling proteins and cancer cell death in NPC cells.

Besides direct tumour cells destruction, PDT is also capable of eliciting various effects in the tumour microenvironment. There is accumulating evidence support that PDT has effect on tumour stroma, which composed of extracellular matrix, vasculature and immune system cells (tumour-associated/-infiltrating immune cells). It has also come to light that application of PDT could develop different immune phenomena, such as inflammation, modulation of cytokines production, and activation of complement cascades (Gollnick, 2012; Sanabria et al., 2013). Membrane lipids, transcription factors NF-kB and AP-1 were observed to be generated after photo-oxidation, which could precipitate in rapid and strong inflammatory reactions (Firczuk et al., 2011; Girotti, 2001; Granville et al., 2001). With better understanding of PDT-induced chemical modulation in the tumour microenvironment, clinicians could develop novel approach in curing tumour. All these evidence provide new insight for PDT treatment.

In spite of the low number of new clinically approved drugs, modification of existing but still underappreciated photosensitizers becomes other therapeutic approaches for PDT. With improvement of photosensitizers, PDT will have increased importance that meets the need of medication for cancer patients in coming future. The future of PDT depends on the ease of use, cost effectiveness, the treatment outcomes and quality of life compared to conventional treatments. The liposomal mTHPC used in this study definitely played a major role to meet these criteria. Another approach could be chemically modified photosensitizers with

sugars to improve solubility, tumour selectivity and decrease toxicity. This opened the possibility to target saccharide specific binding domains that are expressed on tumour-associated macrophages (Bredell et al., 2010; Yano et al., 2011). Photoimmunotherapy (PIT) is another innovative PDT combined with immunomodulation for cancer treatment. For PIT, photosensitizers are conjugated with monoclonal antibodies (MAbs) which targets on an overexpressed tumour marker (cellular) (Qiang, Yow, & Huang, 2008). Despite the encouraging progress made in basic research over the past decades, chemical modification and photoimmunoconjugates to improve PDT efficacy still awaits clinical evaluations for NPC patients (van Dongen et al., 2004).

Further investigations in PDT effect to EBV expressed transcripts, EBV-miRNAs, human miRNAs; modulation of tumour microenvironment and immunity; and modification of photosensitizers or PIT may open up a variety of treatment modalities for nasopharyngeal carcinoma.

7.3 References

Bredell MG, Besic E, Maake C, Walt H. (2010) The application and challenges of clinical PD-PDT in the head and neck region: a short review. *J Photochem Photobiol B, 101*(3), 185-190.

Chen SJ, Chen GH, Chen YH, Liu CY, Chang KP, Chang YS, Chen HC. (2010)Characterization of Epstein-Barr virus miRNAome in nasopharyngeal carcinoma by deep sequencing. *PLoS One, 5*(9). doi: 10.1371/journal.pone.0012745

Cosmopoulos K, Pegtel M, Hawkins J, Moffett H, Novina C, Middeldorp J, Thorley-Lawson DA (2009). Comprehensive profiling of Epstein-Barr virus microRNAs in nasopharyngeal carcinoma. *J Virol, 83*(5), 2357-2367. doi: 10.1128/JVI.02104-08

Dawson, C. W., Port, R. J., & Young, L. S. (2012). The role of the EBV-encoded latent membrane proteins LMP1 and LMP2 in the pathogenesis of nasopharyngeal carcinoma (NPC). *Semin Cancer Biol., 22*(2), 144-153. doi: 10.1016/j.semcancer.2012.01.004

Du ZM, Hu LF, Wang HY, Yan LX, Zeng YX, Shao JY, Ernberg I. (2011) Upregulation of MiR-155 in nasopharyngeal carcinoma is partly driven by LMP1 and LMP2A and downregulates a negative prognostic marker JMJD1A. *PLoS One, 6*(4), e19137.

Firczuk M, Nowis D, Golab J. (2011). PDT-induced inflammatory and host responses. *Photochem Photobiol Sci, 10*(5), 653-663.

Girotti AW. (2001) Photosensitized oxidation of membrane lipids: reaction pathways, cytotoxic effects, and cytoprotective mechanisms. *J Photochem Photobiol B, 63*(1-3), 103-113.

Gollnick SO. (2012) Photodynamic therapy and antitumor immunity. *J Natl Compr Canc Netw, 10 Suppl 2*, S40-43.

Granville DJ, McManus BM,Hunt DW. (2001) Photodynamic therapy: shedding light on the biochemical pathways regulating porphyrin-mediated cell death. *Histol Histopathol, 16*(1), 309-317.

He ML, Luo MX, Lin MC, Kung HF. (2012) MicroRNAs: potential diagnostic markers and therapeutic targets for EBV-associated nasopharyngeal carcinoma. *Biochim Biophys Acta, 1825*(1), 1-10.

Lan YY, Hsiao JR, Chang KC, Chang JS, Chen CW, Lai HC, Chang Y. (2012) Epstein-Barr virus latent membrane protein 2A promotes invasion of nasopharyngeal carcinoma cells through ERK/Fra-1-mediated induction of matrix metalloproteinase 9. *J Virol, 86*(12), 6656-6667.

Li, F., Cheng Y, Lu J, Hu R, Wan Q, Feng H. (2011). Photodynamic therapy boosts anti-glioma immunity in mice: a dependence on the activities of T cells and complement C3. *J Cell Biochem, 112*(10), 3035-3043.

Lo AK, Dawson CW, Jin DY, Lo KW. (2012) The pathological roles of BART miRNAs in nasopharyngeal carcinoma. *J Pathol, 227*(4), 392-403.

Marquitz AR,Raab-Traub N. (2012) The role of miRNAs and EBV BARTs in NPC. *Semin Cancer Biol., 22*(2), 166-172.

Milla Sanabria L, Rodriguez ME, Cogno IS, Rumie Vittar NB, Pansa MF, Lamberti MJ, Rivarola VA. (2013) Direct and indirect photodynamic therapy effects on the cellular and molecular components of the tumor microenvironment. *Biochim Biophys Acta, 1835*(1), 36-45.

Qiang YG, Yow CMN, Huang Z. (2008) Combination of photodynamic therapy and immunomodulation: current status and future trends. *Med Res Rev, 28*(4), 632-644.

Shair KH, Bendt KM, Edwards RH, Nielsen JN, Moore DT, Raab-Traub N. (2012) Epstein-Barr virus-encoded latent membrane protein 1 (LMP1) and LMP2A function cooperatively to promote carcinoma development in a mouse carcinogenesis model. *J Virol, 86*(9), 5352-5365.

Smith P. (2001) Epstein-Barr virus complementary strand transcripts (CSTs/BARTs) and cancer. *Semin Cancer Biol, 11*(6), 469-476.

Smith PR, de Jesus O, Turner D Hollyoake, M Karstegl CE, Griffin BE, Farrell PJ. (2000) Structure and coding content of CST (BART) family RNAs of Epstein-Barr virus. *J Virol, 74*(7), 3082-3092.

Takada K. (2012) Role of EBER and BARF1 in nasopharyngeal carcinoma (NPC) tumorigenesis. *Semin Cancer Biol, 22*(2), 162-165.

van Dongen GA, Visser GW, Vrouenraets MB. (2004) Photosensitizer-antibody conjugates for detection and therapy of cancer. *Adv Drug Deliv Rev, 56*(1), 31-52.

Yano S, Hirohara S, Obata M, Hagiya Y, Ogura Si, Ikeda A, Joh T. (2011) Current states and future views in photodynamic therapy. *Journal of Photochemistry and Photobiology C: Photochemistry Reviews, 12*(1), 46-67.

Zhao Y, Wang Y, Zeng S, Hu X. (2012) LMP1 expression is positively associated with metastasis of nasopharyngeal carcinoma: evidence from a meta-analysis. *J Clin Pathol, 65*(1), 41-45.